

A STUDY OF DARK ENERGY
FROM VARIOUS APPROACHES

THESIS SUBMITTED FOR THE DEGREE OF
DOCTOR OF PHILOSOPHY (SCIENCE)

IN

PHYSICS (THEORETICAL)

BY

NILOK BOSE

DEPARTMENT OF PHYSICS
UNIVERSITY OF CALCUTTA
2013

CONTENTS

I	Introduction	1
1	General Observations	2
1.1	The Scalar Field Approach	5
1.2	Cosmological Backreaction	7
1.3	Outline of Thesis	9
2	Primary Framework	12
2.1	Basics of FRW Cosmology	12
2.1.1	Evolution Equations	12
2.1.2	Evolution of the Universe filled with a perfect fluid	13
2.2	Inflation in the Early Universe	15
2.2.1	Motivation for Inflation	15
2.2.1.1	Flatness Problem	16
2.2.1.2	Horizon Problem	17
2.2.1.3	Relic Particle Abundances	17
2.2.2	How Inflation Helps	17
2.2.3	Basics of Inflation Mechanism	18
2.3	Late-time Acceleration Using Scalar Fields	20
II	Scalar Field Approach Using k-essence	23
3	Unifying Inflation, Dark Energy and Dark Matter using k-essence	24
3.1	Equation of motion of k -essence	24
3.2	Purely kinetic k -essence	26
3.3	Simple unification using purely kinetic k -essence	27
3.4	k -essence Model for Unification	29
3.5	Observational constraints on the model	33
3.6	Summary and Discussion	39

4	Another k-essence Model of Unification	41
4.1	The Model	41
4.2	Observational Constraints on the Model	47
4.3	Summary and Discussion	53
 III Cosmological Backreaction		55
5	The Backreaction Framework	56
5.1	Averaged Einstein equations	56
5.2	Effective Friedmannian Framework	58
5.3	‘Morphed’ Friedmann cosmologies	59
5.3.1	Morphon as k -essence	60
5.4	The Cosmic Quartet	61
5.5	Acceleration and energy conditions	62
5.6	Separation formulae for arbitrary partitions	63
5.7	Consistent split of the dynamical equations	64
6	Effect of Cosmic Backreaction on the Future Evolution of the Universe	66
6.1	Future evolution within the Buchert framework	67
6.1.1	Backreaction and Scalar Curvature	68
6.1.2	Effective Equation of State	70
6.2	Effect of Event Horizon	72
6.2.1	Evolution in a Toy Model	74
6.2.2	Future Deceleration	75
6.2.3	A Different Framework for the Event Horizon	76
6.3	Discussions	79
6.4	Summary	82
7	Backreaction with Multiple Domains	85
7.1	Future Evolution	86
7.2	Discussions	90
7.3	Summary	94
8	Conclusions	96

LIST OF PUBLICATIONS

- “***k*-essence model of inflation, dark matter, and dark energy**” – Nilok Bose and A. S. Majumdar, Phys. Rev. D **79**, 103517 (2009) [arXiv:0812.4131 [astro-ph]].
- “**Unified model of *k*-inflation, dark matter, and dark energy**” – Nilok Bose and A. S. Majumdar, Phys. Rev. D **80**, 103508 (2009) [arXiv:0907.2330 [astro-ph.CO]].
- “**Future deceleration due to cosmic backreaction in presence of the event horizon**” – Nilok Bose and A. S. Majumdar, MNRAS: Letters **418**: L45–L48 (2011) [arXiv:1010.5071 [astro-ph.CO]].
- “**Effect of cosmic backreaction on the future evolution of an accelerating universe**” – Nilok Bose and A. S. Majumdar, [arXiv:1203.0125 [astro-ph.CO]], accepted for publication in Gen. Rel. Grav.
- “**Cosmological backreaction and the future evolution of an accelerating universe**” – Nilok Bose and A. S. Majumdar, [arXiv:1306.2877 [astro-ph.CO]], to appear in the Proceedings of the Thirteenth Marcel Grossmann Meeting.
- “**Study of cosmic backreaction on the future evolution of an accelerating universe using multiple domains**” – Nilok Bose and A. S. Majumdar, [arXiv:1307.5022 [astro-ph.CO]], communicated for publication.

LIST OF FIGURES

6.1	The dimensionless global acceleration parameter $\frac{\ddot{a}_D}{\alpha_D H_D^2}$, plotted vs. time (in units of t/t_0 with t_0 being the current age of the Universe). The parameter values used are: (i) $\alpha = 0.995, \beta = 0.5$, (ii) $\alpha = 0.995, \beta = 0.5$, (iii) $\alpha = 1.02, \beta = 0.66$, (iv) $\alpha = 1.02, \beta = 0.66$. (The curves (i) and (iii) correspond to the case when an event horizon is included in the analysis in Section 6.2.3).	69
6.2	Global backreaction density fraction vs. time. The parameter values used are the same as in Fig. 6.1.	70
6.3	Global scalar curvature density fraction, Ω_R^D plotted vs. time. The parameter values for curves (i) and (ii) are $\alpha = 0.995, \beta = 0.5$, and for curves (iii) and (iv) are $\alpha = 1.02, \beta = 0.66$	71
6.4	Effective equation of state vs. time. The parameter values used are: (i) $\alpha = 0.995, \beta = 0.5$, (ii) $\alpha = 0.995, \beta = 0.5$, (iii) $\alpha = 1.02, \beta = 0.66$, (iv) $\alpha = 1.02, \beta = 0.66$	72
6.5	The dimensionless global acceleration parameter $\frac{\ddot{a}_D}{\alpha_D H_0^2}$ is plotted versus time (s) assuming a constant horizon. The values for the various parameters used are (i) $\alpha = 0.995, \beta = 0.5$, (ii) $\alpha = 0.999, \beta = 0.6$, (iii) $\alpha = 1.0, \beta = 0.5$ and (iv) $\alpha = 1.02, \beta = 0.66$	76
6.6	The dimensionless global acceleration parameter $\frac{\ddot{a}_D}{\alpha_D H_0^2}$ is plotted versus time (s) as obtained through numerical integration, with the ‘initial condition’ of $q_0 = -0.7$. The values for the various parameters used are chosen to be the same as in the corresponding plots of Fig. 6.5.	77

- 6.7 The range of parameters α and β for which future deceleration takes place, shown within the respective contours for the curves (i) and (iii) corresponding to the case with an event horizon, and the curves (ii) and (iv) corresponding to the case where an event horizon is not considered. The value of $\lambda_{\mathcal{M}_0}$ for the curves (i) and (ii) is 0.15 and for curves (iii) and (iv) is 0.2. The shaded region corresponds to the curve (iv) demarcating the parameter space for this case when acceleration vanishes in finite future time. 81
- 7.1 The dimensionless global acceleration parameter $\frac{\ddot{a}_{\mathcal{D}}}{a_{\mathcal{D}}H_0^2}$, plotted vs. time (in units of t/t_0 with t_0 being the current age of the Universe). In curves (i) and (ii) the value of α is in the range 0.990 – 0.999 and that of β is in the range 0.58 – 0.60. In curves (iii) and (iv) the value of α is in the range 1.02 – 1.04 and that of β is in the range 0.58 – 0.60 87
- 7.2 Here also $\frac{\ddot{a}_{\mathcal{D}}}{a_{\mathcal{D}}H_0^2}$ is plotted vs. time. In curves (i) and (ii) the value of α lies in the range 0.990 – 0.999 and that of β is in the range 0.58 – 0.60. For curves (iii) and (iv) the value of α is in the range 0.990 – 0.999 and that of β is in the range 0.55 – 0.65 88
- 7.3 Global backreaction density $\Omega_{\mathcal{Q}}^{\mathcal{D}}$ plotted vs. time (in units of t/t_0). In curves (i) and (ii) the value of α is in the range 0.990 – 0.999 and that of β is in the range 0.58 – 0.60. In curves (iii) and (iv) the value of α is in the range 1.02 – 1.04 and that of β is in the range 0.58 – 0.60 89
- 7.4 Here also $\Omega_{\mathcal{Q}}^{\mathcal{D}}$ is plotted vs. time. In curves (i) and (ii) the value of α lies in the range 0.990 – 0.999 and that of β is in the range 0.58 – 0.60. For curves (iii) and (iv) the value of α is in the range 0.990 – 0.999 and that of β is in the range 0.55 – 0.65 90
- 7.5 We plot $\frac{\ddot{a}_{\mathcal{D}}}{a_{\mathcal{D}}H_0^2}$ vs. t/t_0 for various numbers of subdomains. In all the curves we have α_j in the range 0.990 – 0.999, and β_j in the range 0.58 – 0.60. For curve (i) we consider 100 overdense and underdense subdomains, in (ii) 400 overdense and underdense subdomains and in (iii) 500 overdense and underdense subdomains each. 93

PART I

INTRODUCTION

CHAPTER 1

GENERAL OBSERVATIONS

Our understanding of the Universe has vastly improved in the last century. Edwin Hubble's observation of distant galaxies established in 1929 that the Universe is expanding. The globally homogeneous and isotropic Friedmann-Robertson-Walker (FRW) metric, which is one of the solutions of Einstein's theory of General Relativity, was very successful in explaining our then observed Universe, and became known as the Standard Model of cosmology. Even though the Universe was found to be expanding it was firmly believed that the rate of expansion would be decreasing due to the effect of gravity. However at the end of the last century it was found that the earlier notion was not true and the Universe is in fact in an accelerated expansion. This is one of the most striking result in modern cosmology and it was first reported in Refs. [1]. Over the course of the past decade evidence for this result has been steadily growing. Although it may not have come as such a surprise to a few theorists who were at that time considering the interplay between a number of different types of observations, for the majority it came as something of a bombshell. The Universe is not only expanding, it is accelerating. The results first published in Refs. [1] have caused a significant change in the way we have started thinking about the universe.

The nature of the physical mechanism driving this acceleration is yet unclear, though there exists an increasingly wide variety of approaches that could theoretically account for the present acceleration. The component of the Universe that is responsible for this expansion is required to have negative pressure, something that is not possible with ordinary matter, is believed to be very homogeneous and is not known to interact through any of the fundamental forces other than gravity. Because of the unknown nature of this component it has been innovatively named "Dark Energy". Observations have categorized the energy density of the present

universe to consist of approximately 23% dark matter, which clusters and drives the formation of the large scale structure in the universe, and 73% dark energy, which drives the late-time acceleration of the Universe, with the remaining 5% or so being comprised of matter and radiation (see [2]).

The most simple explanation for the late-time acceleration is provided by a cosmological constant, and is consistent with several important observations such as the redshift of distant supernovae, the power spectrum of the Cosmic Microwave Background (CMB), and the distribution of the large scale structure. However, the introduction of the cosmological constant into our description of the Universe is quite problematic. The current energy density of the cosmological constant, as deduced from observations, is about 10^{-48} (GeV)^4 , which is some 120 orders of magnitude smaller than theoretical expectations. If the energy density were even slightly larger, the repulsive force would cause the Universe to expand too fast so that there would not be enough time for the formation of galaxies or other gravitationally bound systems. This is called the *cosmological constant problem*. Secondly it raises the question of why the value of the cosmological constant was so finely tuned that it came to dominate in a narrow window of time in the present Universe and cause the observed accelerated expansion. This problem is referred as the *cosmic coincidence problem*.

Since the cosmological constant has quite a few problems associated with it [3], so despite its simplicity of approach to explain dark energy driven late-time acceleration a number of alternative routes have been proposed [4]. A few notable examples in this regard are:

- Quintessence models [5] which invoke an evolving canonical scalar field with a potential (effectively providing an inflaton for today) and makes use of the scaling properties and tracker nature of such scalar fields evolving in the presence of other background matter fields.
- A scalar field with a non-canonical kinetic term, known as *k-essence* [6, 7, 8, 9, 10, 11] based on an earlier work known as *k-inflation* [12].
- Modified gravity arising out of both string motivated or more generally General Relativity modified [13] actions which both have the effect of introducing large length scale corrections and modifying the late-time evolution of the Universe.

- Chaplygin gases which attempt to unify dark energy and dark matter under one umbrella by allowing for a fluid with an equation of state which evolves between the two [14].
- The String Landscape arising from the multiple numbers of vacua that exist when the string moduli are made stable as non-abelian fluxes are turned on [15].
- The phenomenon of Cosmological Backreaction whereby the feedback of non-linearities into the evolution equations can significantly change the background evolution and lead to acceleration at late times without introducing any new matter.
- Tachyons arising in string theory [16], Phantom Dark Energy [17] and Ghost Condensates [18], holographic dark energy models [19] and causal sets in the context of Quantum Gravity [20].

These possibilities and more have been discussed in the literature. Since our current observational data are quite favourable towards the presence of a cosmological constant type term today, therefore any dynamically evolving contribution must resemble a cosmological constant today. If we are to see evidence of dynamics in the dark energy equation of state, we have to probe back in time. A number of routes in that direction have been suggested and plans are underway to extend this even further. On the other hand a minority of cosmologists have argued forcefully that the majority of the data as it presently stands can be interpreted without recourse to a cosmological constant, rather we can explain it through other physical processes, for example by relaxing the hypothesis that the fluctuation spectrum can be described by a single power law [21]. Perhaps we do not yet fully understand how Type Ia supernovae evolve and we may have to eventually think of alternative explanations. Although this might well be the case, there is a growing body of evidence for the presence of a cosmological constant which does not rely on the supernova data to support it (see Ref. [22]). However, the more accepted interpretation of the data is that it is becoming clear that consistency between the anisotropies in the CMB [23, 24] and LSS [25] observations imply we live in a Universe where the energy density is dominated by a cosmological constant type contribution. An impressive aspect of this consistency check is the fact that the physics associated with each epoch is completely different and of course it occurs on different time scales. It appears that consistency is obtained for a spatially

flat universe with the fractional energy density in matter contributing today with $\Omega_m^{(0)} \sim 0.3$ whereas for the cosmological constant we have $\Omega_\Lambda^{(0)} \sim 0.7$.

In this thesis we have assumed that dark energy is there in some form and is driving the current accelerated expansion. Our goal was to study both the mechanism behind the current acceleration and also its future evolution. In our work we have dealt with two interesting approaches that try to explain dark energy, namely k -essence and cosmological backreaction, and we mention the main characteristics of these approaches below.

1.1 THE SCALAR FIELD APPROACH

There are several scalar field based models that try to explain the phenomenon of dark energy. But in recent years an interesting branch of this line of study has emerged that deals with non-canonical kinetic terms in the Lagrangian of the scalar field. The first theory of this kind was introduced M. Born and L. Infeld in 1934 [26] to avoid the infinite self-energy of the electron. The non-canonical kinetic terms are quite common in effective field theory models arising from string theory and in particular D-brane models. The idea of k -essence was motivated from the Born-Infeld action of string theory [27] and in cosmology such theories were first studied in the context of k -inflation [12]. Later, it was noted that k -essence could also yield interesting models for dark energy [6, 7, 8, 9, 10, 11] and it was suggested that such models could also solve the cosmic coincidence problem [7]. There have also been attempts to try to describe dark matter through k -essence [28]. As further developments of these ideas we also have the ghost condensation scenario [18], ghost inflation [29] and phantom dark energy [17].

A parallel mechanism for producing the late-time acceleration of the universe through the dynamics of scalar fields, *viz.* quintessence [5], has also gained a lot of popularity in the literature. In most of the quintessence models the late-time dynamics is dominated by the potential for the scalar field. A crucial difference between quintessence and k -essence is that the latter class of models contain non-canonical kinetic terms in the Lagrangian. In this sense quintessence may also be viewed as a special case of k -essence. In fact k -essence can be called the most general possible scalar field model since its Lagrangian encompasses both canonical kinetic terms, such as those present in quintessence, and also of course non-canonical kinetic terms. But in practice only fields that contain non-canonical kinetic terms

are called k -essence fields, and in this text whenever we refer to k -essence we will mean exactly that. Another important subset of k -essence is purely kinetic k -essence in which the Lagrangian contains only a kinetic factor, i.e., a function of the derivatives of the scalar field, and does not depend explicitly on the field itself. Such models were in fact, the first ones investigated in the context of k -inflation [12]. In this context, they successfully yield exponential inflation, but suffer from the “graceful exit” problem.

Much of the early interest in k -essence was due to the fact that it was said to solve the coincidence problem. The addressing of this problem within the context of k -essence is made possible by the existence of fixed points in the radiation and matter era. In order to have these fixed points, it is necessary that the potential has the form $V(\phi) = 1/\phi^2$. It was shown that such models that solve the coincidence problem suffer from superluminal propagation of the field perturbations [30] (which, however, may not affect causality [31]).

Dark matter figures as the majority of matter in the Universe and is probably non-baryonic. Although the evidence for dark matter is considered to be quite overwhelming by many, there is no consensus as to what form it takes. It is quite possible that it interacts with baryonic matter only through gravitational interaction. Since the nature of both dark matter and dark energy are unknown, it is plausible that these two mysterious components of the universe are the manifestations of a single entity. Several examples of attempts to unify dark matter and dark energy can be found in the literature (for instance [32, 33, 34]). Further, it is very strongly believed that there was an early inflationary period of the universe, and the nearly scale independent density perturbations produced during inflation have left a faithful imprint on features of the CMB power spectrum. Since accelerated expansion is a common feature for both the very early and the very late Universe, it is plausible that some common mechanism could be responsible for both. Several models have been constructed to explain inflation and dark energy using a single scalar field (see, for example, quintessential inflation [35]). Apart from the above schemes there are models that try to unify inflation and dark matter (for instance [36]) and also those that attempt to unify all three, *viz.* inflation, dark matter, and dark energy (for instance [37]). An interesting attempt was made to unify dark matter and dark energy using kinetic k -essence in [34]. Though this model had its share of problems extensions of the formalism to extract out dark matter and dark energy components within a unified framework have been used also in subsequent

works [38]. In this thesis we will present two models of k -essence [10, 11] that try to achieve a unification of inflation, dark matter and dark energy using a single scalar field. The first model produces inflation in the early Universe using a standard quadratic potential, whereas the second model achieves this using the process of k -inflation.

1.2 COSMOLOGICAL BACKREACTION

The standard model of cosmology does not, unlike the standard model of particle physics, enjoy appreciable generality. It is based on the simplest conceivable class of (homogeneous–isotropic) solutions of Einstein’s laws of gravitation. The assumption of homogeneity and isotropy was largely made on grounds of simplicity and aesthetic appeal and the standard Big Bang model of cosmology has been very successful based on this assumption. This assumption is even justified to a large extent by our observations of CMB radiation and the large scale structure of the Universe. However the present Universe is certainly not homogeneous and there is a rich variety of structure present in it, from stellar systems to galaxies to clusters of galaxies and even larger systems. Observations tell us that our Universe is inhomogeneous up to at least the scales of super clusters of galaxies. It is clear that the inhomogeneous properties of the Universe cannot be described by such a strong idealization and this calls for, in principle, a modification of the cosmological framework based on the assumption of a globally smooth FRW metric. Taking the global average of the Einstein tensor is unlikely to lead to the same results as taking the average over all the different local metrics and then computing the global Einstein tensor for a nonlinear theory such as general relativity. This realization has led to investigation of the question of how backreaction originating from density inhomogeneities could modify the evolution of the universe as described by the background FRW metric at large scales.

In recent times there is an upsurge of interest on studying the effects of inhomogeneities on the expansion of the Universe. The main obstacle to this investigation is the difficulty of solving the Einstein equations for an inhomogeneous matter distribution and calculating its effect on the evolution of the Universe through tensorial averaging techniques. Approaches have been developed to calculate the effects of inhomogeneous matter distribution on the evolution of the Universe, such as Zalaletdinov’s fully covariant macroscopic gravity [39]; Buchert’s approach

of averaging the scalar parts of Einstein's equations [40, 41] and the perturbation techniques proposed by Kolb *et. al.* [42]. Based on the framework developed by Buchert it has been argued by Räsänen [43] that backreaction from inhomogeneities from the era of structure formation could lead to an accelerated expansion of the Universe. The Buchert framework from a different perspective developed by Wiltshire [44] also leads to an apparent acceleration due to the different lapse of time in underdense and overdense regions. Further, gauge invariant averages in the Buchert framework have also been constructed recently [45].

In spite of numerous creative ideas proposed for the present acceleration, there is still a lack of convincing explanation of this phenomenon. The simplest possible explanation provided by a cosmological constant is endowed with conceptual problems [3]. Alternative mechanisms based on either modifications of the gravitational theory, or invoking extra fields with tailored dynamics mostly suffer from the coincidence problem, as to why the era of acceleration begins around the same era when the Universe becomes structured. The ultimate fate of our Universe remains clouded in considerable mystery. Backreaction from inhomogeneities provides an interesting platform for investigating this issue without invoking additional physics, since the effects of backreaction gain strength as the inhomogeneities develop into structures around the present era.

It needs to be mentioned here that the impact of inhomogeneities on observables [46, 47] of an overall homogeneous FRW model has been debated in the literature. Similar questions have also arisen with regard to the magnitude of backreaction modulated by the effect of shear between overdense and underdense regions [48]. Nevertheless arguments in favour of backreaction seem rather compelling [49]. While upcoming observations may ultimately decide whether backreaction from density inhomogeneities drives the present acceleration, the above studies [40, 50, 42, 43, 49, 44, 45] have highlighted that backreaction could be a crucial ingredient of the present evolution and future fate of our Universe. In this thesis we have not restricted ourselves to exploring the possibility of backreaction producing accelerated expansion, rather we have tried to find out how backreaction can influence the evolution of the Universe once acceleration sets in. Specifically, we have also explored the impact of the event horizon on cosmological backreaction [51]. The presently accelerating epoch dictates the existence of an event horizon since the transition from the previously matter dominated decelerating expansion. Since backreaction is evaluated from the global distribution of

matter inhomogeneities, the event horizon demarcates the spatial regions which are causally connected to us and hence impact the evolution of our part of the Universe. Any contribution from inhomogeneities of scales which cross outside the event horizon due to accelerated expansion, needs to be excluded while computing the overall impact of backreaction. Such an approach had remained unexplored in previous studies of backreaction. We were able to show that backreaction with the event horizon could lead to a surprising possibility of transition to another decelerated future era. We further make a comprehensive analysis of our model, that includes the event horizon, and compare our results with a standard model of backreaction, one that does not include the event horizon. We also make an extension of this study by considering the Universe to be divided into multiple subdomains, and letting each subdomain evolve independently of each other, with the aim of recreating the real Universe much better than in our previous model, and then study the impact of backreaction in the future evolution of the Universe.

1.3 OUTLINE OF THESIS

In Chapter 2 we first briefly outline the basics of the standard Big Bang model of cosmology based on the FRW metric and the evolution equations mentioned here will be used in our work based on k -essence. Here we also give an introduction on the mechanism behind scalar field driven inflationary expansion in the early Universe along with a description of the problems present in the standard model that inflation helps to solve. Later we describe how a traditional scalar field, like quintessence, can give rise to the late time acceleration.

In Chapter 3 we first describe the general framework for k -essence scalar field models and write down the equation of motion and the energy momentum tensor for such cases. Our work on k -essence deals with the flat FRW metric but wherever possible we present the framework equations without assuming any prior metric of the Universe. Further in Section 3.2 we present the framework for an important sub-class of k -essence models, namely purely kinetic k -essence models, and also highlight a very interesting solution for this class of models, one that forms an integral part of our work based on k -essence. In Section 3.3 we will present an important result, that was demonstrated in [10], whereby we show that a purely kinetic k -essence model leads to a static universe when the late-time energy density of the universe is expressed simply as a sum of a cosmological constant and a

dark matter term. We then develop our k -essence model in Section 3.4, that was presented in [10], which contains both a potential and a non-canonical kinetic term for the scalar field, but where it is possible to use a part of the formalism of [34]. We show that our model allows for inflation in the early universe and behaves as purely kinetic k -essence at late times and reproduces a cosmological constant and a dark matter term in the energy density of the Universe. In order to discuss the viability of our model, we further provide estimates of the values of the model parameters that could be obtained from observational constraints.

In Chapter 4 we highlight our work that was presented in the paper [11]. Here we use a form of the k -essence Lagrangian that has been the most widely used [12, 6, 52]. Our motivation is the reproduction of the features of inflation in the early Universe, and also generating dark matter and dark energy at late times. We find that after the early expansion is over, our model can be approximated as kinetic k -essence, i.e., the dynamics becomes dominated by only the kinetic component of the scalar field. We show that the late time energy density reproduces a cosmological constant and a matter like term which we call dark matter. We then consider observational results from the both the early and late eras, which are used to put constraints on the parameters of this model.

In Chapter 5 we present the Buchert framework [40, 41, 53, 50] for studying cosmological backreaction. Besides showing the evolution equations in this framework we also present an interesting aspect of it, called the “morphon” field, which shows that the effects of inhomogeneities in the Universe can be effectively described through a scalar field, and thus provides a realistic source for all the numerous scalar field based models that try to explain dark energy. Further we will show that this morphon field can also be treated as a k -essence field.

In Chapter 6 we will illustrate, using a simple two-scale model, how the Universe evolves in the future by considering the effects of backreaction from inhomogeneities. We will first describe the evolution of the Universe by using the unmodified Buchert framework equations but later on we will take into consideration the effect of the event horizon, which inevitably forms once the Universe enters the accelerated expansion phase. For the latter part we will describe two approaches that were presented in [51] and [54]. We will then compare the evolution of the Universe between the case where we include the event horizon in our calculations and for the case where we don’t consider the event horizon.

In Chapter 7 we will extend our previous model and consider the effects of backreaction on the future evolution of the Universe by assuming the Universe to be partitioned into multiple subdomains, each evolving differently to each other.

Finally we summarize and conclude our work in Chapter 8 with a brief description of possible future areas of work.

CHAPTER 2

PRIMARY FRAMEWORK

2.1 BASICS OF FRW COSMOLOGY

Here we will give a brief review of the basics of FRW cosmology that are mainly required for the chapters on k -essence, but are also helpful when we are dealing with the Buchert framework of backreaction.

We will work with the FRW metric with signature $(+, -, -, -)$ which is written as (by taking the speed of light $c = 1$)

$$ds^2 = dt^2 - a^2(t) \left[\frac{dr^2}{1 - kr^2} + r^2 d\theta^2 + r^2 \sin^2 \theta d\phi^2 \right], \quad (2.1)$$

where $a(t)$ is the scale factor with cosmic time t , k is the curvature parameter and the coordinates r , θ and ϕ are known as comoving coordinates. A freely moving particle comes to rest in these coordinates. The constant k in the metric describes the geometry of the spatial section of space-time, with closed, flat and open universes corresponding to $k = +1, 0, -1$, respectively.

2.1.1 EVOLUTION EQUATIONS

We will consider an ideal perfect fluid as the source of the energy-momentum tensor, which is homogeneous and isotropic in its rest frame and which therefore coincides with the comoving reference frame of the metric. For this the energy-momentum tensor has the form

$$T_{\nu}^{\mu} = \text{Diag} (\rho, -p, -p, -p), \quad (2.2)$$

where ρ is the energy density and p is the pressure of the fluid. We therefore get from the Einstein equations two independent equations

$$H^2 \equiv \left(\frac{\dot{a}}{a}\right)^2 = \frac{8\pi G}{3}\rho - \frac{k}{a^2}, \quad (2.3)$$

$$\frac{\ddot{a}}{a} = -\frac{4\pi G}{3}(\rho + 3p), \quad (2.4)$$

where H is the Hubble parameter. Equation (2.3) is known as the Friedmann equation and we call (2.4) the acceleration equation. From equation (2.4) we see that accelerated expansion occurs for $\rho + 3p < 0$. The energy-momentum tensor is conserved by virtue of the Bianchi identities, leading to the continuity equation

$$\dot{\rho} + 3H(\rho + p) = 0. \quad (2.5)$$

We can rewrite (2.3) in the form

$$\Omega(t) - 1 = \frac{k}{(aH)^2}, \quad (2.6)$$

where $\Omega(t) = \rho(t)/\rho_c(t)$ is the dimensionless density parameter and $\rho_c(t) = 3H^2/8\pi G$ is the critical density. The matter distribution clearly determines the spatial geometry of our universe, i.e.,

$$\Omega > 1 \quad \text{or} \quad \rho > \rho_c \quad \rightarrow \quad k = +1, \quad (2.7)$$

$$\Omega = 1 \quad \text{or} \quad \rho = \rho_c \quad \rightarrow \quad k = 0, \quad (2.8)$$

$$\Omega < 1 \quad \text{or} \quad \rho < \rho_c \quad \rightarrow \quad k = -1. \quad (2.9)$$

Observations have shown that the current universe is very close to a spatially flat geometry ($\Omega \simeq 1$).

2.1.2 EVOLUTION OF THE UNIVERSE FILLED WITH A PERFECT FLUID

The Universe is considered to be filled by a barotropic perfect fluid with which we can associate an equation of state parameter w that is defined as

$$w = \frac{p}{\rho}. \quad (2.10)$$

If we now assume w to be a constant then on solving eqns. (2.3) and (2.4) with $k = 0$ we get

$$H = \frac{2}{3(1+w)(t-t_0)}, \quad (2.11)$$

$$a(t) \propto (t-t_0)^{\frac{2}{3(1+w)}}, \quad (2.12)$$

$$\rho \propto a^{-3(1+w)}, \quad (2.13)$$

where t_0 is a constant. The above solution is valid for $w \neq -1$. For a radiation dominated universe we have $w = 1/3$ and for a dust dominated universe we have $w = 0$. For these two cases we have

$$\text{Radiation: } a(t) \propto (t-t_0)^{1/2}, \quad \rho \propto a^{-4}, \quad (2.14)$$

$$\text{Dust: } a(t) \propto (t-t_0)^{2/3}, \quad \rho \propto a^{-3}. \quad (2.15)$$

Both cases correspond to a decelerated expansion of the universe. From (2.4) we see that in order to have accelerated expansion the equation of state is given by

$$w < -1/3. \quad (2.16)$$

So whatever acts as dark energy it must have an equation of state that satisfies the above condition. For a cosmological constant Λ we have $w = -1$, which gives rise to a constant energy density $\rho_\Lambda = \Lambda/8\pi G$ and consequently the Hubble parameter also has a constant value of $H = \sqrt{\Lambda/3}$. The expression for the scale-factor in this case comes out as

$$a(t) \propto e^{Ht}. \quad (2.17)$$

So far we have restricted our attention to the equation of state: $w \geq -1$. Recent observations suggest that the equation of state which is less than -1 can be also allowed [55]. This specific equation of state corresponds to a phantom (ghost) dark energy [17] component and requires a separate consideration. We first note that

Eq. (2.12) describes a contracting universe for $w < -1$. There is another expanding solution given by

$$a(t) = (t_s - t)^{\frac{2}{3(1+w)}}, \quad (2.18)$$

where t_s is a constant. This corresponds to a super-inflationary solution where the Hubble rate and the scalar curvature grow:

$$H = \frac{n}{t_s - t}, \quad n = -\frac{2}{3(1+w)} > 0, \quad (2.19)$$

$$R = 6 \left(2H^2 + \dot{H} \right) = \frac{6n(2n+1)}{(t_s - t)^2}. \quad (2.20)$$

The Hubble rate diverges as $t \rightarrow t_s$, which corresponds to an infinitely large energy density at a finite time in the future. The curvature also grows to infinity as $t \rightarrow t_s$. Such a situation is referred to as a Big Rip singularity [56]. This cataclysmic conclusion is not inevitable in these models, and can be avoided in specific models of phantom fields with a top-hat potential. It should also be emphasized that we expect quantum effects to become important in a situation when the curvature of the universe becomes large.

2.2 INFLATION IN THE EARLY UNIVERSE

2.2.1 MOTIVATION FOR INFLATION

In the standard Big-Bang model the Universe is taken to be radiation dominated at early times, matter dominated at late-times and as we now know there is a very late transition to dark energy domination. This picture of the Universe has met with a great deal of success and satisfies a variety of observational data, but we may still ask whether the initial conditions that give rise to this Universe are natural. Typically as physicists we look for laws of nature, and imagine that we are free to specify initial conditions and ask how they evolve under such laws. But the Universe seems to have only one set of initial conditions and it seems sensible to wonder if they are relatively generic or finely tuned. At least two features of the Universe seem highly non-generic: its spatial flatness, and its high degree of homogeneity and isotropy. It might be that these conditions are more likely than they appear at first

and there is some dynamical mechanism that can take a wide spectrum of initial conditions and evolve them towards spatial flatness and homogeneity/isotropy. The inflationary universe scenario provides such a mechanism and has become a central organizing principle of modern cosmology, even if we still have not found concrete proof of its existence (See [57] for details on inflation).

Before describing the basics of the inflationary mechanism we will highlight some of the problems that inflation claims to solve.

2.2.1.1 FLATNESS PROBLEM

As we saw in (2.6), we can rewrite the Friedmann equation (2.3) using the density parameter Ω in the following way,

$$\Omega - 1 = \frac{k}{a^2 H^2}. \quad (2.21)$$

For a flat Universe ($k = 0$), we have $\Omega = 1$. If the Universe is flat then it will remain so for all time, otherwise the density parameter simply evolves. The flatness problem is simply that the combination aH is a decreasing function of time for a matter or radiation dominated Universe. For example, for a nearly flat matter dominated Universe we have $|1 - \Omega| \propto t^{2/3}$ and for a nearly flat radiation dominated Universe we have $|1 - \Omega| \propto t$. From observations we know that at present Ω_0 is not very different from unity, at least not more than an order of magnitude. This implies that at earlier times Ω must have been extremely close to unity. To obtain our present Universe, for example at nucleosynthesis which occurred when the Universe was around 1s old, we would need to have

$$|\Omega(t_{nuc}) - 1| \lesssim 10^{-16}. \quad (2.22)$$

At earlier times Ω must have been still more closer to 1. The flatness problem states that such finely tuned initial conditions are extremely unlikely. Almost all initial conditions lead either to a closed Universe that recollapses almost immediately, or to an open Universe that quickly enters the curvature dominated regime and cools below 3K within one second of its existence. For this reason the flatness problem is also sometimes called the age problem – how did our universe get to be so old?

2.2.1.2 HORIZON PROBLEM

In FRW cosmology we have particle horizons, because there is a finite amount of time since the Big Bang singularity and therefore a photon (or a particle traveling at the speed of light) can only travel a finite distance. The horizon problem is simply the fact that the CMB is homogeneous and isotropic to a high degree of precision even though widely separated points on the last scattering surface are completely outside each other's horizons, which imply that there could have been no causal contact between the various regions and thus how homogeneity arose is a mystery.

2.2.1.3 RELIC PARTICLE ABUNDANCES

We know that radiation density reduces with expansion of the Universe as $1/a^4$, therefore if the Universe starts with a very small amount of non-relativistic matter then its slower reduction in density will rapidly bring it to prominence. Particles in the Standard Model of particle interactions don't lead to any problems, because they interact strongly with radiation and thermalization stops them from becoming too prominent. But modern particle physics predicts other particles. The most crucial in originally motivating inflation was a type of particle called magnetic monopole. It is predicted that they were produced in abundance at a very early stage in the Universe, and are also expected to be extraordinarily massive. Such particles would be non-relativistic for almost all the Universe's history, giving them plenty of time to come to dominate over radiation. Since we know the Universe is not dominated by magnetic monopoles now, theories predicting them are incompatible with the standard Big Bang model. While magnetic monopoles were relic particles thought most important at the time inflation was conceived, there are now several other kinds of relic particles also speculated to exist which would cause similar problems.

2.2.2 HOW INFLATION HELPS

Inflationary cosmology is not a modification of the Hot Big Bang model but rather it is an add-on that tries to solve some of the problems associated with this model at early times without disturbing any of its successes. The idea of inflation was first proposed by Alan Guth in 1981 [59] (See also Ref. [60]). The precise defin-

ition of inflation is simply any epoch in which the scale-factor of the Universe is accelerating, i.e.

$$\ddot{a} > 0.$$

There is an equivalent alternative expression of the condition of inflation that gives it a more physical meaning

$$\frac{d}{dt} \frac{1}{aH} < 0. \quad (2.23)$$

Since $1/aH$ is the comoving Hubble length the condition for inflation is that this length decreases with time. Viewed in coordinates fixed with the expansion, the observable Universe actually becomes smaller during inflation because the characteristic scale occupies a smaller and smaller size as inflation proceeds.

If inflation occurs then all the aforementioned problems of the Big Bang model can be solved. The flatness problem is solved because the condition for inflation (2.23) is precisely the condition that drives Ω to 1. The horizon problem can be solved because of the dramatic reduction of the comoving Hubble length during inflation which allows our present observable Universe to originate from a tiny region that was well inside the Hubble radius early on during inflation. The dramatic expansion of the inflationary era dilutes away any unfortunate relic particles because their density is reduced by the expansion more quickly than the other components. Provided enough expansion occurs this dilution can make sure that these particles are not observed today.

2.2.3 BASICS OF INFLATION MECHANISM

The most straightforward way to obtain inflation in the early universe is to use the vacuum energy provided by the potential of a scalar field, the “inflaton”. The energy density and pressure of this homogeneous scalar field $\phi \equiv \phi(t)$ is

$$\rho = \frac{1}{2} \dot{\phi}^2 + V(\phi), \quad (2.24)$$

$$p = \frac{1}{2} \dot{\phi}^2 - V(\phi). \quad (2.25)$$

The term $V(\phi)$ is the potential of the scalar field, which may be derived from some particle physics motivation. Different inflationary models correspond to dif-

ferent choices of the potential. The equations of motion can be obtained by directly substituting these relations into the Friedmann and continuity equations. Assuming a spatially flat Universe we obtain

$$H^2 = \frac{8\pi G}{3} \left[\frac{1}{2} \dot{\phi}^2 + V(\phi) \right], \quad (2.26)$$

$$\ddot{\phi} + 3H\dot{\phi} + \frac{dV}{d\phi} = 0. \quad (2.27)$$

Inflation can occur if the evolution of the field is sufficiently gradual that the potential energy dominates the kinetic energy and the second derivative of ϕ is small enough for this state of affairs to be maintained for a sufficient period. Thus we want

$$\dot{\phi}^2 \ll V(\phi),$$

$$|\ddot{\phi}| \ll |3H\dot{\phi}|, |V'|.$$

This assumption is called the “slow-roll” approximation and under this the equations of motion can now be written as

$$H^2 \simeq \frac{8\pi G}{3} V(\phi), \quad (2.28)$$

$$3H\dot{\phi} \simeq -V'(\phi), \quad (2.29)$$

where $V' = dV/d\phi$. For this approximation to be valid it is necessary for two conditions to hold. These are

$$\epsilon(\phi) \ll 1, \quad |\eta(\phi)| \ll 1, \quad (2.30)$$

where the “slow-roll parameters” ϵ and η are defined by

$$\epsilon = \frac{1}{16\pi G} \left(\frac{V'}{V} \right)^2, \quad (2.31)$$

$$\eta = \frac{1}{8\pi G} \left(\frac{V''}{V} \right). \quad (2.32)$$

Note that $\epsilon \geq 0$ while η can have either sign. Also note that these definitions are not universal as some people like to define them in terms of Hubble parameter rather than the potential. The slow-roll parameters make it easy to see where inflation might occur on a given potential. For example for $V(\phi) = m^2\phi^2/2$, they are satisfied when provided that $\phi^2 > 1/4\pi G$. For such a potential inflation proceeds until the scalar fields gets too close to the minimum for the slow-roll conditions to be maintained, and inflation comes to an end.

The amount of inflation that occurs is quantified by the ratio of the scale-factor at the final time to its value at some initial time. Since this is typically a large quantity a logarithm is taken to give the number of e-foldings N :

$$N(t) \equiv \ln \frac{a(t_{end})}{a(t)}, \quad (2.33)$$

where t_{end} is the time at the end of inflation. This measures the amount of inflation that still has to occur after time t , with N decreasing to zero at the end of inflation. To solve the horizon and flatness problem around 60 - 70 e-foldings of inflation are required. For most purposes, the only knowledge we need is how much more inflation will occur from a given scalar field value ϕ , rather than from a given time. This can be calculated immediately via the slow-roll approximation without any need to solve the equations of motion for the expansion:

$$N \equiv \ln \frac{a(t_{end})}{a(t)} = \int_t^{t_{end}} H dt \simeq 8\pi G \int_{\phi}^{\phi_{end}} \frac{V}{V'} d\phi, \quad (2.34)$$

where ϕ_{end} is defined by $\epsilon(\phi_{end}) = 1$, if inflation ends through the violation of the slow-roll conditions.

2.3 LATE-TIME ACCELERATION USING SCALAR FIELDS

The cosmological constant corresponds to a fluid with a constant equation of state $w = -1$. The current observed energy density attributed to the cosmological constant is not only much smaller than what is expected from order-of-magnitude estimates based on the quantum theory of fields, but is only a few times greater than the present matter density. If we explain dark energy with the help of the cosmological constant then it means that it will behave as a fluid with a constant equation of state and energy density. But observations say little about the time evol-

ution of the equation of state of dark energy, therefore we can consider the scenario where the equation of state of dark energy changes with time, such as in inflationary cosmology. Scalar fields naturally arise in particle physics including string theory and these can act as candidates for dark energy. So far a wide variety of scalar field dark energy models have been proposed. These include quintessence, phantoms, k -essence, tachyon, ghost condensates and dilatonic dark energy amongst many. Below we will describe with the help of a simple quintessence model how late-time acceleration can be achieved.

We will consider an ordinary scalar field ϕ that is minimally coupled to gravity and an unspecified potential $V(\phi)$ (See [58, 4] for details). The action for this quintessence field is given by

$$S = \int d^4x \sqrt{-g} \left[\frac{1}{2} \partial_\mu \phi \partial^\mu \phi - V(\phi) \right]. \quad (2.35)$$

For a flat FRW metric the equation of motion of this field comes out as

$$\ddot{\phi} + 3H\dot{\phi} + \frac{dV}{d\phi} = 0. \quad (2.36)$$

and the energy density and pressure of the field are obtained to be

$$\rho = \frac{1}{2} \dot{\phi}^2 + V(\phi), \quad p = \frac{1}{2} \dot{\phi}^2 - V(\phi). \quad (2.37)$$

Using these values in (2.3) and (2.4) we get

$$H^2 = \frac{8\pi G}{3} \left[\frac{1}{2} \dot{\phi}^2 + V(\phi) \right], \quad (2.38)$$

$$\frac{\ddot{a}}{a} = -\frac{8\pi G}{3} \left[\dot{\phi}^2 - V(\phi) \right]. \quad (2.39)$$

From the above equation it is clear that the Universe accelerates for $\dot{\phi}^2 < V(\phi)$. This means that one requires a flat potential to give rise to an accelerated expansion. The original and simplest example of a quintessence potential is of the type

$$V(\phi) = \frac{M^{4+\alpha}}{\phi^\alpha}, \quad (2.40)$$

where α is a positive number and M is a constant with the unit of mass (taking $\hbar = c = 1$), which gives $V(\phi)$ the dimensions of an energy density. We need to match the energy density of the field to the current critical energy density, that is

$$\rho_0 \approx m_{Pl}^2 H_0^2 \approx 10^{-48} (\text{GeV})^4. \quad (2.41)$$

The mass squared of the field ϕ is given by $m_\phi^2 = \frac{d^2 V}{d\phi^2} \approx \rho/\phi^2$, whereas the Hubble expansion rate is given by $H^2 \approx \rho/m_{Pl}^2$. The universe enters a tracking regime in which the energy density of the field catches up that of the background fluid when m_ϕ^2 decreases to of order H^2 . This shows that the field value at present is of order the Planck mass ($\phi_0 \sim m_{Pl}$), which is typical of most of the quintessence models. Since $\rho_0 \approx V(\phi_0)$, we obtain the mass scale

$$M = (\rho_0 m_{Pl}^\alpha)^{\frac{1}{4+\alpha}}. \quad (2.42)$$

This then constrains the allowed combination of α and M . For example the constraint implies $M = 1$ GeV for $\alpha = 2$. This energy scale can be compatible with the one in particle physics, which means that the severe fine-tuning problem of the cosmological constant is alleviated. Nevertheless a general problem we always have to tackle is finding such quintessence potentials in particle physics.

PART II

SCALAR FIELD APPROACH USING *k*-ESSENCE

CHAPTER 3

UNIFYING INFLATION, DARK ENERGY AND DARK MATTER USING k -ESSENCE

3.1 EQUATION OF MOTION OF k -ESSENCE

For our work in k -essence we will work with a flat FRW metric so that $k = 0$. For such a metric the corresponding Einstein field equations (2.3) and (2.4) are

$$H^2 \equiv \left(\frac{\dot{a}}{a}\right)^2 = \frac{8\pi G}{3}\rho, \quad (3.1)$$

$$\frac{\ddot{a}}{a} = -\frac{4\pi G}{3}(\rho + 3p), \quad (3.2)$$

where ρ is the energy density of the perfect fluid that is considered to fill up the Universe, and p is its pressure. We consider the k -essence field to be minimally coupled to the gravitational field and the k -essence action looks like

$$S_k = \int d^4x \sqrt{-g} \mathcal{L}(\phi, X), \quad (3.3)$$

where ϕ is the k -essence scalar field and X is the kinetic term that is defined as

$$X = \frac{1}{2} \partial_\mu \phi \partial^\mu \phi. \quad (3.4)$$

To preserve the condition of homogeneity and isotropy of the scalar field we must have $\phi = \phi(t)$. So we get the value of X as

$$X = \frac{1}{2}g^{00}\partial_0\phi\partial_0\phi = \frac{1}{2}\dot{\phi}^2. \quad (3.5)$$

The k -essence Lagrangian \mathcal{L} can be any function of the scalar field and X . Traditional scalar field theories, such as quintessence [5], always contained terms that were linear in X , so in a way X can be called the canonical kinetic term. What makes k -essence special is that here the Lagrangian can contain terms that are non-linear in X . The total action describing the dynamics of k -essence and General Relativity is the sum of S_k and the Einstein-Hilbert action:

$$S = \int d^4x \sqrt{-g} \left[-\frac{1}{16\pi G} R + \mathcal{L}(\phi, X) \right], \quad (3.6)$$

where R is the Ricci scalar. If we now vary the action (3.3) with respect to the metric $g_{\mu\nu}$, then we get the energy-momentum tensor of the k -essence field as

$$T_{\mu\nu} = \frac{2}{\sqrt{-g}} \frac{\delta S_k}{\delta g^{\mu\nu}} = \frac{\partial \mathcal{L}}{\partial X} \nabla_\mu \phi \nabla_\nu \phi - g_{\mu\nu} \mathcal{L}, \quad (3.7)$$

where ∇_μ denotes the covariant derivative associated with the metric $g_{\mu\nu}$. Now the k -essence scalar field can be treated as a perfect fluid and for such a case $T_{\mu\nu}$ is of the form

$$T_\nu^\mu = \text{Diag}(\rho, -p, -p, -p), \quad (3.8)$$

where $p = -\frac{1}{3}T_i^i$ is the pressure and is given by the Lagrangian density, $p = \mathcal{L}(\phi, X)$, and the energy density $\rho = T_0^0$ is

$$\rho = 2X \frac{\partial \mathcal{L}}{\partial X} - \mathcal{L}. \quad (3.9)$$

For such a perfect fluid it is conventional to introduce the equation of state parameter w , that is defined as

$$w \equiv \frac{p}{\rho}. \quad (3.10)$$

This definition of w characterises intrinsic properties of k -essence in a coordinate independent way. We can also define an adiabatic sound speed associated with the k -essence fluid, which gives us the speed at which perturbations travel. It is defined as [61]

$$c_s^2 \equiv \frac{\partial p / \partial X}{\partial \rho / \partial X}. \quad (3.11)$$

Note that this definition is different from the usual definition of the adiabatic sound speed (namely, $c_s^2 = \frac{dp}{d\rho}$). However, it has been shown recently [62] that perturbations in such models travel with a speed defined as above, where the authors also define this to be the “phase speed.”

The equation of motion of the k -essence scalar field is given by either varying the Lagrangian with respect to ϕ or inserting the values of ρ and p in the continuity equation (2.5). Doing so we get

$$\ddot{\phi} \frac{\partial \rho}{\partial X} + 3\dot{\phi} H \frac{\partial p}{\partial X} + \frac{\partial \rho}{\partial \phi} = 0. \quad (3.12)$$

Usually k -essence models are restricted to the Lagrangian density of the form

$$\mathcal{L} = F(X)V(\phi), \quad (3.13)$$

which is the most widely studied form and was in fact first proposed in the paper on k -inflation [12]. Another well known variation is of the type $\mathcal{L} = F(X) + V(\phi)$ which has previously been studied in the context of k -essence models in [63] and its properties have been discussed in some detail in [64]. But the important point to note is that the k -essence Lagrangian can in fact be any function of ϕ and X .

3.2 PURELY KINETIC k -ESSENCE

For purely kinetic k -essence the Lagrangian, as the name suggests, will only be a function of the kinetic term X and does not explicitly depend on the field ϕ . We can therefore write the Lagrangian as

$$\mathcal{L} = F(X). \quad (3.14)$$

The energy density ρ (3.9) will therefore be

$$\rho = 2XF_X - F, \quad (3.15)$$

where $F_X = dF/dX$. Now the equation of motion (3.12) of kinetic k -essence field is

$$(F_X + 2XF_{XX})\ddot{\phi} + 3HF_X\dot{\phi} = 0, \quad (3.16)$$

where $F_{XX} = d^2F/dX^2$. If this equation is rewritten in terms of X then it turns out to be

$$(F_X + 2XF_{XX})\dot{X} + 6HF_XX = 0. \quad (3.17)$$

This can be integrated exactly [34] to give the solution

$$\sqrt{X}F_X = ka^{-3}, \quad (3.18)$$

where k is a constant of integration. This solution was previously derived in a slightly different form in [52]. Given any form of $F(X)$ Eq. (3.18) gives the evolution of X as a function of the scale factor a . This result holds irrespective of the spatial curvature of the universe.

3.3 SIMPLE UNIFICATION USING PURELY KINETIC k -ESSENCE

In this section we will demonstrate that a simple unification of dark energy and dark matter is not possible using purely kinetic k -essence, a result that was presented in our paper [10]. As we saw earlier in Section 3.2, for purely kinetic k -essence the Lagrangian can be written as

$$\mathcal{L} = F(X), \quad (3.19)$$

and for this we have a relation between X and the scale factor a

$$\sqrt{X}F_X = ka^{-3}, \quad (3.20)$$

and the energy density is

$$\rho = 2XF_X - F. \quad (3.21)$$

As the most simple choice for the configuration of the late-time energy density, we express the k -essence energy density as

$$\rho = \lambda + \frac{C_1}{a^3}, \quad (3.22)$$

where the energy density is the sum of a cosmological constant and a matter-like term which we call dark matter. Needless to say, such an expression will hold as the true energy density of the universe after matter domination has begun, i.e., when radiation is a negligible fraction of the total energy density of the universe. Now using (3.20) we can rewrite the energy density in (3.22) in terms of X as

$$\rho = \lambda + \frac{C_1}{k} \sqrt{X} F_X. \quad (3.23)$$

By equating (3.21), that is the standard form of the energy density for a purely kinetic k -essence model, with (3.23) we get a differential equation for F given by

$$\frac{F_X}{\lambda + F} = \frac{1}{2X - \frac{C_1}{k} \sqrt{X}}. \quad (3.24)$$

On integrating this equation we get

$$F = -\lambda - C_2 \left(C_1 - 2k\sqrt{X} \right), \quad (3.25)$$

with C_2 being an integration constant. Note here that since X and a are related by Eq. (3.20), the constancy of C_2 with respect to X implies constancy of C_2 with respect to a as well. Now, using the relation (3.20) once again to switch back to the variable a in the expression for F in Eq. (3.25), we obtain

$$C_2 = \frac{1}{a^3}. \quad (3.26)$$

Thus, the only solution compatible with the ansatz [Eq. (3.22)] for the energy density is of a constant scale factor a . Such a solution is indeed consistent with the specific form for $F(X)$ in Eq. (3.25) (actually follows from it). However, since this solution is not compatible with an observationally expanding universe, it rules out our assumption of the energy density to be of the form expressed in Eq. (3.22). We must clarify here that we have assumed that the kinetic k -essence energy density to be exactly of the form of (3.22), whereas in [34, 38] the resultant energy density came out to be approximately of the form of (3.22) under certain assumptions. Therefore, using purely kinetic k -essence we cannot hope to unify dark matter & dark energy, at least exactly in the form of (3.22). Nonetheless, our analysis does not rule out other possible functional categorisations of the late-time energy

density through which dark matter and dark energy could possibly emerge. One could also look into other avenues to achieve the unification, and we try to provide such a way with our model that we will present in the next section.

3.4 *k*-ESSENCE MODEL FOR UNIFICATION

Here we will describe the model for unification that was proposed in our paper [10]. We choose our model to have a Lagrangian density of the form

$$\mathcal{L} = F(X) - V(\phi). \quad (3.27)$$

Although not very common but as stated earlier such forms have been discussed previously in [63]. We choose the functional form of F to be

$$F(X) = KX - m_{Pl}^2 L \sqrt{X} + m_{Pl}^4 M, \quad (3.28)$$

where K , L , and M are dimensionless positive constants, m_{Pl} the Planck mass, and keeping with the spirit of *k*-essence, the second term represents the non-canonical correction ($L^2 > 4KM$) to the kinetic energy. Our choice of the form of $F(X)$ is similar to the type considered in Ref. [52]. Additionally, we include a non-vanishing potential $V(\phi)$ given by

$$V(\phi) = \frac{1}{2} m^2 \phi^2. \quad (3.29)$$

In order to make the subsequent analysis more transparent, especially while applying observational constraints on the parameters, we rewrite the kinetic part of our Lagrangian in the form

$$F(X) = B \left(1 - 2A\sqrt{X} \right)^2 - C, \quad (3.30)$$

where A , B and C can be expressed in terms of our original model parameters as

$$A = m_{Pl}^{-2} \frac{K}{L}; \quad B = m_{Pl}^4 \frac{L^2}{4K}; \quad C = m_{Pl}^4 \left(\frac{L^2}{4K} - M \right). \quad (3.31)$$

The energy density corresponding to our model turns out to be

$$\rho = 2XF_X - F + V = B(4A^2X - 1) + C + \frac{1}{2}m^2\phi^2, \quad (3.32)$$

and the pressure is given by

$$p = B(1 - 2A\sqrt{X})^2 - C - \frac{1}{2}m^2\phi^2. \quad (3.33)$$

The Friedmann equation (3.1) in this case can be written as

$$H^2 = \frac{8\pi G}{3} \left(4A^2BX - B + C + \frac{1}{2}m^2\phi^2 \right). \quad (3.34)$$

The equation of motion (3.12) for the scalar field is obtained to be

$$[F_X + 2XF_{XX}] \ddot{\phi} + 3HF_X \dot{\phi} + \frac{dV}{d\phi} = 0, \quad (3.35)$$

which in terms of the parameters can be written as

$$4A^2B\ddot{\phi} + 12HA^2B\dot{\phi} - 6\sqrt{2}HAB + m^2\phi = 0. \quad (3.36)$$

Considering the standard slow-roll approximation for inflation (see Section 2.2 for details on inflation) we initially take the potential to be much larger than the kinetic part, i.e. we have $V(\phi) \gg 2XF_X - F$. Correspondingly the field equation (3.35) approximates to

$$3HF_X \dot{\phi} + \frac{dV}{d\phi} \simeq 0, \quad (3.37)$$

and we can write Eq. (3.34) as

$$H^2 \simeq \frac{8\pi G}{3} \left(\frac{1}{2}m^2\phi^2 \right). \quad (3.38)$$

The slow-roll parameters for this model are given by ($V' = dV/d\phi$ & $V'' = d^2V/d\phi^2$)

$$\epsilon = \frac{1}{16\pi G} \left(\frac{V'}{V} \right)^2 \frac{1}{F_X}, \quad (3.39)$$

$$\eta = \frac{1}{8\pi G} \frac{V''}{V} \frac{1}{F_X^2}. \quad (3.40)$$

It can be seen that the slow-roll parameters for this model are similar to the standard inflationary scenario (see Eqns. (2.31) and (2.32)), the only difference being the extra factors of F_X . To completely identify with the standard case we demand that $F_X \sim O(1)$. Now equating Eqns. (3.37) and (3.38) we obtain

$$\sqrt{X} \simeq \frac{1}{4\sqrt{2}A^2B} \left(-\frac{m}{\sqrt{12\pi G}} + 2\sqrt{2}AB \right), \quad (3.41)$$

showing that for the duration of inflation X and hence F are practically constant. The number of e-folds of expansion is given by

$$\begin{aligned} N &= \int_{t_i}^{t_e} H dt = 8\pi G \int_{\phi_e}^{\phi_i} \frac{V}{V'} F_X d\phi \simeq 4\pi G F_X \frac{\phi_i^2 - \phi_e^2}{2} \\ &= \frac{4\pi G F_X}{m^2} (V_i - V_e), \end{aligned} \quad (3.42)$$

where the subscript ‘ i ’ refers to the beginning of inflation and ‘ e ’ refers to the end. Inflation ends with $\epsilon \sim 1$, leading to

$$\phi_e^2 \simeq \frac{1}{4\pi G F_X}. \quad (3.43)$$

Using this Eq. (3.42) we get

$$V_i \simeq \frac{m^2}{4\pi G F_X} \left(N + \frac{1}{2} \right). \quad (3.44)$$

So far the inflationary scenario in our model is almost indistinguishable from a standard scalar field inflation involving a chaotic quadratic potential. As inflation ends there will be kinetic domination since now the potential decays and becomes gradually negligible. So for the period of kinetic domination, Eq. (3.35) can be approximated as

$$[F_X + 2X F_{XX}] \ddot{\phi} + 3H F_X \dot{\phi} \simeq 0, \quad (3.45)$$

i.e., we effectively recover Eq. (3.16) for kinetic k -essence. So the formalism described in Section 3.2 carries over. Hence, using Eq. (3.20) we get

$$X = \frac{1}{16A^4B^2} \left(2AB + \frac{k}{a^3} \right)^2. \quad (3.46)$$

Then using Eq. (3.32), and keeping in mind that V was now negligible, the energy density at this stage is given by

$$\rho = C + \frac{k}{Aa^3} + \frac{k^2}{4A^2Ba^6}. \quad (3.47)$$

The subsequent evolution of the universe may be described as follows. During the initial period of kinetic domination the third term in Eq. (3.47) dominates. But that term becomes small quickly (compared to the radiation term $\sim a^{-4}$ that we have not written down explicitly here) and a period of radiation domination in the universe ensues. The second term in Eq. (3.47) gains prominence in the epoch of matter domination, and we identify it with dark matter. But as the universe evolves toward the present era the first term begins to dominate and behaves as a cosmological constant giving rise to the observed accelerated expansion of the universe. The equation of state parameter after the end of inflation is found to be

$$w = \frac{\frac{k^2}{4A^2Ba^6} - C}{C + \frac{k}{Aa^3} + \frac{k^2}{4A^2Ba^6}}. \quad (3.48)$$

We outline the values of w over the various epochs, which further supports the above statements:

$$\begin{aligned} w &\approx 1 \text{ after the end of inflation and before radiation domination} \\ w &\approx 0 \text{ during matter domination} \\ w &\rightarrow -1 \text{ as } a \rightarrow \infty \end{aligned}$$

Using Eq. (7) the adiabatic sound speed turns out to be

$$c_s^2 = \frac{1}{\frac{2ABa^3}{k} + 1}. \quad (3.49)$$

From this equation we see that the sound speed gradually becomes zero as the universe expands. In the next section we will show that it is negligible during the era of matter domination and beyond.

3.5 OBSERVATIONAL CONSTRAINTS ON THE MODEL

We have so far seen that the model considered by us reproduces the primary features of early inflation and gives rise to a matter as well as a dark energy component in the later evolution of the universe. The viability of this model depends of course on the possible values of the parameters. We used various observational features of the universe to constrain the parameters of our model. We first discuss the inflationary dynamics of the early universe. The amplitude of density perturbations produced by inflation is given by

$$\delta_H \simeq \frac{H^2}{4\pi^{3/2}\dot{\phi}}, \quad (3.50)$$

which in our model turns out to be

$$\delta_H = 4\sqrt{\frac{2}{3}}G^{3/2}\frac{V^{3/2}}{V'}F_X = \frac{4}{\sqrt{3}}G^{3/2}mF_X\phi^2. \quad (3.51)$$

According to the COBE normalization $\delta_H \sim 2 \times 10^{-5}$. We assume that 60 e-folds of inflationary expansion takes place. From Eq. (3.44) this then gives

$$\phi_i^2 F_X \simeq \frac{60.5}{2\pi G}. \quad (3.52)$$

Hence using this value in Eq. (3.51) we get $m \sim 10^{13} \text{ GeV} = 10^{-6} m_{Pl}$. Using the last equation we find the slow-roll parameters from Eqns. (3.39) and (3.40) to be

$$\epsilon(\phi_i) = \frac{1}{16\pi G} \frac{4}{\phi_i^2 F_X} = \frac{1}{2(N+1/2)} = 7.63 \times 10^{-3}, \quad (3.53)$$

$$\eta(\phi_i) = \frac{1}{8\pi G} \frac{2}{\phi_i^2 F_X^2} = \frac{1}{2(N+1/2)F_X} \sim O(10^{-3}). \quad (3.54)$$

The tensor-to-scalar ratio turns out to be

$$r = 16 \epsilon(\phi_i) = 0.12. \quad (3.55)$$

Similarly, the spectral index is obtained as

$$n_s = 1 - 6\epsilon(\phi_i) + 2\eta(\phi_i) \approx 0.95. \quad (3.56)$$

Furthermore from Eq. (3.44) we see that the initial value of the potential is

$$V_i \approx 10^{65}(\text{GeV})^4 \ll m_{Pl}^4 = 10^{76}(\text{GeV})^4, \quad (3.57)$$

showing that classical physics remains valid at the beginning of inflation. All the above calculated parameters are of the same magnitude as one would get in a standard model of inflation based on a quadratic chaotic potential. Knowing the value of m we can also estimate the magnitude of the kinetic component during inflation, from Eq. (3.41) to be

$$X = \frac{1}{2}\dot{\phi}^2 \approx 10^{62}(\text{GeV})^4. \quad (3.58)$$

We could estimate the above value because we had assumed that $F_X \sim O(1)$. In view of Eq. (46) and also since $F_X = 4A^2B - \frac{2AB}{\sqrt{X}}$, this assumption leads to

$$K = 4A^2B \sim O(1), \quad (3.59)$$

where we have used Eq. (3.31) in the first equality. When inflation ends then using Eq. (3.43) and the value of m we see that

$$V_e = \frac{m^2}{8\pi GF_X} \approx 10^{62}(\text{GeV})^4 \approx X. \quad (3.60)$$

Thereafter, the magnitude of the potential decreases and the kinetic component begins to dominate, and as we saw from Eq. (3.47) when there is full kinetic domination it will fall off as a^{-6} , quickly paving the way for a radiation dominated universe. After the end of inflation the field ϕ continues to roll down in the absence of any minimum in the potential. Thus reheating could take place only through gravitational particle production. Standard calculations [65, 66] gives the density of particles produced at the end of inflation as

$$\rho_R \sim 0.01gH_e^4 = 0.01g \left(\frac{8\pi G}{3} V_e \right)^2 = 0.01g \left(\frac{m^2}{3F_X} \right)^2, \quad (3.61)$$

where g is the number of fields which produce particles at this stage, likely to be between 10 and 100. The relative densities turns out to be

$$\frac{\rho_R}{\rho_\phi} = 0.01g \left(\frac{m^2}{3F_X} \right)^2 \frac{8\pi GF_X}{m^2} = 7.71 \times 10^{-14} \frac{g}{F_X}. \quad (3.62)$$

The numerical value of the radiation density is

$$\rho_R \simeq 8.46 \times 10^{49} \frac{g}{F_X^2} (\text{GeV})^4, \quad (3.63)$$

which if immediately thermalized will give rise to temperature

$$T_e \simeq \frac{3.03 \times 10^{12}}{F_X^{1/2}} \left(\frac{g}{g_*} \right)^{1/4} \text{GeV}, \quad (3.64)$$

where g_* is the total number of species in the thermal bath and maybe somewhat higher than g . We assume that immediately after the end of inflation there is complete kinetic domination so that $\rho_\phi \propto 1/a^6$. Then we get

$$\frac{\rho_R}{\rho_\phi} \propto a^2. \quad (3.65)$$

Hence from Eq. (3.62) we see that the universe has to expand by a factor of about 10^6 to 10^7 after the end of inflation to become radiation dominated and at which stage the temperature which goes as $T \propto 1/a$ is given by

$$T \simeq \frac{3.03 \times 10^5}{F_X^{1/2}} \text{GeV}. \quad (3.66)$$

So we see that radiation domination sets in comfortably before nucleosynthesis. But the above expression needs some correction to allow for the period between the end of inflation, when $\rho_\phi \propto 1/a^2$, and complete kinetic domination, i.e., when $\rho_\phi \propto 1/a^6$. Although this will reduce the temperature at the onset of radiation domination it will still be high enough for a successful nucleosynthesis, during which a temperature of around 1 MeV is sufficient.

So far we have examined the dynamics of the inflationary era. We now try to impose constraints on the model from the matter dominated era and the present epoch. We have already shown in Eq. (3.47) what the late-time energy density of the universe will be. Observations require that the current magnitude of a cosmological constant be about $10^{-12}(\text{eV})^4$. So we must have

$$C \simeq 10^{-48}(\text{GeV})^4. \quad (3.67)$$

Further, since the current dark matter density is about one-third that of dark energy, one has

$$\frac{C}{3} \simeq \frac{k}{Aa_0^3}, \quad (3.68)$$

the subscript “0” signifying the present epoch. Observations tell us that the fraction of the present total energy density of the universe contained in radiation is $(\Omega_R)_0 \simeq 5 \times 10^{-5}$ and that contained in dark energy is $(\Omega_{DE})_0 \simeq 0.73$. The present radiation density of the universe is thus $(\rho_R)_0 = \frac{(\Omega_R)_0}{(\Omega_{DE})_0} C \simeq 6.94 \times 10^{-53} (\text{GeV})^4$. We denote the third term in (3.47) as ρ_k . It is known that nucleosynthesis occurs at a redshift of $z \sim 10^{10}$. We assume that ρ_R crosses over ρ_k at a redshift of $z \sim 10^{12}$. We then get

$$z^2 \simeq \frac{4A^2 B a_0^6}{k^2} (\rho_R)_0 = 4 \frac{9}{C^2} B (\rho_R)_0. \quad (3.69)$$

Thus one obtains a lower bound on the parameter B given by

$$B \geq 4 \times 10^{-22} (\text{GeV})^4. \quad (3.70)$$

Now using Eq. (3.59) we obtain an upper bound on parameter A given by

$$A \leq 10^{10} (\text{GeV})^{-2}. \quad (3.71)$$

Using the limiting values for the parameters it is found that the crossover between the dark matter density and ρ_k occurred at a redshift of $z \sim 10^9$, and that between dark matter and radiation occurs at a redshift of $z \sim 10^4$, i.e., at the epoch of matter-radiation equality. We also find that the present value of ρ_k is

$$(\rho_k)_0 = \frac{k^2}{4A^2 B a_0^6} \simeq 6.94 \times 10^{-77} (\text{GeV})^4, \quad (3.72)$$

and the adiabatic sound speed at the epoch of matter-radiation equality (at a redshift of about 10^4) is

$$(c_s^2)_{eq} = \frac{1}{\frac{2ABa_{eq}^3}{k} + 1} \simeq \frac{1}{\frac{6B}{Cz_{eq}^3} + 1} \simeq 4.1 \times 10^{-16}. \quad (3.73)$$

We can re-express w from Eq. (3.48) in terms of the redshift z . Since ρ_k is negligible compared to the other components, we have

$$w \approx \frac{-C}{C + \frac{k}{Aa^3}} = \frac{-C}{C + \frac{k}{Aa_0^3} (z+1)^3}. \quad (3.74)$$

Thereafter it is possible to find dw/dz . Its value at the current epoch, i.e., at redshift $z = 0$ using the above limiting values of A and B from Eqns. (3.70), (3.71) turned out to be

$$\left(\frac{dw}{dz}\right)_{z=0} \approx 2.733 \times 10^{-28}. \quad (3.75)$$

On the other hand, observations suggest that inflation ends at a redshift of about $z \sim 10^{28}$. As we saw in the analysis on inflationary dynamics, radiation comes to dominate the kinetic energy density of the scalar field after the universe has expanded by about 10^6 to 10^7 after the end of inflation. Assuming that ρ_R crosses over ρ_k at a redshift of 10^{20} , and proceeding as before for obtaining Eq. (3.70), in this case we obtain an upper bound on the parameter B ,

$$B \leq 4 \times 10^{-6} (\text{GeV})^4, \quad (3.76)$$

and then a corresponding lower bound on the parameter A [using (3.59)] given by

$$A \geq 250 (\text{GeV})^{-2}. \quad (3.77)$$

Using these set of limiting values we find that the crossover between dark matter and ρ_k occurred at a redshift of about 10^{14} , whereas that between dark matter and radiation remained the same as in the earlier case. In this case $(\rho_k)_0$ and $(c_s^2)_{eq}$ are given by

$$(\rho_k)_0 \simeq 6.94 \times 10^{-93} (\text{GeV})^4, \quad (3.78)$$

$$(c_s^2)_{eq} \simeq 4.1 \times 10^{-32}. \quad (3.79)$$

If we use the limiting values of A and B from Eqns. (3.76) and (3.77) in the dw/dz relation obtained from Eq. (3.74), we get

$$\left(\frac{dw}{dz}\right)_{z=0} \approx 1.281 \times 10^{-45}. \quad (3.80)$$

One can also estimate the current value of the equation of state parameter in our model, which using (3.48) turns out to be

$$w_0 \simeq \frac{-C}{C + \frac{k}{Aa_0^3}} \simeq \frac{-C}{C + C/3} \simeq -0.75. \quad (3.81)$$

It should be noted here that the need to determine the value of k explicitly did not arise in our calculations. Its value can be determined from (3.68), provided we know the values of A and C , i.e., k is not an independent parameter in our model. We can further find out at what redshift the universe starts to accelerate due to the presence of dark energy. Knowing that for acceleration to begin we must have $w = -1/3$, from (3.74) we find

$$z_{acc} \approx 0.817. \quad (3.82)$$

Such a value for the redshift is in fact quite compatible with present observations [67]. Finally, using Eqns. (3.70), (3.71), (3.76), and (3.77), in Eq. (3.31), one finds that the parameter L of our model (3.28) is constrained to lie in the range

$$10^{-49} \leq L \leq 10^{-41}. \quad (3.83)$$

and M has to be tuned to satisfy the last relation in Eq. (3.31). We thus see that for a choice of the parameters $K \sim O(1)$ and L in the range given above it is possible to have a k -essence model that not only unifies dark matter and dark energy but also produces inflation in the early universe as well. Note that the requirement of tuning of one of the parameters, *viz.*, M is to be expected, since this is merely a restatement of the fine-tuning problem associated with the cosmological constant. Further, it may be noted that the coincidence problem of the standard Λ CDM cosmology is retained at a similar level within the present framework. In addition to the tuning of the parameter M , as in the Λ CDM model we have used observations to fix the ratio of Ω_m and Ω_Λ effectively through our Eq. (3.68). Though dark matter and dark energy are generated within a unified framework in this model, the late-time behaviour is quite akin to that of the standard Λ CDM model with its coincidence problem.

3.6 SUMMARY AND DISCUSSION

To summarize, we considered a model of k -essence to study the possibility of producing inflation in the early universe, and subsequently generating both dark matter and dark energy during later evolution in appropriate order. We first showed that it was difficult to unify dark matter and dark energy using purely kinetic k -essence, since the ansatz of a late-time energy density expressed simply as a sum of a cosmological constant and a matter term lead to a static universe. We presented an alternative model including a potential for the scalar field that achieved this unification and also behaved effectively as purely kinetic k -essence at late times. We showed that our model generated inflation in the early universe that reproduced the basic features of the standard chaotic inflation model involving a quadratic potential. At the end of inflation when the potential in our model became negligible in comparison to the kinetic component we were able to approximate the model as purely kinetic k -essence. The expression for the energy density in terms of the scale factor a and also for that of adiabatic sound speed were obtained. We found that the resultant energy density contained terms that achieved the unification of dark matter and dark energy. Current observations quite strongly favour a cosmological constant as the source of dark energy. Our model reproduced a cosmological constant at late times. We then used observational constraints ranging from the inflationary era to the subsequent matter and radiation dominated eras and the present accelerated phase as well, to impose a set of bounds on the model parameters. In this way we could provide an estimate of the relative strengths of the various terms of our model Lagrangian. The value of the current equation of state parameter, and the redshift at which the transition to the accelerated phase occurs, that we estimated, lie within observational bounds. The adiabatic sound speed came out to be close to zero when calculated at the epoch of matter-radiation equality, thus posing no problems for structure formation, since the sound speed decreased further as the scale factor increased.

It should be pointed out that the form of the potential chosen for the model, though widely used for its simplicity, is not very realistic and only serves to highlight the features of the model during the inflationary era. Recent Wilkinson Microwave Anisotropy Probe (WMAP) data analysis [68] suggest that the best fit potential for inflation is a trinomial potential and further study of our model could be made by using such a potential. Moreover, it would be interesting to investigate the relation of our model to the dynamics of another widely used class of k -essence models

where the Lagrangian is taken to be of the type $\mathcal{L} = F(X)V(\phi)$. Finally, since the consideration of non-canonical scalar field kinetics in cosmology was originally motivated by the Born-Infeld [27] action of string theory, and there have been many more recent string theoretic inputs in cosmology such as the idea of the landscape [69], it should be worthwhile to explore the possible origin of generalized non-canonical actions such as ours in the low energy limit of specific string theoretic models.

CHAPTER 4

ANOTHER k -ESSENCE MODEL OF UNIFICATION

In the last chapter we described a k -essence model [10] that reproduced the essential features of inflation, dark matter, and dark energy within a unified framework. The Lagrangian chosen in that model was of the form where the kinetic and potential terms were decoupled in the standard way. However, it may be recalled that in most k -essence models [6, 7, 9, 52] including the original k -inflation idea [12], the distinguishing feature was the use of non-canonical kinetic terms in the Lagrangian of the form $F(X)V(\phi)$. In the work that we present below, based on our paper [11], we return to such a Lagrangian with the motivation of reproducing the features of inflation in the early Universe, and also generating dark matter and dark energy at late times. We find that after the early expansion is over, our present model can be approximated as kinetic k -essence, i.e., the dynamics becomes dominated by only the kinetic component of the scalar field. We show that the late time energy density reproduces a cosmological constant and a matter like term which we call dark matter. We then consider observational results from the both the early and late eras, which are used to put constraints on the parameters of this model.

4.1 THE MODEL

As mentioned earlier, unlike the previous model, here we begin with a more traditional form for the k -essence Lagrangian for a scalar field ϕ , which is

$$\mathcal{L} = F(X)V(\phi). \tag{4.1}$$

The functional forms of F and V are taken to be

$$F(X) = KX - m_{Pl}^2 L \sqrt{X} + m_{Pl}^4 M, \quad (4.2)$$

$$V(\phi) = 1 + e^{-\phi/\phi_c}, \quad (4.3)$$

where m_{Pl} denotes the Plank mass, and where the parameters K , L , and M are dimensionless, and were taken to be positive. The parameter ϕ_c is also taken to be positive and clearly has the dimension of ϕ . We work in natural units and consider V to be dimensionless. As is the usual case, the scalar field ϕ has the dimension of mass. From the definition of X it turns out that X , and hence F , has dimension M^4 .

The energy density in this case is given by

$$\rho = V(\phi)(2XF_X - F). \quad (4.4)$$

So substituting the forms of F and V we get

$$\rho = (1 + e^{-\phi/\phi_c})(KX - m_{Pl}^4 M). \quad (4.5)$$

The pressure, which is simply the Lagrangian, turns out to be

$$p = (1 + e^{-\phi/\phi_c})(KX - m_{Pl}^2 L \sqrt{X} + m_{Pl}^4 M). \quad (4.6)$$

The equation of state parameter is given by

$$w = \frac{F}{2XF_X - F}, \quad (4.7)$$

which in our model evaluates to

$$w = \frac{KX - m_{Pl}^2 L \sqrt{X} + m_{Pl}^4 M}{KX - m_{Pl}^4 M}. \quad (4.8)$$

The sound speed, or the speed at which perturbations travel, is defined to be [61]

$$c_s^2 \equiv \frac{\partial p / \partial X}{\partial \rho / \partial X} = \frac{F_X}{2XF_{XX} + F_X}. \quad (4.9)$$

Now, the equation of motion for the k -essence scalar field is given by

$$(2XF_{XX} + F_X)\dot{X} + 6HF_XX + \frac{\dot{V}}{V}(2XF_X - F) = 0, \quad (4.10)$$

which has been written in terms of X . If V is a constant or varies very slowly with time so that the third term in the above equation is negligible then the situation corresponds to kinetic k -essence and the field equation can be written as

$$(2XF_{XX} + F_X)\dot{X} + 6HF_XX = 0, \quad (4.11)$$

and as we saw in Section 3.2 this can be integrated exactly [34] to give the solution

$$\sqrt{X}F_X = \frac{k}{a^3}, \quad (4.12)$$

where k is a constant of integration. The energy conservation equation states that

$$\dot{\rho} = -3H(\rho + p) = -6HF_XXV. \quad (4.13)$$

This shows that the fixed points of the equation correspond to the extrema of F [12], which from Eqns. (4.1) and (4.4) yield $\rho = -p$. Moreover ρ decreases with time when $\rho > -p$ and increases when $\rho < -p$ showing that any point corresponding to $\rho = -p$ is an attractor and, as is well known, will lead to exponential inflation.

In our model the extrema of F corresponds to $X = 0$, or $X = m_{Pl}^4 \frac{L^2}{4K^2}$. The point $X = 0$ is of no significance since that corresponds to energy density and pressure which are constant in time. We take

$$X_0 = m_{Pl}^4 \frac{L^2}{4K^2}, \quad (4.14)$$

which leads from the definition of X , to

$$\dot{\phi}_0 = m_{Pl}^2 \frac{L}{\sqrt{2K}}, \quad (4.15)$$

where we take the positive sign for $\dot{\phi}$. For the above value of X the energy density and pressure turns out to be

$$\rho = V(\phi) \left(\frac{L^2}{4K} - M \right) m_{Pl}^4 = -p. \quad (4.16)$$

Actually, X_0 corresponds to an instantaneous attractive fixed point and X evolves slowly away from that point, which is the analog of “slow-roll” potential driven inflation in which the potential dominates the kinetic term and evolves slowly. Hence, in direct analogy, the above calculated values of ρ and p can be called the slow-roll values. In our model we assume that the exponential term inside V is much larger than 1 during the course of inflation, for which we must have $\phi_0/\phi_c < 0$, and also $|\phi_0/\phi_c| \gg 1$. From Eq. (4.13) we can write $\phi_0 = \dot{\phi}_0 t + C_\phi$, where C_ϕ is an integration constant. This constant can have a negative value, hence making $\phi_0 < 0$. Thus, we choose $\phi_c > 0$, such that the conditions $\phi_0/\phi_c < 0$, and $|\phi_0/\phi_c| \gg 1$ are satisfied during inflation. Since $\dot{\phi}_0 > 0$, it follows that ϕ becomes less and less negative with time. V could be quite accurately approximated as $e^{-\phi/\phi_c}$. This enables us to find the number of e-folds of expansion N , under this slow-roll approximation as

$$N = \int_{t_i}^{t_e} H dt = \int_{\phi_i}^{\phi_e} H \frac{d\phi}{\dot{\phi}}, \quad (4.17)$$

which turns out to be

$$N \simeq \sqrt{\frac{8\pi}{3}} m_{Pl}^{-1} \left(\frac{L^2}{4K} - M \right)^{1/2} \frac{\sqrt{2}K}{L} 2\phi_c \left(\sqrt{V_i} - \sqrt{V_e} \right), \quad (4.18)$$

where the subscripts ‘i’ and ‘e’ refer to the initial and final values, respectively.

The slow-roll condition for k -inflation is given by $[\delta X/X_0] \ll 1$. Now, during the post slow-roll stage we can write $X = X_0 + \delta X$. Also, from Eq. (4.13), we have

$$\frac{F_X}{(KX - m_{Pl}^4 M)} = -\frac{1}{6X} \frac{\dot{V}}{HV}. \quad (4.19)$$

Retaining terms up to the first order in δX we get

$$\frac{\delta X}{X_0} \simeq \frac{\frac{1}{X_0} \left(\frac{L^2}{4K} - M \right)}{\sqrt{3\pi} \frac{L\phi_c}{X_0 m_{Pl}^2} \left(\frac{L^2}{4K} - M \right)^{1/2} \sqrt{V} - \frac{K}{m_{Pl}^4}}. \quad (4.20)$$

Inflation ends when $\frac{\delta X}{X_0} \sim 1$. Using this fact in Eq. (4.18) we find the expression for the final value of the potential, V_e to be

$$\begin{aligned} \sqrt{V_e} \simeq & \frac{m_{Pl}}{\sqrt{3\pi}} \frac{1}{L\phi_c} \left(\frac{L^2}{4K} - M \right)^{1/2} \\ & + \frac{m_{Pl}}{\sqrt{3\pi}} \frac{L}{4K\phi_c} \left(\frac{L^2}{4K} - M \right)^{-1/2}. \end{aligned} \quad (4.21)$$

The kinematics of the inflationary era in our model may be viewed in the following way. We start with some representative point in the (ρ, p) plane corresponding to some initial value of ϕ such that the slow-roll condition is satisfied. In fact, during the first evolutionary stage the representative point takes only a few e-folds to reach the nearest inflationary attractor that corresponds to $\rho = -p$. After this initial stage the representative point follows the post slow-roll motion, $X = X_0 + \delta X$ with $\delta X/X_0 \ll 1$, thereby staying near but not exactly on the $\rho = -p$ line. The value of X is positive (as we will show later in the Section on observational constraints). Hence X slowly moves away from the value X_0 . As the evolution continues, the slow-roll condition is satisfied to a less and lesser extent till a time is reached when the slow-roll condition is actually violated ($\delta X/X_0 \sim 1$), and one naturally exits the inflationary stage.

Now, after inflation ends we have $X > X_0$, meaning that the time evolution of ϕ is faster than during inflation, and hence its value increases very quickly and correspondingly decreases the value of the exponential part in V , so that one gets $V \simeq 1$. In order for such a behaviour to ensue, we must have $\phi/\phi_c > 0$ after inflation is over. Since we have already chosen ϕ_c to be positive, then ϕ has to become positive after inflation where previously it was negative, and this is exactly its behaviour as pointed out earlier, i.e., $\dot{\phi}_0$ was positive. Note that even if the ratio ϕ/ϕ_c is not too big compared to 1, the exponential part of the potential will be negligible. Thus, after the inflationary expansion is over the exponential part in V quickly decays away (we will present an estimate of the time taken for this process in the section on observational constraints on the model). When the exponential term becomes quite negligible we have

$$V \approx 1, \quad \dot{V} \approx 0.$$

So the field equation effectively becomes of the form of Eq. (4.11) and the dynamics can be approximated quite well by the purely kinetic form of k -essence. On using Eq. (4.12) to find X as a function of a we get

$$X = \frac{1}{K^2} \left(m_{Pl}^2 \frac{L}{2} + \frac{k}{a^3} \right)^2. \quad (4.22)$$

Therefore the corresponding expression for the k -essence energy density turns out to be

$$\rho = m_{Pl}^4 \left(\frac{L^2}{4K} - M \right) + m_{Pl}^2 \frac{kL}{Ka^3} + \frac{k^2}{Ka^6}. \quad (4.23)$$

The subsequent evolution of the universe is described as follows. After the end of inflation the universe is in a kinetic dominated period when the third term in Eq. (4.23) dominates, which corresponds to $p = \rho \sim a^{-6}$. But this term becomes small quickly in comparison to radiation which goes as $\sim a^{-4}$ and a period of radiation domination in the universe ensues. The second term in Eq. (4.23) gains prominence in the epoch of matter domination and we identify it with dark matter. But as the universe evolves towards the present era the first term begins to dominate and acts like a cosmological constant giving rise to the late time acceleration of the universe. The equation of state parameter after inflation is over is given by

$$w = \frac{\frac{k^2}{Ka^6} - m_{Pl}^4 \left(\frac{L^2}{4K} - M \right)}{m_{Pl}^4 \left(\frac{L^2}{4K} - M \right) + m_{Pl}^2 \frac{kL}{Ka^3} + \frac{k^2}{Ka^6}}, \quad (4.24)$$

with the following values of w corresponding to the various epochs:

$$w \approx 1 \text{ after the end of inflation and before radiation domination}$$

$$w \approx 0 \text{ during matter domination}$$

$$w \rightarrow -1 \text{ as } a \rightarrow \infty$$

Using Eq. (4.9) the sound speed is found to be

$$c_s^2 = \frac{1}{m_{Pl}^2 \frac{La^3}{2k} + 1}. \quad (4.25)$$

From the above equation it is clear that the sound speed decreases as the Universe expands.

4.2 OBSERVATIONAL CONSTRAINTS ON THE MODEL

So far we have seen that the model considered by us produces the primary features of k -inflation in the early Universe and reproduces dark matter as well as a cosmological constant in the later period of evolution. We will now use various observational features to constrain the parameters of our model. A notable feature [12, 6] in our model is that the potential and the kinetic part are coupled. So parameters that are relevant during the late time era cannot be determined independently of the parameters relevant during the inflationary era. It is thus practical to first carry out the analysis in the late time era and then use the calculated values of the relevant parameters in the inflationary era. We have provided the expression for the k -essence energy density after inflation is over in Eq. (4.23). Using the current observed value of the cosmological constant, we get

$$m_{Pl}^4 \left(\frac{L^2}{4K} - M \right) \simeq 10^{-48} (\text{GeV})^4. \quad (4.26)$$

Also, observations put the current dark matter density to be about one-third of the current dark energy density. This enables us to write

$$\frac{kL}{Ka_0^3} \approx \frac{1}{3} m_{Pl}^2 \left(\frac{L^2}{4K} - M \right), \quad (4.27)$$

where the subscript '0' signifies the present epoch. We know from observations that the fraction of the current energy density contained in radiation is $(\Omega_R)_0 \simeq 5 \times 10^{-5}$ corresponding to the present radiation density $(\rho_R)_0 \simeq 6.94 \times 10^{-53} (\text{GeV})^4$. Denoting the third term in Eq. (4.23) as ρ_k , and assuming that ρ_R crosses over ρ_k at a redshift of $z \sim 10^{12}$ (prior to the nucleosynthesis at a redshift of 10^{10}), we get

$$z^2 = \frac{(\rho_R)_0 Ka_0^6}{k^2} \Rightarrow \frac{k}{a_0^3} = \frac{K^{1/2}}{z} (\rho_R)_0^{1/2}. \quad (4.28)$$

Now from Eqns. (4.27) and (4.28) we get

$$m_{Pl}^2 \frac{L}{K^{1/2}} \simeq 4 \times 10^{-11} (\text{GeV})^{-2}. \quad (4.29)$$

From Eqns. (4.28) and (4.29) it can be seen that the cross-over between dark matter and ρ_k occurs at a redshift of $\sim 10^9$ and that between radiation and dark matter at a redshift of $\sim 10^4$, i.e., at the epoch of matter-radiation equality. We also find the present value of ρ_k to be

$$(\rho_k)_0 = \frac{k^2}{K a_0^6} = \frac{(\rho_R)_0}{z^2} \approx 6.94 \times 10^{-77} (\text{GeV})^4. \quad (4.30)$$

The sound speed at the epoch of matter-radiation equality turns out to be

$$(c_s^2)_{eq} = \frac{1}{m_{Pl}^2 \frac{L a_{eq}^3}{2k} + 1} = \frac{1}{m_{Pl}^2 \frac{L a_0^3}{2z_{eq}^3 k} + 1} \simeq 4.1 \times 10^{-16}. \quad (4.31)$$

Now, we can re-express w from Eq. (4.24) in terms of the redshift z . Since ρ_k is negligible in comparison to the other components, we have

$$w \approx \frac{-\left(\frac{L^2}{4K} - M\right)}{\left(\frac{L^2}{4K} - M\right) + m_{Pl}^{-2} \frac{kL}{K a_0^3} (z+1)^3}. \quad (4.32)$$

Thereafter, it is possible to find dw/dz . Its value at the current epoch, i.e., at redshift $z = 0$ using Eqns. (4.26) and (4.27) turns out to be

$$\left(\frac{dw}{dz}\right)_0 \approx 2.733 \times 10^{-28}. \quad (4.33)$$

One can also estimate the current value of the equation of state parameter in our model, which using (4.32) and putting $z = 0$ turns out to be

$$w_0 \approx -0.75. \quad (4.34)$$

We can further find out the value of the redshift at which the Universe started its transition from the matter dominated decelerating era to its presently accelerating era. Knowing that for acceleration to begin we must have $w = -1/3$, from Eq. (4.32) we find that

$$z_{acc} \approx 0.817. \quad (4.35)$$

Such a value for the redshift is quite compatible with present observations [67]. But, from Eqns. (4.26) and (4.29) we find that

$$m_{Pl}^4 M = 4 \times 10^{-22} - 10^{-48} (\text{GeV})^4, \quad (4.36)$$

showing that a tuning of the parameter M is needed. This is expected since it is simply a rephrasing of the coincidence problem associated with the present window of acceleration of the Universe.

We now revisit the inflationary era for analyzing the observational constraints pertaining to it. From Ref. [61] the spectrum of scalar density perturbations in k -inflation is given by

$$\begin{aligned} P &= \frac{16}{9} \frac{m_{Pl}^{-4}}{c_s} \frac{\rho}{1+p/\rho} = -\frac{16}{9} \frac{m_{Pl}^{-4}}{c_s} \sqrt{\frac{8\pi G}{3}} \frac{\rho^{5/2}}{\dot{\rho}} \\ &= \frac{32\sqrt{2}}{3\sqrt{3}} \frac{\sqrt{\pi} m_{Pl}^{-1}}{c_s} \frac{\sqrt{2} K \phi_c}{L} \left(\frac{L^2}{4K} - M \right)^{3/2} V_i^{3/2}, \end{aligned} \quad (4.37)$$

where in the second step we have used the energy conservation law and also used the Friedmann equation. Using the COBE normalization $\sqrt{P} \sim 2 \times 10^{-5}$ and assuming that 60 e-folds of expansion took place, we can rewrite Eq. (4.37) to get an expression for V_i to be

$$\sqrt{V_i} = \frac{(27)^{1/6}}{4} \frac{c_s^{1/3} m_{Pl}^{-1/3}}{\pi^{1/6}} \left(\frac{PL}{K\phi_c} \right)^{1/3} \left(\frac{L^2}{4K} - M \right)^{-1/2}. \quad (4.38)$$

Using Eqns. (4.21) and (4.38) in Eq. (4.18) we can write

$$c_s^{1/3} \phi_c^{2/3} = \frac{4}{(27)^{1/6}} \pi^{1/6} m_{Pl}^{2/3} \left(\frac{K}{PL} \right)^{1/3} \quad (4.39)$$

$$\left[\frac{1}{\sqrt{3\pi}} \frac{1}{L} \left(\frac{L^2}{4K} - M \right) + \frac{1}{\sqrt{3\pi}} \frac{L}{4K} + \frac{NL}{2^{3/2}K} \sqrt{\frac{3}{8\pi}} \right].$$

Now from Eq. (4.9) we see that in slow-roll approximation when $F_X = 0$ we get $c_s^2 = 0$. But, in the post slow-roll stage, $X = X_0 + \delta X$, and F_X does not vanish. To first order in δX we can write $F_X \approx (F_{XX})_0 \delta X$. Using this in Eq. (4.9) we get

$$c_s^2 \simeq \frac{\delta X}{2X_0}. \quad (4.40)$$

Stability requires $X > 0$ and we show now that this is indeed the case. From Eqns. (4.20) and (4.38) we calculate $\delta X/X_0$ when $V = V_i$, to get

$$\frac{\delta X}{X_0} = \frac{\frac{4K^2}{L^2} \left(\frac{L^2}{4K} - M \right)}{\sqrt{3\pi} \frac{4K^2}{L} \left[\frac{1}{\sqrt{3\pi}} \frac{1}{L} \left(\frac{L^2}{4K} - M \right) + \frac{1}{\sqrt{3\pi}} \frac{L}{4K} + \frac{NL}{2^{3/2}K} \sqrt{\frac{3}{8\pi}} \right] - K}. \quad (4.41)$$

It is to be noted that in order to evaluate the above equation the actual value of K or L is not required, instead the ratio L/\sqrt{K} from Eq. (4.29) serves the purpose. Substituting the various values we find that

$$\frac{\delta X}{X_0} \simeq 2.748 \times 10^{-29}, \quad (4.42)$$

which is positive as claimed. The sound speed is therefore found to be

$$c_s^2 \simeq \frac{1}{2} \frac{\delta X}{X_0} \simeq 1.374 \times 10^{-29}. \quad (4.43)$$

Having found the sound speed and using the values of P and N , we now use Eq. (4.29) in Eq. (4.39) to get

$$\frac{1}{\phi_c \sqrt{K}} \simeq 3.23 \times 10^{15} (\text{GeV})^{-1}. \quad (4.44)$$

We now have all the parameter values to evaluate the value of V at the beginning and at the end of k -inflation which we write below:

$$V_i \simeq 9.166 \times 10^{97}, \quad (4.45)$$

$$V_e \simeq 1.107 \times 10^{94}. \quad (4.46)$$

The corresponding energy densities are

$$\rho_i = V_i \left(\frac{L^2}{4K} - M \right) m_{Pl}^4 \simeq 9.166 \times 10^{49} (\text{GeV})^4, \quad (4.47)$$

$$\rho_e = V_e \left(\frac{L^2}{4K} - M \right) m_{Pl}^4 \simeq 1.107 \times 10^{46} (\text{GeV})^4. \quad (4.48)$$

The tensor-to-scalar ratio is given by [61]

$$\begin{aligned} r &= 24c_s \left(1 + \frac{p}{\rho}\right) = -\frac{24c_s m_{Pl}}{\sqrt{24\pi}} \frac{\dot{\rho}}{\rho^{3/2}} \\ &= \sqrt{\frac{24}{\pi}} \frac{c_s}{\phi_c} \left(\frac{L^2}{4K} - M\right)^{-1/2} \frac{L}{\sqrt{2K}} \frac{1}{\sqrt{V_i}}. \end{aligned} \quad (4.49)$$

where in the second step we have used the energy conservation and Friedmann's equation. On substituting the parameter values we get

$$r = 9.776 \times 10^{-16}. \quad (4.50)$$

The scalar spectral index can be obtained from the relation [61]

$$\begin{aligned} n_s - 1 &= -3 \left(1 + \frac{p}{\rho}\right) - \frac{1}{H} \frac{d}{dt} \ln \left(1 + \frac{p}{\rho}\right) - \frac{1}{H} \frac{d}{dt} \ln c_s \\ &= \frac{2\dot{\rho}}{\rho H} - \frac{\ddot{\rho}}{\rho H} + \frac{\dot{H}}{H^2} - \frac{1}{H} \frac{\dot{c}_s}{c_s}. \end{aligned} \quad (4.51)$$

To evaluate n_s the values of the following quantities are required:

$$\begin{aligned} \frac{\dot{\rho}}{\rho} = \frac{\ddot{\rho}}{\dot{\rho}} = -\frac{\dot{\phi}_0}{\phi_c} &= -\frac{m_{Pl}^2}{\phi_c} \frac{L}{\sqrt{2K}} = -9.136 \times 10^4 \text{GeV}, \\ H &= \sqrt{\frac{8\pi G}{3}} \rho_i = 2.771 \times 10^6 \text{GeV}, \\ \dot{H} &= -\frac{4\pi G}{3} (\rho_i + p_i) = \frac{4\pi G}{9} \frac{\dot{\rho}_i}{H} = -4.219 \times 10^{10} (\text{GeV})^2, \\ \frac{\dot{c}_s}{c_s} &= 2.519 \times 10^{-94} \text{GeV}. \end{aligned}$$

All the above values have been calculated using the slow-roll approximation pertaining to the beginning of k -inflation. Therefore, using these values in Eq. (4.51) we get

$$n_s = 0.96514. \quad (4.52)$$

This value is quite close to what is predicted by models of potential driven inflation. Equation (4.51) differs from the appropriate expression in the case of

usual inflation by the term proportional to the derivative of the sound speed. Since in standard inflation $c_s = 1$, this term vanishes and one obtains n_s to be very close to 1, i.e., a scale invariant spectrum. But in k -inflation models, $c_s \neq 1$, and a tilted spectrum with $n_s < 1$ is generally predicted. However, in our model this term in Eq. (4.51) makes a vanishingly small contribution, and hence we get a spectral index that is again quite close to 1. Only the value of the tensor-to-scalar ratio in our model makes it distinguishable from standard inflation where typically a value of about 0.12 to 0.15 is obtained.

Now, the duration of inflation in our model is found to be

$$t_e - t_i = \int_{\phi_i}^{\phi_e} \frac{d\phi}{\dot{\phi}} = \frac{\sqrt{2}K}{L} (\phi_e - \phi_i) m_{Pl}^{-1} \approx 6.9 \times 10^{-29} \text{s}. \quad (4.53)$$

After the end of inflation, the stage of kinetic dominated evolution sets in very quickly. In order to have an idea as to how much time it takes for the exponential part of the potential to become negligible, we assume that for argument's sake, $X \simeq X_0$. This assumption is only made to perform a simple calculation and get an upper bound on the time required for the exponential part to decay (the actual time taken is much smaller since $X > X_0$ and ϕ evolves more rapidly compared to its linear evolution during inflation). The time taken after inflation for the exponential part to attain the value $e^{-\phi/\phi_c} \simeq 0.01$, is about 1.7×10^{-27} s. Thus, the time required for the k -essence field to effectively behave as kinetic k -essence is of the order of 10^{-27} s. This again justifies our analysis of the previous section pertaining to the post inflationary period being dominated by the dynamics of purely kinetic k -essence. It should be noted that the estimate for the time required for the Universe to enter into a kinetic dominated era after inflation is actually an upper bound. In reality the time required is much shorter since $X > X_0$ and the scalar field evolves more rapidly with time than during the inflationary era (the potential decreases very quickly to assume an almost constant value).

Reheating in this model could be caused by gravitational particle production. The process of gravitational reheating in the presence of kinetic domination by a scalar field is not yet understood very well [70]. However, standard calculations [65, 66] give the density of particles produced at the end of inflation to be $\rho_R \simeq 8.67 \times 10^{15} g(\text{GeV})^4$ where g is the number of fields which produce particles at this stage, likely to be between 10 and 100. This energy density, if immediately thermalized,

would give rise to a temperature of $T_e \simeq 9.65 \times 10^3 \left(\frac{g}{g_*}\right)^{1/4}$ GeV, where g_* is the total number of species in the thermal bath and maybe somewhat higher than g . Assuming that immediately after the end of inflation there is complete kinetic domination so that the scalar field density falls as a^6 , it is estimated that in our model the Universe has to expand by a factor of about 10^{15} for radiation domination to set in. After that expansion the temperature which goes as $T \propto 1/a$ comes out as $T \simeq 9.65 \times 10^{-12} \left(\frac{g}{g_*}\right)^{1/4}$ GeV. So we see that the temperature is not high enough for a successful nucleosynthesis for which a temperature around 1 MeV is needed. Now, if we change our parameters somewhat such that the value of the redshift for the crossover between ρ_R and ρ_k is 10^6 , then we find that the reheat temperature turns out to be $T \simeq 9.65 \times 10^{-5} \left(\frac{g}{g_*}\right)^{1/4}$ GeV which is roughly about the order of 0.1 MeV. There have been some recent studies which indicate that very low reheating temperatures could also be a viable option for successful nucleosynthesis (see, for instance [71]). These ideas have to be analyzed in detail in the context of k -essence scenarios in order to check how far gravitational reheating could be successful in our model.

4.3 SUMMARY AND DISCUSSION

To summarize we have considered a k -essence model that produces inflationary expansion in the early Universe by the process of k -inflation and later on generates both dark matter and dark energy at appropriate subsequent stages. For our Lagrangian we have considered that form which has been widely used for k -essence models [6, 7, 8, 9]. In contrast to the earlier model studied by us [10], the potential and the kinetic parts of the scalar field were not decoupled, leading to coupling between the inflationary era and the late time parameters. A significant feature of this fact can be found in the expression for the energy density. It thus follows that the generated cosmological constant which dominates the dynamics at late times derives its value from inflationary parameters. It needs to be mentioned here that our model was unable to address the coincidence problem and we also saw that the fine-tuning problem associated with the cosmological constant reemerged as a fine-tuning requirement of one of our model parameters.

Our model was able to reproduce the basic features of k -inflation. Although in general k -inflation predicts that $n_s < 1$, our model gave rise to a value which was nearly the same with what is obtained in standard potential driven inflation, predicting an almost scale invariant density perturbation spectrum. But, the value of the calculated tensor-to-scalar ratio was quite different from what is obtained in standard inflationary models. After the inflation was over the potential quickly became constant and we were able to approximate the model as purely kinetic k -essence. The late time energy density and the sound speed in terms of the scale factor a were obtained. The resultant energy density contained terms that achieved the desired unification of dark matter and dark energy. We showed that the sound speed calculated at the epoch of matter-radiation equality came out to be very small, thus posing no problem for structure formation, since it further decreased as the Universe expanded. Our estimation of the current equation of state and the redshift at which the current acceleration of the Universe started, lie within observational bounds. Further studies would be needed to see if gravitational reheating could be a viable feature of such a scheme.

PART III

COSMOLOGICAL BACKREACTION

CHAPTER 5

THE BACKREACTION FRAMEWORK

5.1 AVERAGED EINSTEIN EQUATIONS

In the framework developed by Buchert [40] (also see [72] for a review on this), the Universe is considered to be filled with an irrotational fluid of dust and the spacetime is foliated into flow-orthogonal hypersurfaces featuring the line-element

$$ds^2 = -dt^2 + g_{ij}dX^i dX^j, \quad (5.1)$$

where the proper time t labels the hypersurfaces and X^i are Gaussian normal coordinates (locating free-falling fluid elements or generalized fundamental observers) in the hypersurfaces. g_{ij} is the full inhomogeneous three metric of the hypersurfaces of constant proper time. Note here that in the second paper in [40], the framework was later refined to be applicable to perfect fluid matter models.

On these hypersurfaces we want to study the evolution of compact spatial domains \mathcal{D} , comoving with the fluid. This latter property ensures that the domain is frozen into the general three-metric, i.e. its shape encodes the geometrical structure of the local inhomogeneities. One fundamental quantity characterizing such a domain is its volume, which is the only such measure used, since we wish to address questions related to the size of the domains and its time-derivatives only,

$$|\mathcal{D}|_g = \int_{\mathcal{D}} d\mu_g, \quad (5.2)$$

where $d\mu_g = \sqrt{{}^{(3)}g(t, X^1, X^2, X^3)}dX^1 dX^2 dX^3$. From the domain's volume one may define a scale factor

$$a_{\mathcal{D}}(t) = \left(\frac{|\mathcal{D}|_g}{|\mathcal{D}_i|_g} \right)^{1/3}, \quad (5.3)$$

encoding the average stretch of all directions of the domain. For wild changes of the shape of the initial domain \mathcal{D}_i one might want to know more about the evolution of other morphological characteristics to deduce directional expansion information, and would therefore have to extend the analysis.

Concentrating on the volume and the effective scale factor alone, one can derive, from the Einstein equations with a pressure-less fluid source, the following set of equations governing its evolution:

$$3 \frac{\ddot{a}_{\mathcal{D}}}{a_{\mathcal{D}}} = -4\pi G \langle \rho \rangle_{\mathcal{D}} + \mathcal{Q}_{\mathcal{D}} + \Lambda, \quad (5.4)$$

$$3H_{\mathcal{D}}^2 = 8\pi G \langle \rho \rangle_{\mathcal{D}} - \frac{1}{2} \langle \mathcal{R} \rangle_{\mathcal{D}} - \frac{1}{2} \mathcal{Q}_{\mathcal{D}} + \Lambda, \quad (5.5)$$

$$0 = \partial_t \langle \rho \rangle_{\mathcal{D}} + 3H_{\mathcal{D}} \langle \rho \rangle_{\mathcal{D}}, \quad (5.6)$$

where the average over scalar quantities is defined as

$$\langle f \rangle_{\mathcal{D}}(t) = \frac{\int_{\mathcal{D}} f(t, X^1, X^2, X^3) d\mu_g}{\int_{\mathcal{D}} d\mu_g} = |\mathcal{D}|_g^{-1} \int_{\mathcal{D}} f d\mu_g, \quad (5.7)$$

and where ρ , \mathcal{R} and $H_{\mathcal{D}}$ denote the local matter density, the Ricci scalar of the three-metric g_{ij} , and the domain dependent Hubble rate $H_{\mathcal{D}} = \dot{a}_{\mathcal{D}}/a_{\mathcal{D}}$, respectively. The kinematical backreaction $\mathcal{Q}_{\mathcal{D}}$ is defined as

$$\mathcal{Q}_{\mathcal{D}} = \frac{2}{3} (\langle \theta^2 \rangle_{\mathcal{D}} - \langle \theta \rangle_{\mathcal{D}}^2) - 2\sigma_{\mathcal{D}}^2, \quad (5.8)$$

where θ is the local expansion rate and $\sigma^2 = 1/2 \sigma_{ij} \sigma^{ij}$ is the squared rate of shear. Note that $H_{\mathcal{D}}$ is defined as $H_{\mathcal{D}} = 1/3 \langle \theta \rangle_{\mathcal{D}}$. $\mathcal{Q}_{\mathcal{D}}$ is composed of the variance of the local expansion rates, $\langle \theta^2 \rangle_{\mathcal{D}} - \langle \theta \rangle_{\mathcal{D}}^2$, and the averaged shear scalar $\sigma_{\mathcal{D}}^2$ on the domain under consideration. For a homogeneous domain it is zero. It therefore encodes the departure from homogeneity and is supposed to be particularly important in the late, inhomogeneous phase of the Universe at the epoch of structure formation.

The integrability condition connecting Eqns. (5.4) and (5.5) reads

$$\frac{1}{a_{\mathcal{D}}^2} \partial_t (a_{\mathcal{D}}^2 \langle \mathcal{R} \rangle_{\mathcal{D}}) + \frac{1}{a_{\mathcal{D}}^6} \partial_t (a_{\mathcal{D}}^6 \mathcal{Q}_{\mathcal{D}}) = 0, \quad (5.9)$$

which already shows an important feature of the averaged equations as they in general couple the evolution of the backreaction term, and hence extrinsic curvature inhomogeneities (or in this picture matter inhomogeneities), to the average intrinsic curvature. Unlike in the case of a standard Friedmannian evolution the curvature term here is not restricted to an $a_{\mathcal{D}}^{-2}$ scaling behaviour but is dynamical in the sense that it may be an arbitrary function of $a_{\mathcal{D}}$. It should be noted that the essential effect of backreaction models is not a large magnitude of $\mathcal{Q}_{\mathcal{D}}$, but a dynamical coupling of a non-vanishing $\mathcal{Q}_{\mathcal{D}}$ to the averaged scalar curvature, changing the temporal behaviour of this latter.

5.2 EFFECTIVE FRIEDMANNIAN FRAMEWORK

We may also recast the general equations (5.4), (5.5), (5.6) and (5.9) by appealing to the Friedmannian framework. This amounts to re-interpretation of geometrical terms, that arise through averaging, as effective sources within a Friedmannian setting. In the present case the averaged equations may be written as standard zero-curvature Friedmann equations for an effective perfect fluid energy momentum tensor with new effective sources :

$$\rho_{eff}^{\mathcal{D}} = \langle \rho \rangle_{\mathcal{D}} - \frac{1}{16\pi G} \mathcal{Q}_{\mathcal{D}} - \frac{1}{16\pi G} \langle \mathcal{R} \rangle_{\mathcal{D}}, \quad (5.10)$$

$$p_{eff}^{\mathcal{D}} = -\frac{1}{16\pi G} \mathcal{Q}_{\mathcal{D}} + \frac{1}{48\pi G} \langle \mathcal{R} \rangle_{\mathcal{D}}, \quad (5.11)$$

and the evolution equations become

$$3 \frac{\ddot{a}_{\mathcal{D}}}{a_{\mathcal{D}}} = -4\pi G (\rho_{eff}^{\mathcal{D}} + 3p_{eff}^{\mathcal{D}}) + \Lambda, \quad (5.12)$$

$$3H_{\mathcal{D}}^2 = 8\pi G \rho_{eff}^{\mathcal{D}} + \Lambda, \quad (5.13)$$

$$0 = \dot{\rho}_{eff}^{\mathcal{D}} + 3H_{\mathcal{D}} (\rho_{eff}^{\mathcal{D}} + p_{eff}^{\mathcal{D}}). \quad (5.14)$$

We notice that $\mathcal{Q}_{\mathcal{D}}$, if interpreted as a source, introduces a component with ‘stiff equation of state’, $p_{\mathcal{Q}}^{\mathcal{D}} = \rho_{\mathcal{Q}}^{\mathcal{D}}$, suggesting a correspondence with a free scalar field

(discussed in the next section), while the averaged scalar curvature introduces a component with ‘curvature equation of state’ $p_{\mathcal{R}}^{\mathcal{D}} = -1/3\rho_{\mathcal{R}}^{\mathcal{D}}$. Although we are dealing with dust matter, we appreciate a ‘geometrical pressure’ in the effective energy–momentum tensor.

5.3 ‘MORPHED’ FRIEDMANN COSMOLOGIES

In the above introduced framework we distinguish the averaged matter source on the one hand, and averaged sources due to geometrical inhomogeneities stemming from extrinsic and intrinsic curvature (kinematical backreaction terms) on the other. As shown above, the averaged equations can be written as standard Friedmann equations that are sourced by both. Thus, we have the choice to consider the averaged model as a (scale–dependent) ‘standard model’ with matter source evolving in a mean field of backreaction terms. This form of the equations is closest to the standard model of cosmology. It is a ‘morphed’ Friedmann cosmology, sourced by matter and ‘morphed’ by a (minimally coupled) scalar field, the morphon field [73]. We write (recall that we have no matter pressure source here):

$$\rho_{eff}^{\mathcal{D}} = \langle \rho \rangle_{\mathcal{D}} + \rho_{\phi}^{\mathcal{D}} ; p_{eff}^{\mathcal{D}} = p_{\phi}^{\mathcal{D}}, \quad (5.15)$$

with

$$\rho_{\phi}^{\mathcal{D}} = \varepsilon \frac{1}{2} \dot{\phi}_{\mathcal{D}}^2 + U_{\mathcal{D}} ; p_{\phi}^{\mathcal{D}} = \varepsilon \frac{1}{2} \dot{\phi}_{\mathcal{D}}^2 - U_{\mathcal{D}}, \quad (5.16)$$

where $\varepsilon = +1$ for a standard scalar field (with positive kinetic energy), and $\varepsilon = -1$ for a phantom scalar field (with negative kinetic energy). Thus, in view of Eq. (5.10), we obtain the following correspondence:

$$-\frac{1}{8\pi G} \mathcal{Q}_{\mathcal{D}} = \varepsilon \dot{\phi}_{\mathcal{D}}^2 - U_{\mathcal{D}} ; -\frac{1}{8\pi G} \langle \mathcal{R} \rangle_{\mathcal{D}} = 3U_{\mathcal{D}}. \quad (5.17)$$

Inserting this equation into the integrability condition (5.9) then implies that $\phi_{\mathcal{D}}$, for $\dot{\phi}_{\mathcal{D}} \neq 0$, obeys the (scale–dependent) Klein–Gordon equation:

$$\ddot{\phi}_{\mathcal{D}} + 3H_{\mathcal{D}}\dot{\phi}_{\mathcal{D}} + \varepsilon \frac{\partial}{\partial \phi_{\mathcal{D}}} U_{\mathcal{D}}(\phi_{\mathcal{D}}, \langle \rho \rangle_{\mathcal{D}}) = 0. \quad (5.18)$$

Note that the potential $U_{\mathcal{D}}$ is not restricted to depend only on $\phi_{\mathcal{D}}$ explicitly. An explicit dependence on the averaged density and on other variables of the sys-

tem (that can, however, be expressed in terms of these two variables) is generic. The above correspondence allows us to interpret the kinematical backreaction effects in terms of properties of scalar field cosmologies, notably quintessence or phantom–quintessence scenario that are here routed back to models of inhomogeneities. Dark Energy emerges as unbalanced kinetic and potential energies due to structural inhomogeneities. More precisely, kinematical backreaction appears as excess of kinetic energy density over the ‘virial balance’, while the averaged scalar curvature of space sections is directly proportional to the potential energy density; e.g. a void (a ‘classical vacuum’) with on average negative scalar curvature (a positive potential) can be attributed to a negative potential energy of a morphon field (‘classical vacuum energy’).

5.3.1 MORPHON AS k -ESSENCE

We just saw how the effects of backreaction can be related to a scalar field called “morphon”. But the Buchert framework treats this field as a traditional scalar field (such as quintessence) whose equation of motion is given by the Klein-Gordon equation. We now show that it is not necessary to restrict the morphon to such behaviour and we can treat it as a k -essence field, i.e. a field which has non-canonical kinetic terms in the Lagrangian.

Let us assume that the Lagrangian of the morphon has the form

$$\mathcal{L} = F(X)V(\phi), \quad (5.19)$$

which we know to be a traditional form of k -essence Lagrangian. For this the energy density and pressure of the morphon will look like

$$\rho_{\phi}^{\mathcal{D}} = V(2XF_X - F), \quad (5.20)$$

$$p_{\phi}^{\mathcal{D}} = FV, \quad (5.21)$$

using which we can write the effective energy density and pressure of Eqns. (5.4), (5.5) and (5.6), just as before

$$\rho_{eff}^{\mathcal{D}} = \langle \rho \rangle_{\mathcal{D}} + \rho_{\phi}^{\mathcal{D}} ; p_{eff}^{\mathcal{D}} = p_{\phi}^{\mathcal{D}}. \quad (5.22)$$

Therefore using the above equations in (5.4) and (5.5) we see that we can write

$$Q_{\mathcal{D}} = -8\pi G V (X F_X + F), \quad (5.23)$$

$$\langle \mathcal{R} \rangle_{\mathcal{D}} = 24\pi G V (F - X F_X). \quad (5.24)$$

Inserting these values of $Q_{\mathcal{D}}$ and $\langle \mathcal{R} \rangle_{\mathcal{D}}$ in the integrability condition (5.9) gives us

$$(2X F_{XX} + F_X) \dot{X} + 6H F_X X + \frac{\dot{V}}{V} (2X F_X - F) = 0, \quad (5.25)$$

which as we know is the equation of motion of a k -essence field that has a Lagrangian of the form we have chosen, and hence as stated we can take the morphon to behave as a k -essence field. Note that although in the above example we took the Lagrangian for the k -essence field as $\mathcal{L} = F(X)V(\phi)$, we are certainly not restricted to that form only. We could also have taken the Lagrangian to be of the form $\mathcal{L} = F(X) + V(\phi)$, or for that matter any function of ϕ and X , and the morphon would still act as a k -essence field with the appropriate equation of motion.

5.4 THE COSMIC QUARTET

We start by dividing the volume averaged Hamiltonian constraint (5.5) by the squared volume Hubble functional $H_{\mathcal{D}} = \dot{a}_{\mathcal{D}}/a_{\mathcal{D}}$ introduced before. Then, expressed through the following set of ‘parameters’

$$\begin{aligned} \Omega_m^{\mathcal{D}} &= \frac{8\pi G}{3H_{\mathcal{D}}^2} \langle \rho \rangle_{\mathcal{D}}, \\ \Omega_{\Lambda}^{\mathcal{D}} &= \frac{\Lambda}{3H_{\mathcal{D}}^2}, \\ \Omega_{\mathcal{R}}^{\mathcal{D}} &= -\frac{\langle \mathcal{R} \rangle_{\mathcal{D}}}{6H_{\mathcal{D}}^2}, \\ \Omega_Q^{\mathcal{D}} &= -\frac{Q_{\mathcal{D}}}{6H_{\mathcal{D}}^2}, \end{aligned} \quad (5.26)$$

the averaged Hamiltonian constraint assumes the form of a cosmic quartet

$$\Omega_m^{\mathcal{D}} + \Omega_\Lambda^{\mathcal{D}} + \Omega_{\mathcal{R}}^{\mathcal{D}} + \Omega_{\mathcal{Q}}^{\mathcal{D}} = 1, \quad (5.27)$$

showing that the solution space of an averaged inhomogeneous cosmology is three-dimensional in the present framework. In this set, the averaged scalar curvature parameter and the kinematical backreaction parameter are directly expressed through $\langle \mathcal{R} \rangle_{\mathcal{D}}$ and $\mathcal{Q}_{\mathcal{D}}$, respectively.

5.5 ACCELERATION AND ENERGY CONDITIONS

Let us look at the general acceleration law (5.4), and ask when we would find volume acceleration on a given patch of the spatial hypersurface

$$3 \frac{\ddot{a}_{\mathcal{D}}}{a_{\mathcal{D}}} = -4\pi G \langle \rho \rangle_{\mathcal{D}} + \mathcal{Q}_{\mathcal{D}} + \Lambda > 0. \quad (5.28)$$

We find that, if there is no cosmological constant, the necessary condition $\mathcal{Q}_{\mathcal{D}} > 4\pi G \langle \rho \rangle_{\mathcal{D}}$ must be satisfied on a sufficiently large scale, at least at the present time. This requires that $\mathcal{Q}_{\mathcal{D}}$ is positive, i.e. shear fluctuations are superseded by expansion fluctuations and, what is crucial, that $\mathcal{Q}_{\mathcal{D}}$ decays less rapidly than the averaged density. It is not obvious that this latter condition could be met in view of our remarks above. We conclude that backreaction has only a chance to be relevant in magnitude compared with the density (e.g. as defined through the inequality Eq. (5.28) today), if its decay rate substantially deviates from its ‘quasi-Newtonian’ behaviour and, more precisely, its decay rate must be weaker than that of the averaged density (or at least comparable, depending on initial data for the magnitude of Early Dark Energy).

Another model of Dark Energy is to assume the existence of a scalar field source, a so-called quintessence field. However, a usual scalar field source in a Friedmannian model, attributed e.g. to phantom quintessence that leads to acceleration, will violate the strong energy condition $\rho + 3p > 0$, i.e.:

$$3 \frac{\ddot{a}}{a} = -4\pi G (\rho + 3p) = -4\pi G (\rho_H + \rho_\phi + 3p_\phi) > 0. \quad (5.29)$$

Previously we have introduced a mean field description of kinematical backreaction in terms of a morphon field. For such an effective scalar field the strong energy

condition is not violated for the true content of the Universe, that is ordinary dust matter. In this line it is interesting that we can identify ‘violation’ of an effective ‘strong energy condition’ with the acceleration condition above (cf. Eqns. (5.10), (5.15))

$$\begin{aligned} 3\frac{\ddot{a}_{\mathcal{D}}}{a_{\mathcal{D}}} &= -4\pi G (\rho_{eff}^{\mathcal{D}} + 3p_{eff}^{\mathcal{D}}) \\ &= -4\pi G (\langle \rho \rangle_{\mathcal{D}} + \rho_{\phi}^{\mathcal{D}} + 3p_{\phi}^{\mathcal{D}}) \\ &= -4\pi G \langle \rho \rangle_{\mathcal{D}} + \mathcal{Q}_{\mathcal{D}}, \end{aligned} \quad (5.30)$$

which has to be positive, if the acceleration condition (5.28) is met.

5.6 SEPARATION FORMULAE FOR ARBITRARY PARTITIONS

So far we have focussed our attention on a single domain \mathcal{D} , but now we will consider \mathcal{D} to be some kind of ‘global’ domain that is assumed to be separated into subregions \mathcal{F}_{ℓ} , which themselves consist of elementary space entities $\mathcal{F}_{\ell}^{(\alpha)}$ that may be associated with some averaging length scale [50]. In mathematical terms $\mathcal{D} = \cup_{\ell} \mathcal{F}_{\ell}$, where $\mathcal{F}_{\ell} = \cup_{\alpha} \mathcal{F}_{\ell}^{(\alpha)}$ and $\mathcal{F}_{\ell}^{(\alpha)} \cap \mathcal{F}_{m}^{(\beta)} = \emptyset$ for all $\alpha \neq \beta$ and $\ell \neq m$. The average of the scalar valued function f on the domain \mathcal{D} (5.7) may then be split into the averages of f on the subregions \mathcal{F}_{ℓ} in the form,

$$\langle f \rangle_{\mathcal{D}} = \sum_{\ell} |\mathcal{D}|_g^{-1} \sum_{\alpha} \int_{\mathcal{F}_{\ell}^{(\alpha)}} f d\mu_g = \sum_{\ell} \lambda_{\ell} \langle f \rangle_{\mathcal{F}_{\ell}}, \quad (5.31)$$

where $\lambda_{\ell} = |\mathcal{F}_{\ell}|_g / |\mathcal{D}|_g$, is the volume fraction of the subregion \mathcal{F}_{ℓ} . The above equation directly provides the expression for the separation of the scalar quantities ρ , \mathcal{R} and $H_{\mathcal{D}} = 1/3 \langle \theta \rangle_{\mathcal{D}}$. However, $\mathcal{Q}_{\mathcal{D}}$, as defined in (5.8), does not split in such a simple manner due to the $\langle \theta \rangle_{\mathcal{D}}^2$ term. Instead the correct formula turns out to be

$$\mathcal{Q}_{\mathcal{D}} = \sum_{\mathcal{D}} \lambda_{\ell} \mathcal{Q}_{\ell} + 3 \sum_{\ell \neq m} \lambda_{\ell} \lambda_m (H_{\ell} - H_m)^2, \quad (5.32)$$

where \mathcal{Q}_{ℓ} and H_{ℓ} are defined in \mathcal{F}_{ℓ} in the same way as $\mathcal{Q}_{\mathcal{D}}$ and $H_{\mathcal{D}}$ are defined in \mathcal{D} . The shear part $\langle \sigma^2 \rangle_{\mathcal{F}_{\ell}}$ is completely absorbed in \mathcal{Q}_{ℓ} , whereas the variance of

the local expansion rates $\langle \theta^2 \rangle_{\mathcal{D}} - \langle \theta \rangle_{\mathcal{D}}^2$ is partly contained in \mathcal{Q}_ℓ but also generates the extra term $3 \sum_{\ell \neq m} \lambda_\ell \lambda_m (H_\ell - H_m)^2$. This is because the part of the variance that is present in \mathcal{Q}_ℓ , namely $\langle \theta^2 \rangle_{\mathcal{F}_\ell} - \langle \theta \rangle_{\mathcal{F}_\ell}^2$, only takes into account points inside \mathcal{F}_ℓ . To restore the variance that comes from combining points of \mathcal{F}_ℓ with others in \mathcal{F}_m , the extra term containing the averaged Hubble rate emerges. Note here that the above formulation of the backreaction holds in the case when there is no interaction between the overdense and the underdense subregions.

Analogous to the scale-factor for the global domain, a scale-factor a_ℓ for each of the subregions \mathcal{F}_ℓ can be defined such that $|\mathcal{D}|_g = \sum_\ell |\mathcal{F}_\ell|_g$, and hence,

$$a_{\mathcal{D}}^3 = \sum_\ell \lambda_{\ell_i} a_\ell^3, \quad (5.33)$$

where $\lambda_{\ell_i} = |\mathcal{F}_{\ell_i}|_g / |\mathcal{D}|_g$ is the initial volume fraction of the subregion \mathcal{F}_ℓ . If we now twice differentiate this equation with respect to the foliation time and use the result for \dot{a}_ℓ from (5.5), we then get the expression that relates the acceleration of the global domain to that of the sub-domains:

$$\frac{\ddot{a}_{\mathcal{D}}}{a_{\mathcal{D}}} = \sum_\ell \lambda_\ell \frac{\ddot{a}_\ell(t)}{a_\ell(t)} + \sum_{\ell \neq m} \lambda_\ell \lambda_m (H_\ell - H_m)^2. \quad (5.34)$$

As an immediate consequence one can see that even when the subregions decelerate, the second term of the above equation may counterbalance the first one to lead to global accelerated expansion.

5.7 CONSISTENT SPLIT OF THE DYNAMICAL EQUATIONS

In the last section we saw how we can relate between the quantities on the subregions with those on the global domain \mathcal{D} . We now try to see how the separation affects the evolution equations for those quantities. We therefore insert the expressions (5.31) for $H_{\mathcal{D}}$, $\langle \rho \rangle_{\mathcal{D}}$ and $\langle \mathcal{R} \rangle_{\mathcal{D}}$ and (5.32) for $\mathcal{Q}_{\mathcal{D}}$ into (5.4), (5.5) and (5.9). A straightforward calculation shows that the equations take the following form

$$0 = \sum_{\ell} \lambda_{\ell} \left[8\pi G \langle \rho \rangle_{\ell} - \frac{\mathcal{Q}_{\ell} + \langle \mathcal{R} \rangle_{\ell}}{2} + \Lambda - 3H_{\ell}^2 \right] \quad (5.35)$$

$$0 = \sum_{\ell} \lambda_{\ell} \left[-4\pi G \langle \rho \rangle_{\ell} + \mathcal{Q}_{\ell} + \Lambda - 3 \frac{\ddot{a}_{\ell}(t)}{a_{\ell}(t)} \right] \quad (5.36)$$

$$0 = \sum_{\ell} \lambda_{\ell} \left[\frac{1}{a_{\ell}^2} \partial_t (a_{\ell}^2 \langle \mathcal{R} \rangle_{\ell}) + \frac{1}{a_{\ell}^6} \partial_t (a_{\ell}^6 \mathcal{Q}_{\ell}) \right], \quad (5.37)$$

i.e. they may be split into a sum in which the equations on the subregions take the same form as those of the global region (5.4)-(5.6) and their contribution is weighted with the volume fraction of the respective subregion. As equations (5.4)-(5.6) hold for an arbitrary domain \mathcal{D} and therefore also for the subregions \mathcal{F}_{ℓ} , equations (5.35)-(5.37) show that the separation advocated in the previous section is also consistent at the level of the evolution equations. This is not surprising as the separation procedure is straightforward and the equations are supposed to hold on any domain, but was, especially in view of the nonlinear form of (5.32), not entirely clear when just looking at the formulae. The consistent split assures that, if we have found a solution for the quantities on the subregions \mathcal{F}_{ℓ} and use the relations of the previous section to calculate those on the global domain, then we will automatically obtain a solution of the averaged equations (5.4)-(5.6) on this global domain.

CHAPTER 6

EFFECT OF COSMIC BACKREACTION ON THE FUTURE EVOLUTION OF THE UNIVERSE

We will now try to see what happens to the evolution of the Universe once the present stage of acceleration sets. The work described in this chapter is based on our papers [51] and [54]. We will first study the evolution of the Universe by using the evolution equations of the Buchert framework. However, the acceleration of the universe leads to a future event horizon from beyond which it is not possible for any signal to reach us. The currently accelerating epoch dictates the existence of an event horizon since the transition from the previously matter-dominated decelerating expansion. Since backreaction is evaluated from the global distribution of matter inhomogeneities, the event horizon demarcates the spatial regions which are causally connected to us and hence impact the evolution of our part of the Universe. Therefore we will investigate the consequences of backreaction in presence of the horizon by taking into consideration the effect of the horizon in the Buchert framework. Such an approach has remained unexplored in previous studies of backreaction. It may be noted that the formalism of backreaction [40, 53, 50] has been criticized on the grounds that the average is taken on a space-like hypersurface, while observations are made along and inside the past light cone [46]. Our present analysis, by considering an effect due to the event horizon, introduces an element of light cone physics from a somewhat different perspective. We will also perform a comparative analysis between the case where we include the event horizon in our calculations and the case where we don't.

6.1 FUTURE EVOLUTION WITHIN THE BUCHERT FRAMEWORK

We now try to see what happens to the evolution of the Universe once the present stage of acceleration sets in. Note, henceforth, we do not need to necessarily assume that the acceleration is due to backreaction [43, 50]. For the purpose of our present analysis, it suffices to consider the observed accelerated phase of the universe [74] that could occur due to any of a variety of mechanisms [4].

We work with a compact spatial domain \mathcal{D} that we consider to be a ‘‘global’’ domain that is large enough for a scale of homogeneity to be associated with it. This allows us to write

$$|\mathcal{D}|_g = \int_{\mathcal{D}} \sqrt{-g} d^3X \approx f(r)a_F^3(t), \quad (6.1)$$

where $f(r)$ is a function of the comoving FRW radial coordinate r and a_F is the FRW scale-factor. From the definition of the volume average scale-factor (5.3) it then follows that

$$a_{\mathcal{D}} = \left(\frac{f(r)}{|\mathcal{D}|_g} \right)^{1/3} a_F \equiv c_F a_F, \quad (6.2)$$

where c_F is a constant in time. Thus, $H_F \approx H_{\mathcal{D}}$, where H_F is the FRW Hubble parameter associated with \mathcal{D} . Though in general $H_{\mathcal{D}}$ and H_F can differ on even large scales [50], the above approximation is valid for small metric perturbations.

Following the simplifying assumption of [50], we consider the global domain \mathcal{D} to be divided into a collection of overdense regions $\mathcal{M} = \cup_j \mathcal{M}^j$ (called ‘wall’), with total volume $|\mathcal{M}|_g = \sum_j |\mathcal{M}^j|_g$ and undersense regions $\mathcal{E} = \cup_j \mathcal{E}^j$ (called ‘void’) with corresponding volume $|\mathcal{E}|_g = \sum_j |\mathcal{E}^j|_g$, such that $\mathcal{D} = \mathcal{M} \cup \mathcal{E}$ and also $H_{\mathcal{D}} = \lambda_{\mathcal{M}} H_{\mathcal{M}} + \lambda_{\mathcal{E}} H_{\mathcal{E}}$, with similar expressions for $\langle \rho \rangle_{\mathcal{D}}$ and $\langle \mathcal{R} \rangle_{\mathcal{D}}$. Since we are essentially dealing with two subregions so Eq. (5.34) in this case becomes

$$\frac{\ddot{a}_{\mathcal{D}}}{a_{\mathcal{D}}} = \lambda_{\mathcal{M}} \frac{\ddot{a}_{\mathcal{M}}}{a_{\mathcal{M}}} + \lambda_{\mathcal{E}} \frac{\ddot{a}_{\mathcal{E}}}{a_{\mathcal{E}}} + 2\lambda_{\mathcal{M}}\lambda_{\mathcal{E}}(H_{\mathcal{M}} - H_{\mathcal{E}})^2. \quad (6.3)$$

Here $\lambda_{\mathcal{M}} + \lambda_{\mathcal{E}} = 1$ with $\lambda_{\mathcal{M}} = |\mathcal{M}|/|\mathcal{D}|$ and $\lambda_{\mathcal{E}} = |\mathcal{E}|/|\mathcal{D}|$. We assume that the scale-factors of the regions are respectively given by $a_{\mathcal{E}^j} = c_{\mathcal{E}^j} t^{\alpha}$ and $a_{\mathcal{M}^j} = c_{\mathcal{M}^j} t^{\beta}$, where $\alpha, \beta, c_{\mathcal{M}^j}$ and $c_{\mathcal{E}^j}$ are constants. This then gives us

$$a_{\mathcal{E}}^3 = c_{\mathcal{E}}^3 t^{3\alpha}; \quad a_{\mathcal{M}}^3 = c_{\mathcal{M}}^3 t^{3\beta}, \quad (6.4)$$

where $c_{\mathcal{E}}^3 = \frac{\sum_j c_{\mathcal{E}_j}^3 |\mathcal{E}_j^j|_g}{|\mathcal{E}|_g}$ is a constant, and similarly for $c_{\mathcal{M}}$. The volume fraction of the subdomain \mathcal{M} is given by $\lambda_{\mathcal{M}} = \frac{|\mathcal{M}|_g}{|\mathcal{D}|_g}$ which can be rewritten in terms of the corresponding scale-factors as $\lambda_{\mathcal{M}} = \frac{a_{\mathcal{M}}^3 |\mathcal{M}_i|_g}{a_{\mathcal{D}}^3 |\mathcal{D}_i|_g}$. Therefore the global acceleration for this case (6.3) becomes

$$\begin{aligned} \frac{\ddot{a}_{\mathcal{D}}}{a_{\mathcal{D}}} &= \frac{g_{\mathcal{M}_h}^3 t^{3\beta} \beta(\beta-1)}{a_{\mathcal{D}}^3 t^2} + \left(1 - \frac{g_{\mathcal{M}_h}^3 t^{3\beta}}{a_{\mathcal{D}}^3}\right) \frac{\alpha(\alpha-1)}{t^2} \\ &+ 2 \frac{g_{\mathcal{M}_h}^3 t^{3\beta}}{a_{\mathcal{D}}^3} \left(1 - \frac{g_{\mathcal{M}_h}^3 t^{3\beta}}{a_{\mathcal{D}}^3}\right) \left(\frac{\beta}{t} - \frac{\alpha}{t}\right)^2, \end{aligned} \quad (6.5)$$

where $g_{\mathcal{M}_h}^3 = \frac{\lambda_{\mathcal{M}_0} a_{\mathcal{D}_0}^3}{t_0^{3\beta}}$ is a constant. We obtain numerical solutions of the above equation for various parameter values (see curves (ii) and (iv) of Fig. 6.1). The expansion factor β for the overdense subdomain (wall) is chosen to lie between 1/2 and 2/3 (since the expansion is assumed to be faster than in the radiation dominated case, and is upper limited by the value for matter dominated expansion).

Note here that using our ansatz for the subdomain scale factors given by Eq. (6.4), one may try to determine the global scale factor through Eq. (5.33). In order to do so, one needs to know the initial volume fractions λ_{ℓ_i} which are in turn related to the $c_{\mathcal{E}}$ and $c_{\mathcal{M}}$. However, in our approach based upon the Buchert framework [40, 41, 50] we do not need to determine $c_{\mathcal{E}}$ and $c_{\mathcal{M}}$, but in stead, obtain from Eq. (6.5) the global scale factor numerically by the method of recursive iteration, using the value $\lambda_{\mathcal{M}_0} = 0.09$ determined through numerical simulations in the earlier literature [50]. We later compare these solutions for the global scale factor with the solutions of the model with an explicit event horizon studied in Section 6.2.3.

6.1.1 BACKREACTION AND SCALAR CURVATURE

It is of interest to study separately the behaviour of the backreaction term in the Buchert model [40, 50]. The backreaction $\mathcal{Q}_{\mathcal{D}}$ is obtained from (5.4) to be

$$\mathcal{Q}_{\mathcal{D}} = 3 \frac{\ddot{a}_{\mathcal{D}}}{a_{\mathcal{D}}} + 4\pi G \langle \rho \rangle_{\mathcal{D}}. \quad (6.6)$$

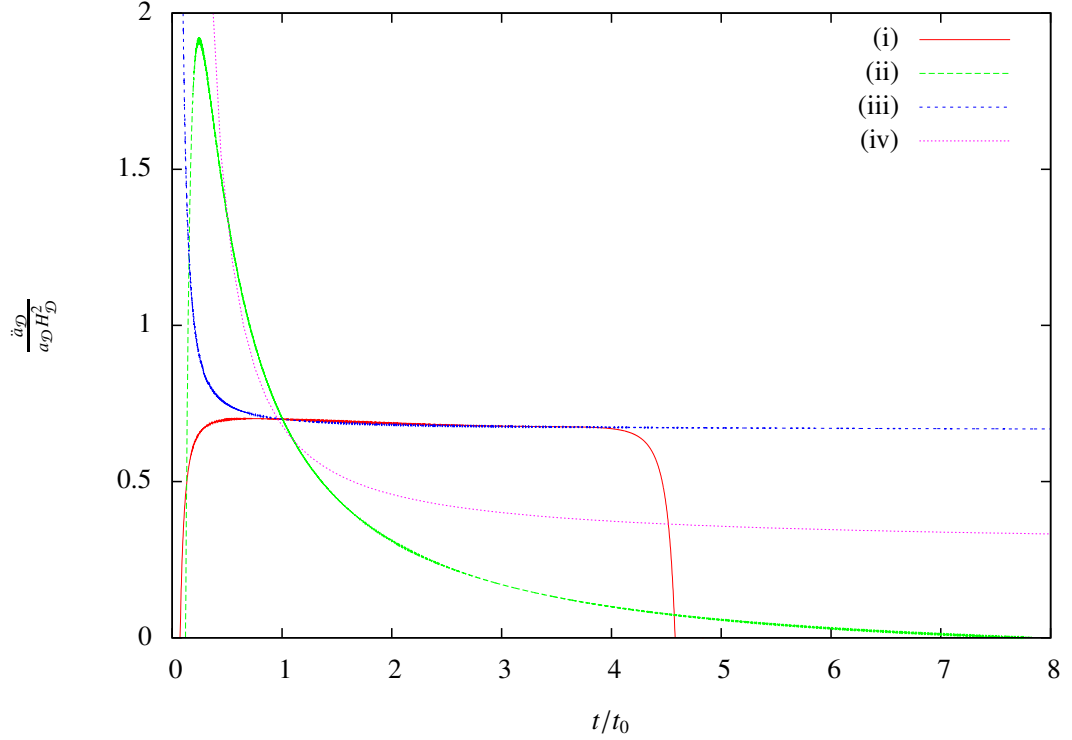


Figure 6.1: The dimensionless global acceleration parameter $\frac{\ddot{a}_D}{a_D H_D^2}$, plotted vs. time (in units of t/t_0 with t_0 being the current age of the Universe). The parameter values used are: (i) $\alpha = 0.995$, $\beta = 0.5$, (ii) $\alpha = 0.995$, $\beta = 0.5$, (iii) $\alpha = 1.02$, $\beta = 0.66$, (iv) $\alpha = 1.02$, $\beta = 0.66$. (The curves (i) and (iii) correspond to the case when an event horizon is included in the analysis in Section 6.2.3).

Note that we are not considering the presence of any cosmological constant Λ as shown in (5.4). We can assume that $\langle \rho \rangle_D$ behaves like the matter energy density, i.e. $\langle \rho \rangle_D = \frac{c_\rho}{a_D^3}$, where c_ρ is a constant. Now, observations tell us that the current matter energy density fraction (baryonic and dark matter) is about 27% and that of dark energy is about 73%. Assuming the dark energy density to be of the order of $10^{-48}(\text{GeV})^4$, we get $\langle \rho \rangle_{D_0} \approx 3.699 \times 10^{-49}(\text{GeV})^4$. Thus, using the values for the global acceleration computed numerically, the future evolution of the backreaction term Q_D can also be computed (see curves (ii) and (iv) of Fig. 6.2, where we have plotted the backreaction density fraction $\Omega_Q^D = -\frac{Q_D}{6H_D^2}$). Once we compute the backreaction it is straightforward to calculate the scalar curvature $\langle \mathcal{R} \rangle_D$ as

$$\langle \mathcal{R} \rangle_D = 16\pi G \langle \rho \rangle_D - Q_D - 6H_D^2. \quad (6.7)$$

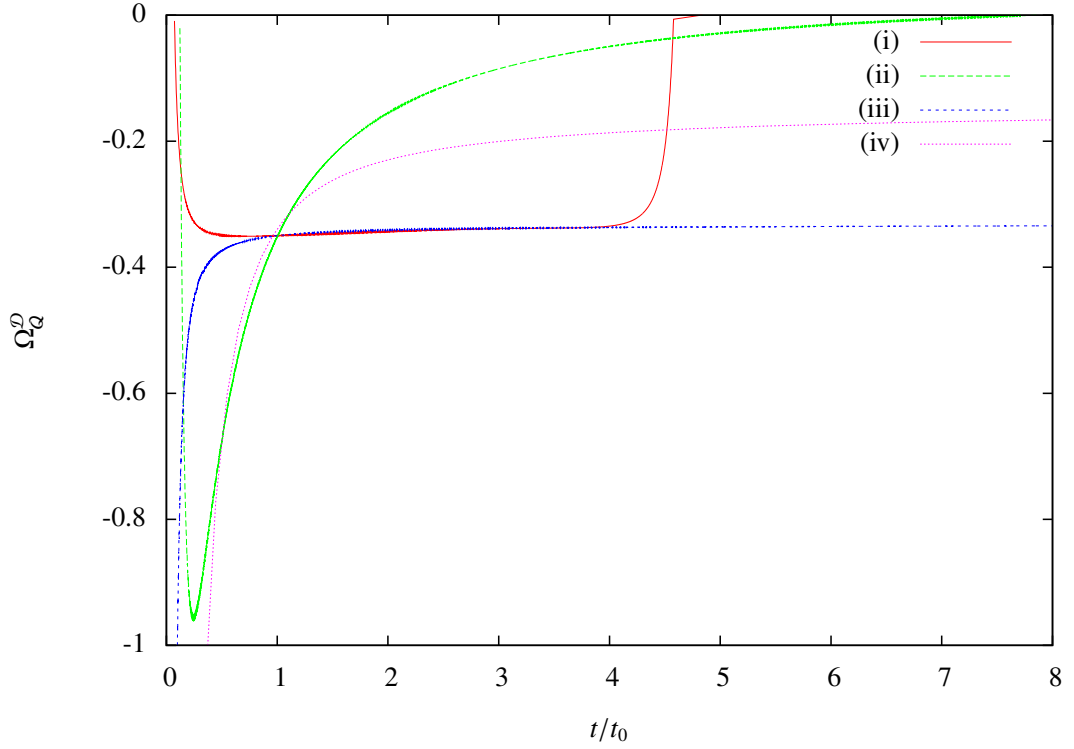


Figure 6.2: Global backreaction density fraction vs. time. The parameter values used are the same as in Fig. 6.1.

6.1.2 EFFECTIVE EQUATION OF STATE

As we have seen before, we can rewrite the Buchert equations in the standard form of Friedmann equations by re-interpreting the geometrical terms as effective sources in the Friedmann equation. We therefore get

$$\begin{aligned} 3\frac{\ddot{a}_{\mathcal{D}}}{a_{\mathcal{D}}} &= -4\pi G (\rho_{eff}^{\mathcal{D}} + 3p_{eff}^{\mathcal{D}}), \\ 3H_{\mathcal{D}}^2 &= 8\pi G \rho_{eff}^{\mathcal{D}}, \end{aligned} \quad (6.8)$$

where the effective energy density and pressure are defined as

$$\begin{aligned} \rho_{eff}^{\mathcal{D}} &= \langle \rho \rangle_{\mathcal{D}} - \frac{1}{16\pi G} \mathcal{Q}_{\mathcal{D}} - \frac{1}{16\pi G} \langle \mathcal{R} \rangle_{\mathcal{D}}, \\ p_{eff}^{\mathcal{D}} &= -\frac{1}{16\pi G} \mathcal{Q}_{\mathcal{D}} + \frac{1}{48\pi G} \langle \mathcal{R} \rangle_{\mathcal{D}}. \end{aligned} \quad (6.9)$$

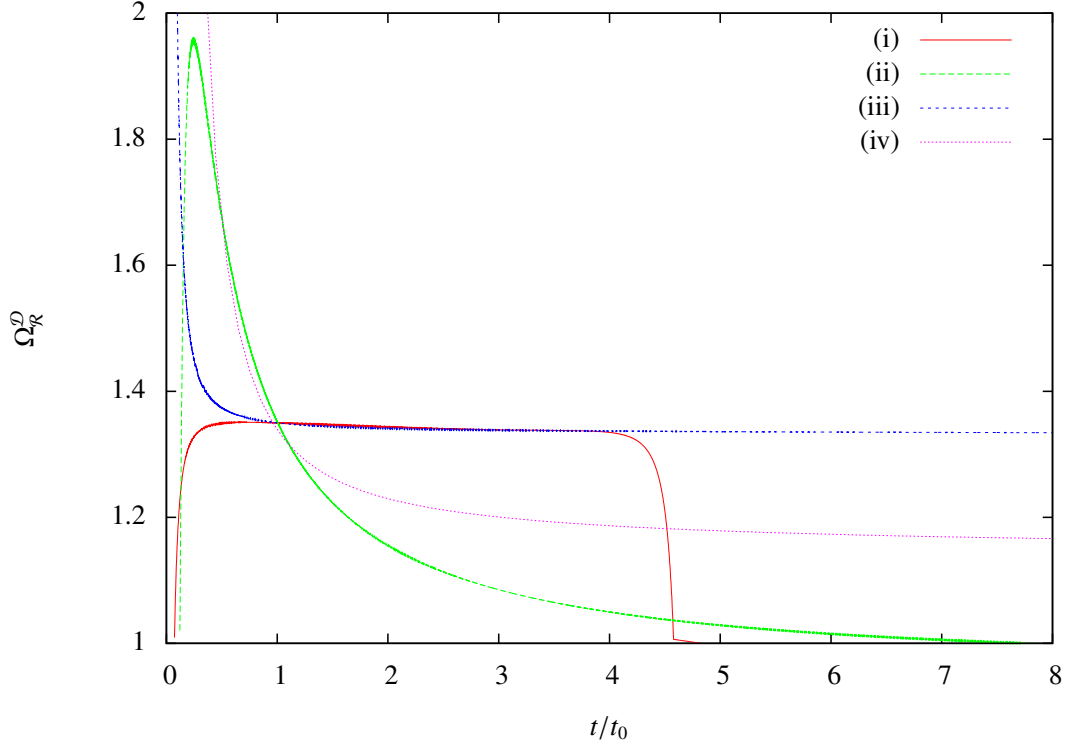


Figure 6.3: Global scalar curvature density fraction, $\Omega_{\mathcal{R}}^{\mathcal{D}}$ plotted vs. time. The parameter values for curves (i) and (ii) are $\alpha = 0.995$, $\beta = 0.5$, and for curves (iii) and (iv) are $\alpha = 1.02$, $\beta = 0.66$.

Note that as in (6.6), here also we are not considering the presence of any cosmological constant Λ . In this sense, $\mathcal{Q}_{\mathcal{D}}$ and $\langle \mathcal{R} \rangle_{\mathcal{D}}$ may be combined to some kind of dark fluid component that is commonly referred to as X-matter. One quantity characterizing this X-matter is its equation of state given by

$$w_{\Lambda,eff}^{\mathcal{D}} = \frac{p_{eff}^{\mathcal{D}}}{\rho_{eff}^{\mathcal{D}} - \langle \rho \rangle_{\mathcal{D}}} = \frac{\mathcal{Q}_{\mathcal{D}} - \frac{1}{3}\langle \mathcal{R} \rangle_{\mathcal{D}}}{\mathcal{Q}_{\mathcal{D}} + \langle \mathcal{R} \rangle_{\mathcal{D}}} = \frac{\Omega_{\mathcal{Q}}^{\mathcal{D}} - \frac{1}{3}\Omega_{\mathcal{R}}^{\mathcal{D}}}{\Omega_{\mathcal{Q}}^{\mathcal{D}} + \Omega_{\mathcal{R}}^{\mathcal{D}}}, \quad (6.10)$$

which is an effective one due to the fact that backreaction and curvature give rise to effective energy density and pressure. We plot this effective equation of state by computing its value numerically (see curves (ii) and (iv) of Fig. 6.4), and later we will compare the results with those obtained by considering the effect of an event horizon.

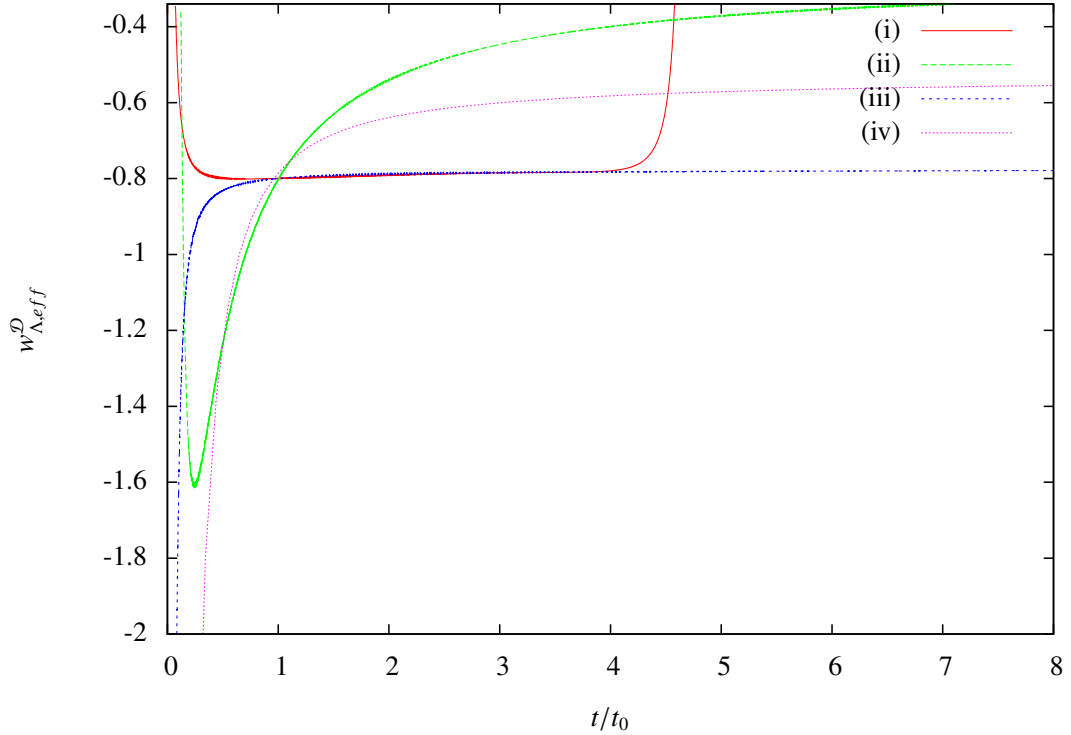


Figure 6.4: Effective equation of state vs. time. The parameter values used are: (i) $\alpha = 0.995$, $\beta = 0.5$, (ii) $\alpha = 0.995$, $\beta = 0.5$, (iii) $\alpha = 1.02$, $\beta = 0.66$, (iv) $\alpha = 1.02$, $\beta = 0.66$

6.2 EFFECT OF EVENT HORIZON

As already stated, we do not need to assume that the current acceleration of the Universe is caused by cosmic backreaction [43, 50]. For the purposes of our analysis it suffices to consider the present acceleration to be caused by any of a variety of mechanisms [4]. Given that we are undergoing a stage of acceleration since transition from an era of structure formation, our aim here was to explore the subsequent evolution of the Universe due to the effects of backreaction in presence of the cosmic event horizon.

In the same spirit as considering $a_{\mathcal{D}} \approx c_F a_F$, we are able to write the expression for the event horizon, which forms at the onset of acceleration, to a good approximation by

$$r_h = a_{\mathcal{D}} \int_t^{\infty} \frac{dt'}{a_{\mathcal{D}}(t')}, \quad (6.11)$$

although spatial and light cone distances and corresponding accelerations can be different, as shown explicitly in the framework of Lemaitre–Tolman–Bondi (LTB) models [75]. The concept of the event horizon just ensures that the effect of backreactions are computed by taking into account only the causally connected processes, but leaving out the processes that are not causally connected, i.e., the effect of inhomogeneities from regions that lie outside the event horizon. Now, from its very definition the event horizon is observer dependent. For example, the event horizon for an observer ‘A’ based, say, in our group of local galaxies, is different from the event horizon for another hypothetical observer ‘B’ based, say, somewhere in a very distant region of the universe. This means that certain regions in the universe that are causally connected to ‘A’ may not be connected to ‘B’, and vice-versa. The regions not causally connected to ‘A’ have no impact on the physics, i.e., the space-time metric for ‘A’ is unaffected by the backreaction from inhomogeneities at those regions. Hence, in a two scale void-wall model that we are using, the event horizon has to be chosen with respect to either ‘A’ (say, wall), or ‘B’ (say, void). However, the important assumption here is that there is indeed a scale of global homogeneity which lies within the horizon volume, and the physics is translationally invariant over such large scales. The void-wall symmetry of Eq. (6.3) thereby ensures that the conclusions are similar whether one chooses to define the event horizon with respect to the wall or with respect to the void.

Since an event horizon forms only those regions of \mathcal{D} that are within the horizon are accessible to us. Hence in this case an apparent volume fraction, given by $\lambda_{\mathcal{M}_h} = \frac{a_{\mathcal{M}_h}^3 |\mathcal{M}_i|_g}{\frac{4}{3}\pi r_h^3}$, is introduced. From equation (6.4) it then follows that

$$\lambda_{\mathcal{M}_h} = \frac{c_{\mathcal{M}_h}^3 t^{3\beta}}{r_h^3}, \quad (6.12)$$

where $c_{\mathcal{M}_h}^3 = c_{\mathcal{M}}^3 |\mathcal{M}_i|_g / \frac{4}{3}\pi$ is a constant. Normalizing the total accessible volume in the presence of the event horizon, we can write

$$\lambda_{\mathcal{E}_h} = 1 - \lambda_{\mathcal{M}_h}, \quad (6.13)$$

where $\lambda_{\mathcal{E}_h}$ is the apparent volume fraction for the subdomain \mathcal{E} . It hence follows that the global acceleration equation (5.34) is now given by

$$\begin{aligned} \frac{\ddot{a}_{\mathcal{D}}}{a_{\mathcal{D}}} = & \frac{c_{\mathcal{M}_h}^3 t^{3\beta}}{r_h^3} \frac{\beta(\beta-1)}{t^2} + \left(1 - \frac{c_{\mathcal{M}_h}^3 t^{3\beta}}{r_h^3}\right) \frac{\alpha(\alpha-1)}{t^2} \\ & + 2 \frac{c_{\mathcal{M}_h}^3 t^{3\beta}}{r_h^3} \left(1 - \frac{c_{\mathcal{M}_h}^3 t^{3\beta}}{r_h^3}\right) \left(\frac{\beta}{t} - \frac{\alpha}{t}\right)^2. \end{aligned} \quad (6.14)$$

6.2.1 EVOLUTION IN A TOY MODEL

In order to obtain the future evolution of the universe with backreaction in presence of the event horizon, one has to solve the above equation for the scale-factor with the event horizon r_h given by equation (6.11). We will eventually obtain numerical solutions of the above integro-differential equations, however, we find that it is instructive to first obtain some physical insight of the evolution by taking recourse to a simple approximation.

To this end, let us for the moment model the onset of the present acceleration of the Universe by an exponential expansion, keeping our analysis close to observations. Specifically, we set $a_{\mathcal{D}} \propto e^{H_{\mathcal{D}} t}$ in equation (6.11) only. (We will see later that this rather crude approximation does indeed give rise to results that are qualitatively similar to the ones obtained through numerical analysis.) Using $H_F = H_{\mathcal{D}}$, where H_F is the FRW Hubble parameter associated with \mathcal{D} , it follows that $r_H = H_F^{-1}$, a constant which we substituted in equation (6.14). With this substitution, the global acceleration $\ddot{a}_{\mathcal{D}}$ vanishes at times given by

$$t^{3\beta} = \frac{r_h^3}{4(\beta-\alpha)c_{\mathcal{M}_h}^3} \left[(3\beta - \alpha - 1) \pm \sqrt{(3\beta - \alpha - 1)^2 + 8\alpha(\alpha - 1)} \right]. \quad (6.15)$$

The scale-factor of the ‘wall’ grows as t^β , where $1/2 \leq \beta \leq 2/3$. The above equation corresponds to real time solutions for $\alpha \geq \frac{1}{3} \left[(\beta + 1) + 2\sqrt{2\beta(1-\beta)} \right]$.

We will now consider two separate cases and describe the evolution of the Universe accordingly.

Case I: $\alpha < 1$ and $\beta \leq 2/3$. There exist two real solutions (6.15) corresponding to two values of time when the global acceleration vanishes. In Fig. 6.5, we have plotted a dimensionless global acceleration parameter $\frac{\ddot{a}_{\mathcal{D}}}{a_{\mathcal{D}} H_0^2}$ with time using equation (6.14). The curves (i) and (ii) correspond to this case showing that the Universe first enters the epoch of acceleration due to backreaction, which sub-

sequently slows down and finally vanishes at the onset of another decelerating era in the future.

Case II: $\alpha \geq 1$ and $\beta \leq 2/3$. From (6.15) it follows that there is only one real solution (minus sign for the square root). This case models the Universe which accelerates due to some other mechanism (not backreaction), but subsequently enters an epoch of deceleration due to backreaction of inhomogeneities in the presence of the event horizon [see curves (iii) and (iv) of Fig. 6.5].

The plots in Fig. 6.5 were done taking the standard values of the parameters $r_h = H_{\mathcal{D}_0}^{-1} = 4.36 \times 10^{17}$ s, while choosing the appropriate range of the parameters α and β , as given in the figure caption. Based on the N-body simulation values used in [50] we also take $\lambda_{\mathcal{M}_{h_0}} = 0.09$. Using the relation $z_T = \exp[H_{\mathcal{D}_0}(t_0 - t_T)] - 1$ where t_T corresponds to the transition time in the past, the redshifts for the transition could be estimated. For example, for the data used in curve (i), the transition from deceleration to acceleration occurs at $z_T \simeq 0.844$, and for curve (ii) we have $z_T \simeq 0.914$ [which are close to the Λ Cold Dark Matter (CDM) value for the standard transition redshift [67]].

6.2.2 FUTURE DECELERATION

We now study the acceleration equation (6.14) numerically without assuming a priori any behaviour for the horizon. Keeping with the spirit of our analysis, we assume that the Universe has entered the accelerated stage and thus a cosmic event horizon has formed. This ensures that r_h defined by (6.11) will be finite valued, enabling us to replace the integral equation (6.11) by

$$\dot{r}_h = \frac{\dot{a}_{\mathcal{D}}}{a_{\mathcal{D}}} r_h - 1. \quad (6.16)$$

Thus, the evolution of the scale-factor is now governed by the set of coupled differential equations (6.14) and (6.16). We numerically integrate these equations by using as an ‘initial condition’ the observational constraint $q_0 \approx -0.7$, where q_0 is the current value of the deceleration parameter, and using the solution for the scale-factor plot the global acceleration versus time in Fig. 6.6 [thus, all the curves in Fig. 6.6 are set to intersect at the point (t_0, q_0)]. The values of the other parameters including α and β are chosen to be the same as in the corresponding curves of the exponential case. As can be seen from Fig. 6.6, the nature of the plots is quite similar to the ones that are obtained in the case assuming a constant event

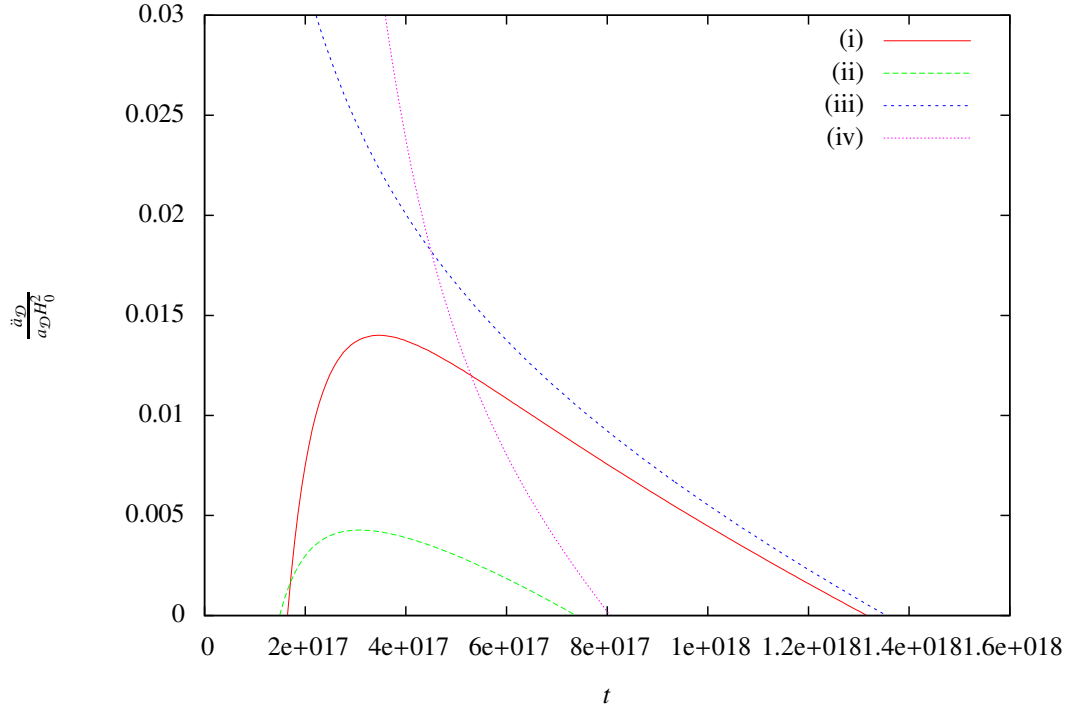


Figure 6.5: The dimensionless global acceleration parameter $\frac{\ddot{a}_D}{a_D H_0^2}$ is plotted versus time (s) assuming a constant horizon. The values for the various parameters used are (i) $\alpha = 0.995$, $\beta = 0.5$, (ii) $\alpha = 0.999$, $\beta = 0.6$, (iii) $\alpha = 1.0$, $\beta = 0.5$ and (iv) $\alpha = 1.02$, $\beta = 0.66$.

horizon, with the $\alpha > 1$ curves signifying only one transition between acceleration and deceleration in the future. The differences in the various slopes and also in the scale for the dimensionless global acceleration parameter in the two cases arise as a result of the approximation of constant horizon used in the former, as well as due to the choice of the condition $q_0 \approx -0.7$ used in the latter.

6.2.3 A DIFFERENT FRAMEWORK FOR THE EVENT HORIZON

Here we will describe a slightly different approach in taking into consideration the effect of the event horizon on the Buchert framework. Since an event horizon forms, only those regions of \mathcal{D} that are within the event horizon are causally accessible to us. We hence define a new fiducial global domain as that contained within the horizon, which naturally is smaller than the original global domain \mathcal{D} that we dealt with in Section 6.1. We assume that the entire Buchert formalism, as outlined in Chapter 5, holds in this new global domain. Note that even if conservation of total

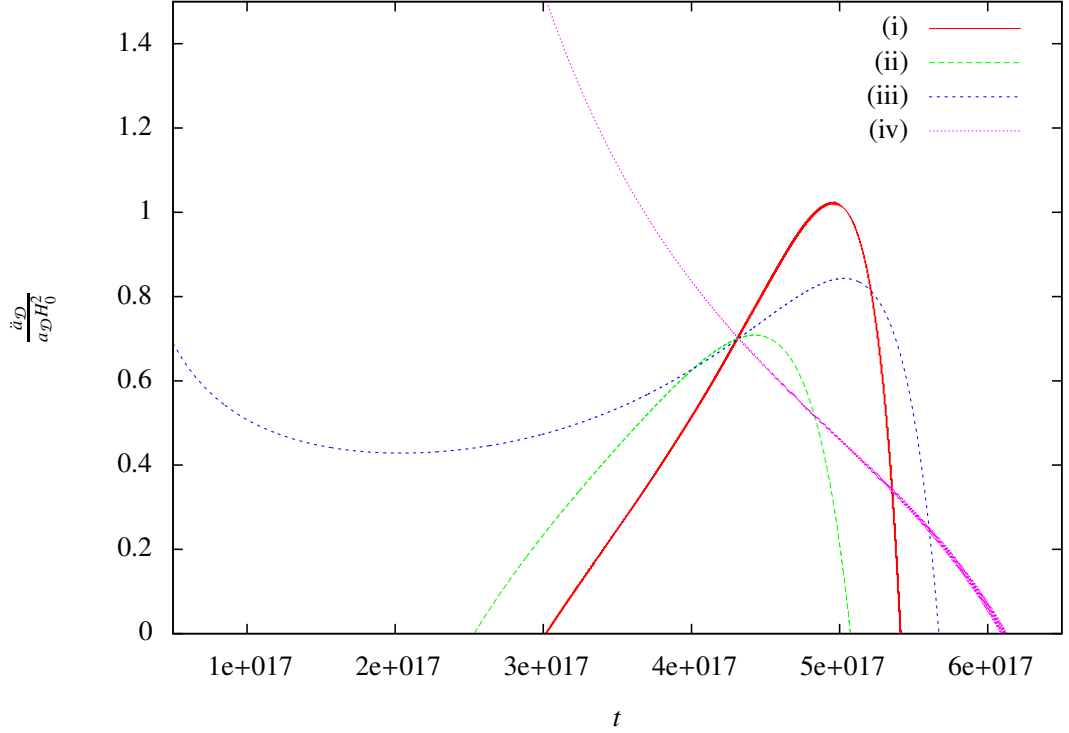


Figure 6.6: The dimensionless global acceleration parameter $\frac{\ddot{a}_{\mathcal{D}}}{a_{\mathcal{D}}H_0^2}$ is plotted versus time (s) as obtained through numerical integration, with the ‘initial condition’ of $q_0 = -0.7$. The values for the various parameters used are chosen to be the same as in the corresponding plots of Fig. 6.5.

rest mass is not strictly or exactly obeyed inside this fiducial global domain, the magnitude of violation is assumed to be rather small since the volume and mass contained within the event horizon is huge, and inflow or outflow is assumed to be a rather insignificant fraction of the total amount. Therefore, in our subsequent analysis we work under the assumption that the Buchert framework is valid up to this approximation. Denoting this domain as $\tilde{\mathcal{D}}$, and the corresponding volume as $|\tilde{\mathcal{D}}|_g$, the volume scale-factor is defined as

$$a_{\tilde{\mathcal{D}}}^3 = \frac{|\tilde{\mathcal{D}}|_g}{|\tilde{\mathcal{D}}_i|_g} = \frac{\frac{4}{3}\pi r_h^3}{|\tilde{\mathcal{D}}_i|_g}, \quad (6.17)$$

where $|\tilde{\mathcal{D}}_i|_g$ is the volume of the fiducial global domain at some initial time, which we can take to be the time when the transition from deceleration to accel-

eration occurs. The average of a scalar valued function (Eq. (5.7)) in $\tilde{\mathcal{D}}$ will be written as

$$\langle f \rangle_{\tilde{\mathcal{D}}}(t) = \frac{\int_{\tilde{\mathcal{D}}} f(t, X^1, X^2, X^3) d\mu_g}{\int_{\tilde{\mathcal{D}}} d\mu_g} = |\tilde{\mathcal{D}}|_g^{-1} \int_{\tilde{\mathcal{D}}} f d\mu_g. \quad (6.18)$$

The Einstein equations (5.4), (5.5) and (5.6) are also assumed to hold in this new domain, after we replace \mathcal{D} with $\tilde{\mathcal{D}}$ in the equations. The domain $\tilde{\mathcal{D}}$ is considered to be divided into several subregions and the average of the scalar valued function f on the domain $\tilde{\mathcal{D}}$ can then be split into the averages of f on the subregions $\tilde{\mathcal{F}}_\ell$ in the form

$$\langle f \rangle_{\tilde{\mathcal{D}}} = \sum_{\ell} |\tilde{\mathcal{D}}|_g^{-1} \sum_{\alpha} \int_{\tilde{\mathcal{F}}_\ell^{(\alpha)}} f d\mu_g = \sum_{\ell} \lambda_{\ell} \langle f \rangle_{\tilde{\mathcal{F}}_\ell}, \quad (6.19)$$

where $\lambda_{\ell} = |\tilde{\mathcal{F}}_\ell|_g / |\tilde{\mathcal{D}}|_g$, is the volume fraction of the subregion $\tilde{\mathcal{F}}_\ell$. Just like in Section 6.1 here also we consider the global domain $\tilde{\mathcal{D}}$ to be divided into a collection of overdense regions $\mathcal{M} = \cup_j \mathcal{M}^j$, with total volume $|\mathcal{M}|_g = \sum_j |\mathcal{M}^j|_g$, and underdense regions $\mathcal{E} = \cup_j \mathcal{E}^j$ with total volume $|\mathcal{E}|_g = \sum_j |\mathcal{E}^j|_g$. We also assume that the scale-factors of the regions \mathcal{E} and \mathcal{M} are, respectively, given by $a_{\mathcal{E}} = c_{\mathcal{E}} t^{\alpha}$ and $a_{\mathcal{M}} = c_{\mathcal{M}} t^{\beta}$ where $\alpha, \beta, c_{\mathcal{E}}$ and $c_{\mathcal{M}}$ are constants. The volume fraction of the subdomain \mathcal{M} is given by $\lambda_{\mathcal{M}} = \frac{|\mathcal{M}|_g}{|\tilde{\mathcal{D}}|_g}$, which can be rewritten in terms of the corresponding scale factors as $\lambda_{\mathcal{M}} = \frac{a_{\mathcal{M}}^3 |\mathcal{M}|_g}{a_{\tilde{\mathcal{D}}}^3 |\tilde{\mathcal{D}}|_g}$.

We can then find the acceleration of this new global domain $\tilde{\mathcal{D}}$, just like we did in Section 6.1. So in this case the global acceleration for $\tilde{\mathcal{D}}$ is given by

$$\begin{aligned} \frac{\ddot{a}_{\tilde{\mathcal{D}}}}{a_{\tilde{\mathcal{D}}}} &= \frac{\tilde{c}_{\mathcal{M}}^3 t^{3\beta}}{a_{\tilde{\mathcal{D}}}^3} \frac{\beta(\beta-1)}{t^2} + \left(1 - \frac{\tilde{c}_{\mathcal{M}}^3 t^{3\beta}}{a_{\tilde{\mathcal{D}}}^3} \right) \frac{\alpha(\alpha-1)}{t^2} \\ &+ 2 \frac{\tilde{c}_{\mathcal{M}}^3 t^{3\beta}}{a_{\tilde{\mathcal{D}}}^3} \left(1 - \frac{\tilde{c}_{\mathcal{M}}^3 t^{3\beta}}{a_{\tilde{\mathcal{D}}}^3} \right) \left(\frac{\beta}{t} - \frac{\alpha}{t} \right)^2. \end{aligned} \quad (6.20)$$

But we can see from (6.17) that $a_{\tilde{\mathcal{D}}} \propto r_h$, so we can write $\frac{\ddot{a}_{\tilde{\mathcal{D}}}}{a_{\tilde{\mathcal{D}}}} = \frac{\ddot{r}_h}{r_h}$ and hence the above equation can be written as

$$\begin{aligned} \frac{\ddot{r}_h}{r_h} = & \frac{c_{\mathcal{M}_h}^3 t^{3\beta}}{r_h^3} \frac{\beta(\beta-1)}{t^2} + \left(1 - \frac{c_{\mathcal{M}_h}^3 t^{3\beta}}{r_h^3}\right) \frac{\alpha(\alpha-1)}{t^2} \\ & + 2 \frac{c_{\mathcal{M}_h}^3 t^{3\beta}}{r_h^3} \left(1 - \frac{c_{\mathcal{M}_h}^3 t^{3\beta}}{r_h^3}\right) \left(\frac{\beta}{t} - \frac{\alpha}{t}\right)^2. \end{aligned} \quad (6.21)$$

Note here that the global domain $\tilde{\mathcal{D}}$ is a fiducial one defined with respect to the observer-dependent event horizon for the purpose of our intermediate analysis, and ultimately we are interested to obtain the evolution of the global domain \mathcal{D} . In order to get the acceleration of the global domain \mathcal{D} we first convert (6.11) to a differential form,

$$\dot{r}_h = \frac{\dot{a}_{\mathcal{D}}}{a_{\mathcal{D}}} r_h - 1. \quad (6.22)$$

Thus, the evolution of the scale-factor $a_{\mathcal{D}}$ is now governed by the set of coupled differential equations (6.21) and (6.22). We numerically integrate these equations by using as an ‘initial condition’ the observational constraint $q_0 = -0.7$, where q_0 is the current value of the deceleration parameter. The global acceleration obtained from these equations is plotted in Fig. 6.1 (curves (i) and (iii)). The expression for q_0 is a completely analytic function of α , β and t_0 , but we since we are studying the effect of inhomogeneities therefore the Universe cannot strictly be described based on a FRW model and hence the current age of the Universe (t_0) cannot be fixed based on current observations which use the FRW model to fix the age. Instead for each combination of values of the parameters α and β we find out the value of t_0 for our model from (6.20) by taking $q_0 = -0.7$. Note that we use the same technique for finding t_0 in Section 6.1, where we use (6.5).

6.3 DISCUSSIONS

Let us now compare the nature of acceleration of the Universe for the two models described respectively, in Sections 6.1 and 6.2.3. The global acceleration for the two models have been plotted in Fig. 6.1. Here curves (i) and (iii) are for the case when an event horizon is included, and curves (ii) and (iv) correspond to the case without an event horizon. For $\alpha < 1$ the acceleration becomes negative in the future for both the cases. The acceleration reaches a much greater value when no event

horizon is present and that too very quickly, but decreases much more gradually than when an event horizon is included. This behaviour could be due to the fact that the inclusion of the event horizon somehow limits the global volume of domain \mathcal{D} in such a way that the available volume of the underdense region \mathcal{E} is lesser than when an event horizon is not included. This causes the overdense region \mathcal{M} to start dominating much earlier and thus causing global deceleration much more quickly. When $\alpha > 1$ the acceleration decreases and reaches a positive constant value asymptotically when an event horizon is not included (curve (iv)), and also when it is included (curve (iii)). Here also we can see that when we include an event horizon in our calculations then there is much more rapid deceleration, the reason for which is mentioned above. Initially the curves for the two cases are almost identical qualitatively, but later on they diverge due to the faster deceleration for the case when an event horizon is included.

A similar comparison of the backreaction for the two models is presented in Fig. 6.2. From the expression of $\Omega_{\mathcal{Q}}^{\mathcal{D}}$ and (5.8) it can be seen that the backreaction will be dominated by the variance of the local expansion rate θ . Here we observe that even for the model where an event horizon is not included, $\Omega_{\mathcal{Q}}^{\mathcal{D}}$ is negative for the duration over which the acceleration is positive. For $\alpha < 1$ the backreaction density first reaches a minimum and then keeps on rising. For the case where an event horizon is included (curve (i)) the backreaction density remains almost constant after reaching a minimum but then when it rises it does so very rapidly as compared to the case where an event horizon is not included (curve (ii)). For $\alpha > 1$ the backreaction density keeps on rising monotonically. Here curves for both the models are initially very similar qualitatively but later on they diverge.

When we look at Fig. 6.3, where the scalar curvature density has been plotted we observe that the scalar curvature turns out to be negative for the duration when the Universe is in accelerated phase, which is what we expect from our knowledge of FRW cosmology. For $\alpha < 1$ the curvature density increases to a maximum and then decreases, the rise to the maximum being much more fast for the case where an event horizon is not included (curve (ii)) whereas the fall from the maximum being much more fast for the case where the event horizon is included (curve (i)). For $\alpha > 1$ the curvature density keeps on decreasing monotonically for both the cases.

We next consider the effective equation of state $w_{\Lambda,eff}^{\mathcal{D}}$ (Fig. 6.4). It remains negative for the entire duration over which the acceleration is positive. For $\alpha <$

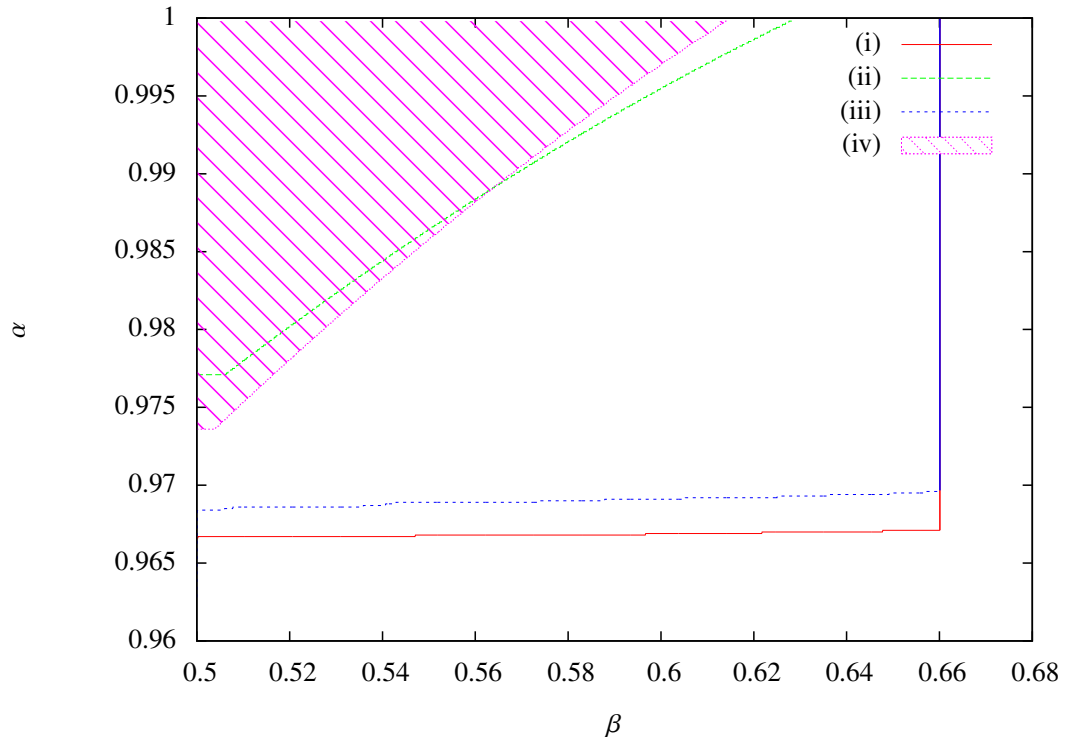


Figure 6.7: The range of parameters α and β for which future deceleration takes place, shown within the respective contours for the curves (i) and (iii) corresponding to the case with an event horizon, and the curves (ii) and (iv) corresponding to the case where an event horizon is not considered. The value of λ_{M_0} for the curves (i) and (ii) is 0.15 and for curves (iii) and (iv) is 0.2. The shaded region corresponds to the curve (iv) demarcating the parameter space for this case when acceleration vanishes in finite future time.

1, $w_{\Lambda,eff}^{\mathcal{D}}$ first reaches a minimum and then keeps on rising. The falling to the minimum is much faster for the model where an event horizon is not included (curve (ii)) whereas for the case with an event horizon the equation of state remains almost constant after reaching the minimum but then rises very rapidly (curve(i)). For $\alpha > 1$ the curves for the two cases are very similar initially qualitatively (again like backreaction plots) but later on they diverge.

From our analysis so far it is clear that the acceleration of the Universe could become negative in the future for certain values of the parameters α and β , which represent the growth rates of the scale factors corresponding to the void and wall, respectively. The range of values of α and β for which a future transition to deceleration is possible, is depicted in Fig. 6.7. We provide a contour plot of α versus β demarcating the range in parameter space (inside of the contours) for which

acceleration vanishes in finite future time. We see that the curves for the model with an event horizon (curves (i) and (iii)) have almost the same value of α for various values of β . This shows that for this case there is no dependence on the value of β to make the acceleration negative in the future. For the case where there is no event horizon (curves (ii) and (iv)), initially the values of α are the same for various values of β , but later on the values of α begin to change and increases as β increases. Since the acceleration has no chance of becoming negative when we have $\alpha > 1$, therefore the maximum limit of α for all the cases is depicted by the line $\alpha = 1$.

6.4 SUMMARY

To summarize, in this work we performed a detailed analysis of the various aspects of the future evolution of the presently accelerating Universe in the presence of matter inhomogeneities. The backreaction of inhomogeneities on the global evolution is calculated within the context of the Buchert framework for a two-scale non-interacting void-wall model [40, 41, 53, 50]. We first analyzed the future evolution using the Buchert framework by computing various dynamical quantities such as the global acceleration, strength of backreaction, scalar curvature and equation of state. Though in this case we did not consider explicitly the effect of the event horizon, it may be argued that a horizon scale is implicitly set by the scale of global homogeneity labelled by the global scale-factor. We show that the Buchert framework allows for the possibility of the global acceleration vanishing at a finite future time, provided that none of the subdomains accelerate individually (both α and β are less than 1).

We next considered in detail a model with an explicit event horizon, for which we described two approaches, the first was presented in [51] and the second in [54]. The observed present acceleration of the universe dictates the occurrence of a future event horizon since the onset of the present accelerating era. It may be noted that though the event horizon is observer dependent, the symmetry of the equation (6.3) ensures that our analysis would lead to similar conclusions for a ‘void’ centric observer, as it does for a ‘wall’ centric one. We showed that the presence of the cosmic event horizon causes the acceleration to slow down significantly with time. Our results indicate the fascinating possibility of backreaction being responsible for not only the present acceleration as shown in earlier works [43, 50], but also

leading to a transition to another decelerated era in the future. Another possibility following from our analysis is that the Universe is currently accelerating due to a different mechanism [4], but with backreaction [40, 53, 50] later causing acceleration to slow down. Our prediction of the future slowing down of acceleration seems to fit smoothly with the earlier era of structure formation and the transition to acceleration in the standard Λ CDM model, as shown here (transition redshift $z_T \approx 0.8$). In order to understand better the underlying physics behind the slowing down of the global acceleration, we explored the nature of the global backreaction, scalar curvature and effective equation of state. We then provided a quantitative comparison of the evolution of these dynamical quantities of this model with the case when an event horizon is not included.

Our analysis showed that, in comparison with the model without an event horizon, during the subsequent future evolution the global acceleration decreases more quickly at late times when we include an event horizon. The reason for this effect is that in the latter model an effective reduction of the volume fraction for the void leads to the overdense region starting to dominate much earlier and hence, causes faster deceleration of the universe. We also found that the acceleration does not vanish in finite time, but in stead goes asymptotically to a constant value for $\alpha > 1$ for both the cases. Nonetheless, when $\alpha > 1$, the curves for acceleration, backreaction, scalar curvature, and effective equation of state for both the cases are very similar qualitatively and only diverge later on. We finally demarcated the region in the parameter space of the growth rates of the void and the wall, where it is possible to obtain a transition to deceleration in the finite future.

Before concluding, in context of the formalism used in the present work it may be worthwhile to recapitulate some of the present debate in the literature regarding averaging on a space-like hypersurface [40, 53, 50] as compared to taking the average on the past light cone. The usefulness of the expansion rate averaged on any hypersurface is determined by relating it to observed quantities. It has been observed that the redshift and distance can be expressed in terms of the average geometry alone, provided that the contribution of the null shear is negligible [76]. Observationally, the shear is known to be indeed small [77]. Nonetheless, it has been claimed that neither averaging on a constant time hypersurface nor light cone averaging is easy to connect with the observations corresponding to parameters of the Λ CDM model [78]. The task of developing a procedure for light cone averaging is an ambitious programme and till date there is no standard formalism to do so.

In a recent paper, three different types of light cone averaging have been proposed [79], though much work remains to be done in order to apply their technique to the problem of cosmic acceleration. On the other hand, our present work introduces an element of light cone physics from another perspective by considering an effect due to the event horizon.

CHAPTER 7

BACKREACTION WITH MULTIPLE DOMAINS

So far we have studied the effects of cosmic backreaction within the Buchert framework using a simple two-scale model [51], and our model indicated the possibility of a transition to a future era. The Buchert framework has been further extended in [50] so as to facilitate the study of backreaction in the case where the universe is considered to be divided into multiple domains and subdomains. But the model that was considered in [50] was a simple model consisting of one overdense subdomain and one underdense subdomain, like that used in [51]. Such a simple model is attractive because it simplifies the evolution equations and eases the process of understanding the effect of backreaction on the evolution of the Universe. But the real Universe cannot be partitioned simply into one overdense subdomain and one underdense subdomain. To the best of our knowledge, so far there has been no study on the effect of backreaction from inhomogeneities by considering multiple subdomains. Using the formalism proposed in [50], in the present work, which is based on our paper [80], we improve upon our previous two-scale model and consider the Universe as a global domain \mathcal{D} which is partitioned into multiple overdense and underdense regions, and all these subdomains are taken to evolve differently to each other. This is done in order to recreate the real Universe as much as possible in our simple model. Our aim here is to study the future evolution of the Universe by taking into consideration its current accelerated expansion. The accelerated expansion of the Universe can be assumed to be caused by backreaction or any other mechanism [4]. We consider two different partitioning cases of the Universe and explore the future evolution of the Universe for these two cases and then perform a comparative analysis for the two.

7.1 FUTURE EVOLUTION

We consider \mathcal{D} to be partitioned into equal numbers of overdense and underdense domains. We label all overdense domains as \mathcal{M} (called ‘Wall’) and all underdense domains as \mathcal{E} (called ‘Void’), such that $\mathcal{D} = (\cup_j \mathcal{M}^j) \cup (\cup_j \mathcal{E}^j)$. In this case one obtains $H_{\mathcal{D}} = \sum_j \lambda_{\mathcal{M}_j} H_{\mathcal{M}_j} + \sum_j \lambda_{\mathcal{E}_j} H_{\mathcal{E}_j}$, with similar expressions for $\langle \rho \rangle_{\mathcal{D}}$ and $\langle \mathcal{R} \rangle_{\mathcal{D}}$ and also $\sum_j \lambda_j = 1$. For such a partitioning the global acceleration (5.34) can be written as

$$\begin{aligned} \frac{\ddot{a}_{\mathcal{D}}}{a_{\mathcal{D}}} &= \sum_j \lambda_{\mathcal{M}_j} \frac{\ddot{a}_{\mathcal{M}_j}}{a_{\mathcal{M}_j}} + \sum_j \lambda_{\mathcal{E}_j} \frac{\ddot{a}_{\mathcal{E}_j}}{a_{\mathcal{E}_j}} \\ &\quad + \sum_{j \neq k} \lambda_{\mathcal{M}_j} \lambda_{\mathcal{M}_k} (H_{\mathcal{M}_j} - H_{\mathcal{M}_k})^2 \\ &\quad + \sum_{j \neq k} \lambda_{\mathcal{E}_j} \lambda_{\mathcal{E}_k} (H_{\mathcal{E}_j} - H_{\mathcal{E}_k})^2 \\ &\quad + 2 \sum_{j, k} \lambda_{\mathcal{M}_j} \lambda_{\mathcal{E}_k} (H_{\mathcal{M}_j} - H_{\mathcal{E}_k})^2. \end{aligned} \quad (7.1)$$

We assume that the scale-factors of the regions \mathcal{E}^j and \mathcal{M}^j are, respectively, given by $a_{\mathcal{E}_j} = c_{\mathcal{E}_j} t^{\alpha_j}$ and $a_{\mathcal{M}_j} = c_{\mathcal{M}_j} t^{\beta_j}$ where α_j , β_j , $c_{\mathcal{E}_j}$ and $c_{\mathcal{M}_j}$ are constants. The volume fraction of the subdomain \mathcal{M}^j is given by $\lambda_{\mathcal{M}_j} = \frac{|\mathcal{M}^j|_g}{|\mathcal{D}|_g}$, which can be rewritten in terms of the corresponding scale factors as $\lambda_{\mathcal{M}_j} = \frac{a_{\mathcal{M}_j}^3 |\mathcal{M}_i^j|_g}{a_{\mathcal{D}}^3 |\mathcal{D}_i|_g}$, and similarly for the \mathcal{E}^j subdomains. We therefore find that the global acceleration equation (7.1) becomes

$$\begin{aligned} \frac{\ddot{a}_{\mathcal{D}}}{a_{\mathcal{D}}} &= \sum_j \frac{g_{\mathcal{M}_j}^3 t^{3\beta_j}}{a_{\mathcal{D}}^3} \frac{\beta_j(\beta_j - 1)}{t^2} + \sum_j \frac{g_{\mathcal{E}_j}^3 t^{3\alpha_j}}{a_{\mathcal{D}}^3} \frac{\alpha_j(\alpha_j - 1)}{t^2} \\ &\quad + \sum_{j \neq k} \frac{g_{\mathcal{M}_j}^3 t^{3\beta_j}}{a_{\mathcal{D}}^3} \frac{g_{\mathcal{M}_k}^3 t^{3\beta_k}}{a_{\mathcal{D}}^3} \left(\frac{\beta_j}{t} - \frac{\beta_k}{t} \right)^2 \\ &\quad + \sum_{j \neq k} \frac{g_{\mathcal{E}_j}^3 t^{3\alpha_j}}{a_{\mathcal{D}}^3} \frac{g_{\mathcal{E}_k}^3 t^{3\alpha_k}}{a_{\mathcal{D}}^3} \left(\frac{\alpha_j}{t} - \frac{\alpha_k}{t} \right)^2 \\ &\quad + 2 \sum_{j, k} \frac{g_{\mathcal{M}_j}^3 t^{3\beta_j}}{a_{\mathcal{D}}^3} \frac{g_{\mathcal{E}_k}^3 t^{3\alpha_k}}{a_{\mathcal{D}}^3} \left(\frac{\beta_j}{t} - \frac{\alpha_k}{t} \right)^2, \end{aligned} \quad (7.2)$$

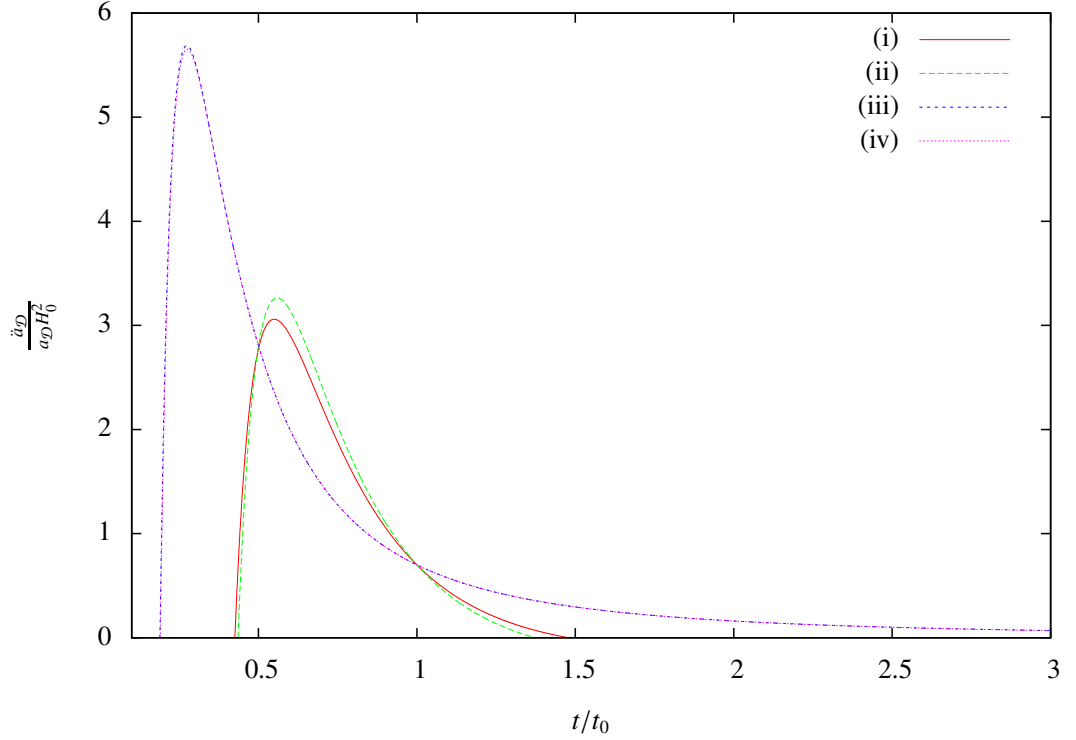


Figure 7.1: The dimensionless global acceleration parameter $\frac{\ddot{a}_{\mathcal{D}}}{a_{\mathcal{D}}H_0^2}$, plotted vs. time (in units of t/t_0 with t_0 being the current age of the Universe). In curves (i) and (ii) the value of α is in the range $0.990 - 0.999$ and that of β is in the range $0.58 - 0.60$. In curves (iii) and (iv) the value of α is in the range $1.02 - 1.04$ and that of β is in the range $0.58 - 0.60$

where $g_{\mathcal{M}_j}^3 = \frac{\lambda_{\mathcal{M}_j} a_{\mathcal{D}0}^3}{t_0^{3\beta_j}}$ and $g_{\mathcal{E}_j}^3 = \frac{\lambda_{\mathcal{E}_j} a_{\mathcal{D}0}^3}{t_0^{3\alpha_j}}$ are constants.

We will perform a comparative study of two cases where (i) the global domain \mathcal{D} is considered to be divided into 50 overdense and underdense subdomains each and (ii) 100 overdense and underdense subdomains each. We will obtain numerical solutions of equation (7.2) for various ranges of parameter values. In order to do this we consider the range of values for the parameters α_j and β_j as a Gaussian distribution, which is of the form $\frac{1}{\sigma\sqrt{2\pi}} \exp\left[-\frac{(x-\mu)^2}{2\sigma^2}\right]$, where σ is the standard deviation and μ is the mean (the range of values corresponds to the full width at half maximum of the distribution). We also assign values for the volume fractions $\lambda_{\mathcal{M}_j}$ and $\lambda_{\mathcal{E}_j}$ based on a Gaussian distribution and impose the restriction that the total volume fraction of all the overdense subdomains at present time should be 0.09, a value that has been determined through numerical simulations in the earlier literature [50]. Note here that using our ansatz for the

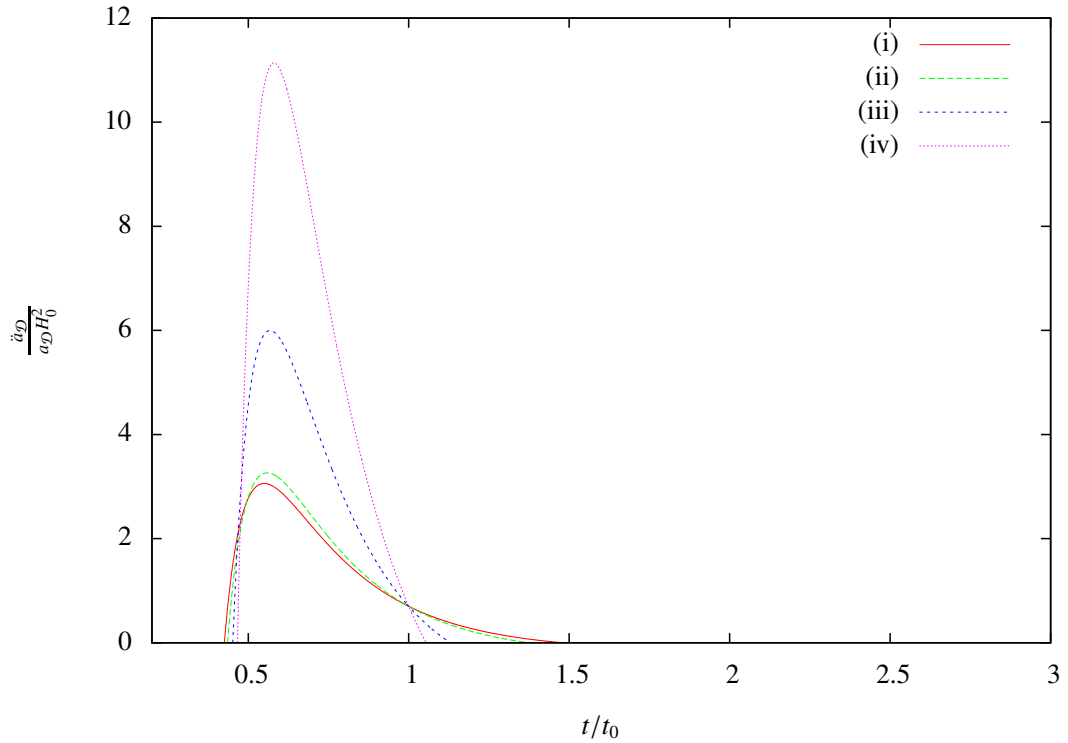


Figure 7.2: Here also $\frac{\ddot{a}_D}{a_D H_0^2}$ is plotted vs. time. In curves (i) and (ii) the value of α lies in the range $0.990 - 0.999$ and that of β is in the range $0.58 - 0.60$. For curves (iii) and (iv) the value of α is in the range $0.990 - 0.999$ and that of β is in the range $0.55 - 0.65$

subdomain scale factors one may try to determine the global scale factor through Eq. (5.33). In order to do so, one needs to know the initial volume fractions λ_{ℓ_i} which are in turn related to the $c_{\mathcal{E}_j}$ and $c_{\mathcal{M}_j}$. However, in our approach based upon the Buchert framework [40, 41, 50] we did not need to determine $c_{\mathcal{E}_j}$ and $c_{\mathcal{M}_j}$, but instead, obtained from Eq. (7.2) the global scale factor numerically by the method of recursive iteration, using as an ‘initial condition’ the observational constraint $q_0 = -0.7$, where q_0 is the current value of the deceleration parameter. The expression for q_0 is a completely analytic function of α_j , β_j and t_0 , but since we are studying the effect of inhomogeneities therefore the Universe cannot strictly be described based on a FRW model and hence the current age of the Universe (t_0) cannot be fixed based on current observations which use the FRW model to fix the age. Instead for each combination of values of the parameters α_j and β_j we find out the value of t_0 for our model from (7.2) by taking $q_0 = -0.7$.

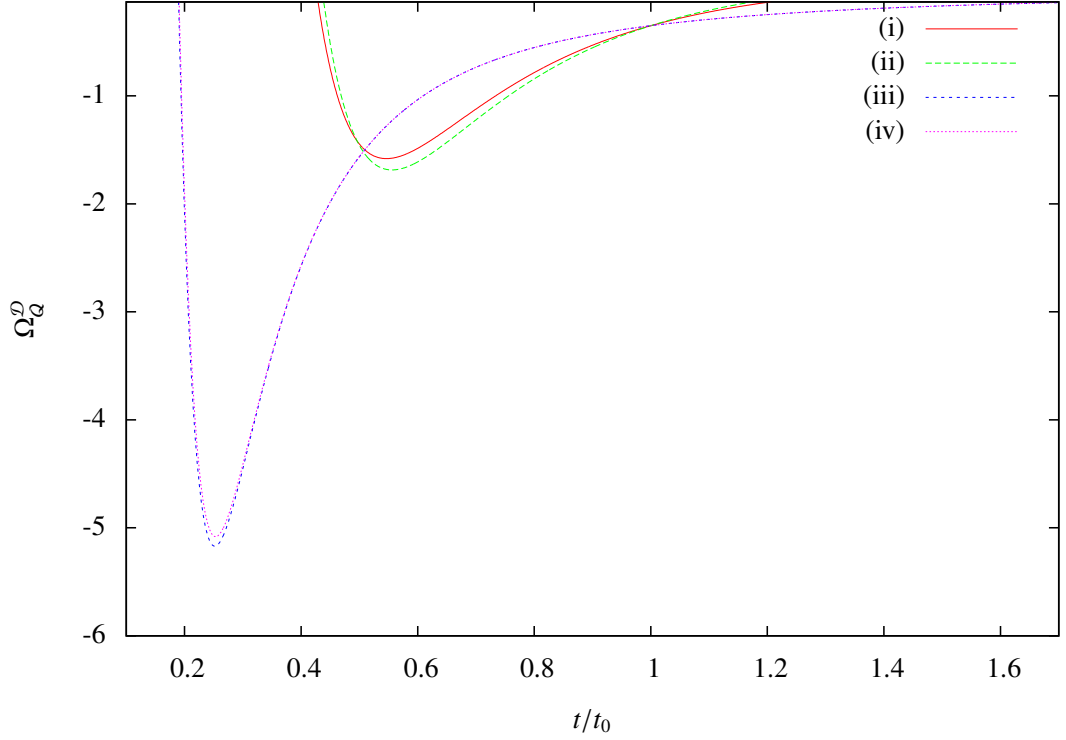


Figure 7.3: Global backreaction density $\Omega_{\mathcal{Q}}^{\mathcal{D}}$ plotted vs. time (in units of t/t_0). In curves (i) and (ii) the value of α is in the range $0.990 - 0.999$ and that of β is in the range $0.58 - 0.60$. In curves (iii) and (iv) the value of α is in the range $1.02 - 1.04$ and that of β is in the range $0.58 - 0.60$

It is of interest to study separately the behaviour of the backreaction term in the Buchert model [40, 50]. The backreaction $\mathcal{Q}_{\mathcal{D}}$ is obtained from (5.4) to be

$$\mathcal{Q}_{\mathcal{D}} = 3 \frac{\ddot{a}_{\mathcal{D}}}{a_{\mathcal{D}}} + 4\pi G \langle \rho \rangle_{\mathcal{D}}. \quad (7.3)$$

Note that we are not considering the presence of any cosmological constant Λ as shown in (5.4). We can assume that $\langle \rho \rangle_{\mathcal{D}}$ behaves like the matter energy density, i.e. $\langle \rho \rangle_{\mathcal{D}} = \frac{c_{\rho}}{a_{\mathcal{D}}^3}$, where c_{ρ} is a constant. Now, observations tell us that the current matter energy density fraction (baryonic and dark matter) is about 27% and that of dark energy is about 73%. Assuming the dark energy density to be of the order of $10^{-48} (GeV)^4$, we get $\rho_{\mathcal{D}_0} \simeq 3.699 \times 10^{-49} (GeV)^4$. Thus, using the values for the global acceleration computed numerically, the future evolution of the backreaction term $\mathcal{Q}_{\mathcal{D}}$ can also be computed (see Figs. 7.3 and 7.4, where we have plotted the backreaction density fraction $\Omega_{\mathcal{Q}}^{\mathcal{D}} = -\frac{\mathcal{Q}_{\mathcal{D}}}{6H_{\mathcal{D}}^2}$).

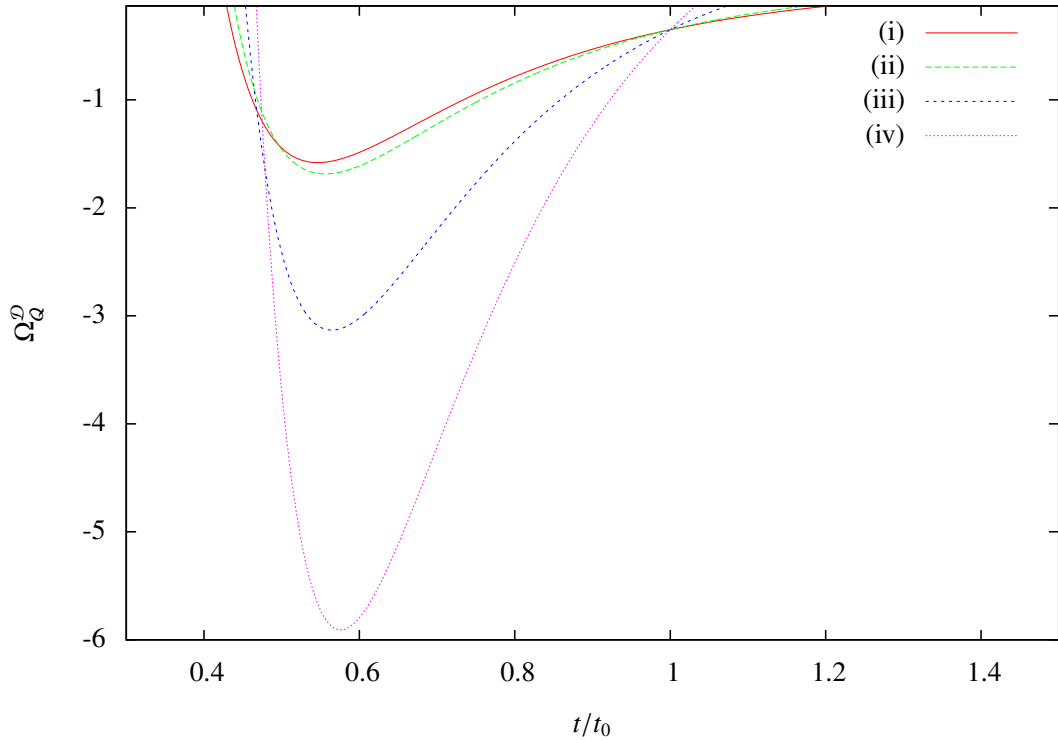


Figure 7.4: Here also $\Omega_{\mathcal{Q}}^{\mathcal{D}}$ is plotted vs. time. In curves (i) and (ii) the value of α lies in the range $0.990 - 0.999$ and that of β is in the range $0.58 - 0.60$. For curves (iii) and (iv) the value of α is in the range $0.990 - 0.999$ and that of β is in the range $0.55 - 0.65$

7.2 DISCUSSIONS

Let us now compare the nature of acceleration of the Universe for the two cases described in the previous section. The global acceleration for the two cases have been plotted in Figs. 7.1 and 7.2. In both the figures curves (i) and (iii) are for the case where \mathcal{D} is partitioned into 50 overdense and underdense subdomains each, and curves (ii) and (iv) correspond to the case where \mathcal{D} is partitioned into 100 overdense and underdense subdomains each. The values for the expansion parameters β_j of the overdense subdomains is taken to lie between $1/2$ and $2/3$ since the expansion is assumed to be faster than in the radiation dominated case, and is upper limited by the value for matter dominated expansion. In Fig. 7.1 the behaviour of global acceleration is shown for values of $\alpha_j < 1$ and also $\alpha_j > 1$, keeping the range of values of β_j quite narrow and also the same for all four curves. We have kept the value of α_j close to 1 when $\alpha_j < 1$ because if α_j is less than a certain value, which depends on the value of β_j , then the acceleration becomes

undefined as we do not get real solutions from (7.2). In order to demonstrate this fact analytically let us consider a toy model where \mathcal{D} is divided into one overdense subdomain \mathcal{M} and one underdense subdomain \mathcal{E} . In this case (7.2) can be written as

$$\begin{aligned} \frac{\ddot{a}_{\mathcal{D}}}{a_{\mathcal{D}}} &= \frac{g_{\mathcal{M}}^3 t^{3\beta}}{a_{\mathcal{D}}^3} \frac{\beta(\beta-1)}{t^2} + \frac{g_{\mathcal{E}}^3 t^{3\alpha}}{a_{\mathcal{D}}^3} \frac{\alpha(\alpha-1)}{t^2} \\ &+ 2 \frac{g_{\mathcal{M}}^3 t^{3\beta}}{a_{\mathcal{D}}^3} \frac{g_{\mathcal{E}}^3 t^{3\alpha}}{a_{\mathcal{D}}^3} \left(\frac{\beta}{t} - \frac{\alpha}{t} \right)^2. \end{aligned} \quad (7.4)$$

Now we must have $\lambda_{\mathcal{M}} + \lambda_{\mathcal{E}} = 1$, so we can write $\frac{g_{\mathcal{E}}^3 t^{3\beta}}{a_{\mathcal{D}}^3} = 1 - \frac{g_{\mathcal{M}}^3 t^{3\beta}}{a_{\mathcal{D}}^3}$. Therefore the above equation now becomes

$$\begin{aligned} \frac{\ddot{a}_{\mathcal{D}}}{a_{\mathcal{D}}} &= \frac{g_{\mathcal{M}}^3 t^{3\beta}}{a_{\mathcal{D}}^3} \frac{\beta(\beta-1)}{t^2} + \left(1 - \frac{g_{\mathcal{M}}^3 t^{3\beta}}{a_{\mathcal{D}}^3} \right) \frac{\alpha(\alpha-1)}{t^2} \\ &+ 2 \frac{g_{\mathcal{M}}^3 t^{3\beta}}{a_{\mathcal{D}}^3} \left(1 - \frac{g_{\mathcal{M}}^3 t^{3\beta}}{a_{\mathcal{D}}^3} \right) \left(\frac{\beta}{t} - \frac{\alpha}{t} \right)^2. \end{aligned} \quad (7.5)$$

From this equation we see that the global acceleration vanishes at times given by

$$\begin{aligned} t^{3\beta} a_{\mathcal{D}}^3 &= \frac{1}{4(\beta-\alpha)g_{\mathcal{M}}^3} [(3\beta-\alpha-1) \\ &\pm \sqrt{(3\beta-\alpha-1)^2 + 8\alpha(\alpha-1)}]. \end{aligned} \quad (7.6)$$

This shows us that we get real time solutions for $\alpha \geq \frac{1}{3} \left[(\beta+1) + 2\sqrt{2\beta(1-\beta)} \right]$. If we now consider $\beta = 0.5$ (its lowest possible value) then we get $\alpha \geq 0.971404521$ and if we consider $\beta = 0.66$ (its highest possible value) then we get $\alpha \geq 0.999950246$. Hence as stated earlier, for a particular value of β we have a lower limit on the value of α .

In Fig. 7.1, for $\alpha_j < 1$ the acceleration becomes negative in the future for both cases of partitioning (curves (i) and (ii)). The acceleration reaches a greater value and at a slightly later time when \mathcal{D} is partitioned into 100 overdense and underdense subdomains (curve (ii)) and also becomes negative at an earlier time as

compared to the case where \mathcal{D} is partitioned into 50 overdense and underdense subdomains (curve (i)). When $\alpha_j > 1$ then we see that the acceleration curves for the two cases are almost identical, with the maximum value being very slightly larger for partition type (i) (curve (iii)). After reaching the maximum the acceleration decreases and goes asymptotically to a small positive value. When $\alpha_j < 1$ then the first two terms of (7.2) are negative, but the last term, which is always positive, gains prominence as the number of subdomains increases thus increasing the acceleration. When $\alpha_j > 1$ then only the first term in (7.2) is negative and hence the acceleration curves for the two partition cases (curves (iii) and (iv)) are very similar, the only visible difference being the slightly higher maximum value when \mathcal{D} is partitioned into a lower number of subdomains.

In Fig. 7.2 we have illustrated the behaviour of the global acceleration by taking narrow and broad ranges of values of β_j and keeping $\alpha_j < 1$ and the same for all the curves. As seen in Fig. 7.1 here also the acceleration becomes negative in the future for all the curves because we have $\alpha_j < 1$ for all of them, but we see that the difference between the acceleration curves for the two partition cases is very small when we consider a narrow range of values of β_j (curves (i) and (ii)) and the difference increases considerably when we consider a broad range of values of β_j (curve (iii) and (iv)). The acceleration attains a much greater value when \mathcal{D} is partitioned into a larger number of subdomains and also becomes negative quicker. The reason for the latter behaviour is that the broad range of values of β_j makes the third term in (7.2) gain more prominence when we consider a larger number of subdomains thus resulting in greater positive acceleration.

A similar comparison of the backreaction for the two models is presented in Figs. 7.3 and 7.4 where we have plotted the backreaction density for the duration over which the global acceleration is positive. We see in these figures that the backreaction density is negative and from the expression of $\Omega_{\mathcal{Q}}^{\mathcal{D}}$ and (5.8) it can be seen that the backreaction will be dominated by the variance of the local expansion rate θ . In Fig. 7.3 we see that for $\alpha_j < 1$, the backreaction density reaches a minimum, which is also greater in magnitude, for partition type (ii) (curve (ii)) as compared to partition type (i) (curve (i)). For $\alpha_j > 1$ the curves for the two cases are almost identical, the only difference being that for partition type (i) (curve (iii)) the backreaction density reaches a minimum of greater magnitude. In Fig. 7.4 we see that, just like the acceleration curves, the difference between the backreaction plots for the two partition cases is much smaller when we consider a narrow range

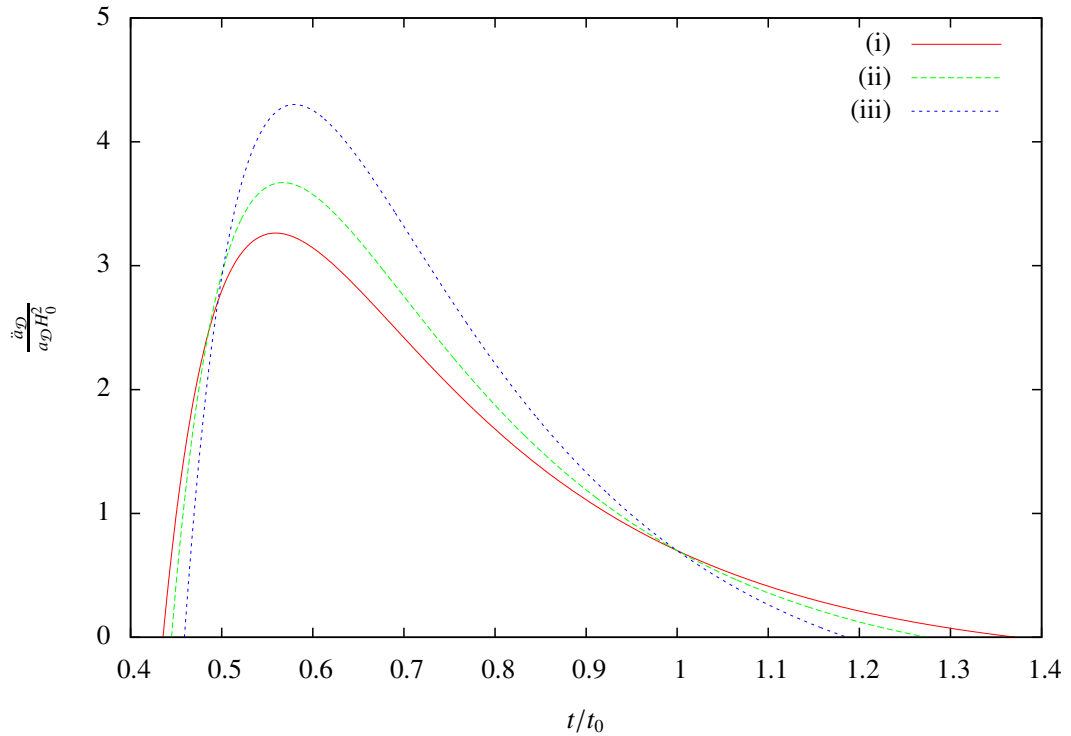


Figure 7.5: We plot $\frac{\ddot{a}_{\mathcal{D}}}{a_{\mathcal{D}}H_0^2}$ vs. t/t_0 for various numbers of subdomains. In all the curves we have α_j in the range $0.990 - 0.999$, and β_j in the range $0.58 - 0.60$. For curve (i) we consider 100 overdense and underdense subdomains, in (ii) 400 overdense and underdense subdomains and in (iii) 500 overdense and underdense subdomains each.

of values of β_j , but the difference becomes quite large when we consider a broad range of values of β_j . The behaviour of the backreaction as illustrated in Figs. 7.3 and 7.4 is quite similar to the global acceleration, as seen in Figs. 7.1 and 7.2, and that is expected because from (5.8) we see that $\mathcal{Q}_{\mathcal{D}}$ is linearly proportional to the global acceleration.

In order to see how the global acceleration behaves based on the number of subdomains we have in Fig. 7.5 plotted the global acceleration vs. time for three partition cases where we consider (i) 100 overdense and underdense subdomains, (ii) 400 overdense and underdense subdomains and (iii) 500 overdense and underdense subdomains each. For all three cases we have kept the range of values of α_j and β_j the same and taken $\alpha_j < 1$. It is clearly seen from the plot that the global acceleration increases in magnitude as the number of subdomains increases, and the maximum is obtained later in time with increase in the number of subdomains.

We also see that the acceleration becomes negative faster when the number of subdomains increases.

7.3 SUMMARY

To summarize, in this work we performed a detailed analysis of the various aspects of the future evolution of the presently accelerating universe in the presence of matter inhomogeneities. The effect of backreaction from inhomogeneities on the global evolution is calculated within the context of the Buchert framework by considering the universe to be divided into multiple underdense and overdense domains, each evolving independently, in order to recreate the real universe more accurately [40, 41, 53, 50]. We analyzed the future evolution of the universe using the Buchert framework by computing the global acceleration and strength of backreaction. We showed that the Buchert framework allows for the possibility of the global acceleration vanishing at a finite future time, provided that none of the subdomains accelerate individually (both α_j and β_j are less than 1).

Our analysis shows that if the β_j parameters are distributed over a narrow range of values and $\alpha_j < 1$ then the global acceleration reaches a greater maximum, when the number of subdomains is larger, showing that the last term in (7.2), which is always positive, has more prominence for a large number of subdomains. This difference between the accelerations for the two partition cases decreases even more when $\alpha_j > 1$, because then only the first term in (7.2) has a negative contribution. However when we consider a broad range of values of β_j then the difference between the accelerations for the two cases becomes much larger, the acceleration being greater for a larger number of subdomains. The cause for this is attributed to the dominance of the third term in (7.2) when we have a larger number of subdomains and a broad range of values of β_j . We also saw that the behaviour of the backreaction mimics the behaviour of the global acceleration, and that is expected because as seen from (5.8), we have Q_D linearly proportional to the acceleration.

Our results indicate that backreaction can not only be responsible for the current accelerated expansion, as shown in earlier works [43, 50], but can also cause the acceleration to slow down and even lead to a future decelerated era in some cases. In drawing this conclusion it was not necessary for us to assume that the

current acceleration is caused by backreaction, and the acceleration could have been caused by any other mechanism [4].

CHAPTER 8

CONCLUSIONS

The current accelerated expansion of the Universe is one of the most important unsolved problems in modern cosmology and physicists are coming up with ever innovative ideas to explain the nature of Dark Energy, the component of the Universe that is said to cause the acceleration. There are a wide variety of theories [4] that cover a broad spectrum of approaches. The ideas started with scalar field models of dark energy, shifting to modifying the framework of gravity in order to explain the phenomenon, and new ideas are being proposed regularly. The most simple explanation for the current acceleration is offered by the cosmological constant, which has a constant energy density and an equation of state of -1 , and which is consistent with several important observations such as the redshift of distant supernovae, the power spectrum of the CMB, and the distribution of the large scale structure. But there are several problems associated with this approach [3], most notable of them being the *cosmological constant problem* and the *cosmic coincidence problem*. Therefore despite the simplicity of the above approach alternate ideas are being proposed to explain the acceleration and these theories almost always present a dynamic dark energy component, one whose energy density and equation of state varies with time. Since our current observational data are quite favourable towards the presence of a cosmological constant type term today, therefore any dynamically evolving contribution must resemble a cosmological constant today.

There are several scalar field based models that try to explain the phenomenon of dark energy and in this thesis we have discussed about the k -essence scalar field approach. The distinguishing feature of k -essence is that the Lagrangian of the scalar field contains non-canonical kinetic terms. It is widely believed that the early Universe went through a period of rapid accelerated expansion which is known as “inflation” and since accelerated expansion is a common feature in the

both the early and the late Universe it is plausible that some common mechanism could be responsible for both. Several models have been constructed to explain inflation and dark energy using a single scalar field. Dark matter figures as the majority of matter in the Universe and its true nature is also unknown to us. Since the nature of both dark matter and dark energy are unknown, it is plausible that these two mysterious components of the universe are the manifestations of a single entity. Several examples of attempts to unify dark matter and dark energy can be found in the literature. An important subset of models of k -essence is purely kinetic k -essence, where the Lagrangian of the scalar field depends only on the kinetic component and does not explicitly depend on the field itself. We have been able to show that using a purely kinetic k -essence model it is not possible to unify dark energy and dark matter using the most simple unification scheme. However it did not rule out the possibility of exploring other avenues in order to achieve a unification using purely kinetic k -essence.

In our work with k -essence we were able to unify inflation, dark energy and dark matter using a single scalar field. In the first model that we presented the inflation in the early Universe was identical to that obtained from a standard chaotic inflation model involving a quadratic potential. At the end of inflation when the potential in our model became negligible in comparison to the kinetic component we were able to approximate the model as purely kinetic k -essence. We found that the resultant energy density contained terms that achieved the unification of dark matter and dark energy, the dark energy component being identical to a cosmological constant. In our other model based on k -essence we also tried to achieve a triple unification like in the first model, but in this case inflation in the early Universe was produced through the process of k -inflation. Although in both models we were able to obtain accelerated expansion in the late Universe with a scalar field but our models also had the fine tuning problem associated with the cosmological constant. Despite these problems both models demonstrated how k -essence, especially using the features of purely kinetic k -essence, can be used to not only explain dark energy but at the same time inflation and dark matter as well, a triple unification that had not been done before. The form of the potential chosen for the first model, though widely used for its simplicity, is not very realistic and only serves to highlight the features of the model during the inflationary era. Recent WMAP data analysis [68] suggest that the best fit potential for inflation is a trinomial potential and further study of our model could be made by using such a potential. We also saw that in

the second model gravitational reheating was not able to produce sufficiently high temperatures after inflation was over in order to have a successful nucleosynthesis. There have been some recent studies which indicate that very low reheating temperatures could also be a viable option for a successful nucleosynthesis [71]. These ideas have to be analyzed in detail in the context of k -essence scenarios in order to check how far gravitational reheating could be successful in our model. Further the k -essence Lagrangian used in our models is certainly a simple example of a Lagrangian with a non-canonical kinetic term and it will be possible to generalize it and create a more broad class of k -essence models with rich features. Some work in this regard has already been done in [81].

It is well known from observations that our Universe is inhomogeneous up to at least the scales of super clusters of galaxies and has a rich variety of structure in it. But the standard Big Bang model of the Universe, although quite successful, is based on the assumption of homogeneity and isotropy. It has been realized that a modification of the standard cosmological framework is required in order to account for the presence of inhomogeneities, and this realization has led to investigation of the question of how backreaction originating from density inhomogeneities could modify the evolution of the universe as described by the background FRW metric at large scales. The main obstacle to this investigation is the difficulty of solving the Einstein equations for an inhomogeneous matter distribution and calculating its effect on the evolution of the Universe through tensorial averaging techniques. Many approaches have been proposed to calculate the effects of inhomogeneous matter distribution on the evolution of the Universe. In this thesis we have focused on the approach proposed by Buchert [40, 53]. It has been shown that backreaction from inhomogeneities from the era of structure formation could lead to an accelerated expansion of the Universe. This is exciting because if this turns out to be true then we can explain dark energy and the current accelerated expansion of the Universe without taking recourse to exotic scalar fields or modifying Einstein's theory of gravity, but by only refining our current cosmological framework. The Buchert framework also shows that we can describe the effects of inhomogeneities with the help of an effective scalar field called the morphon. This is an interesting result and it shows that we can interpret all existing scalar field models as originating from the effects of inhomogeneities. Although the original work by Buchert et. al. showed that the morphon was a traditional scalar field like quintessence, we have been able to show that the morphon can even be taken to behave as a k -essence

field. Thus the morphon provides a realistic source for all the various scalar field models of dark energy. The impact of inhomogeneities on observables of an overall homogenous FRW model has been debated in the literature. Similar questions have also arisen with regard to the magnitude of backreaction modulated by the effect of shear between overdense and underdense regions. Nevertheless arguments in favour of backreaction seem rather compelling. While upcoming observations may ultimately decide whether backreaction from density inhomogeneities drives the present acceleration, the above studies have highlighted that backreaction could be a crucial ingredient of the present evolution and future fate of our Universe.

Most of the work that has been done on dark energy focuses on how the current acceleration occurs, whether that work is based on scalar fields or backreaction. In our work on backreaction instead of going in this direction, we have tried to explore how dark energy and the current acceleration will behave in the future. The presently accelerating epoch dictates the existence of an event horizon since the transition from the previously matter dominated decelerating expansion. Since backreaction is evaluated from the global distribution of matter inhomogeneities, the event horizon demarcates the spatial regions which are causally connected to us and hence impact the evolution of our part of the Universe. Any contribution from inhomogeneities of scales which cross outside the event horizon due to accelerated expansion, needs to be excluded while computing the overall impact of backreaction. Such an approach has remained unexplored in previous studies of backreaction. Using a simple two-scale model we were able to show that backreaction with the event horizon could lead to a surprising possibility of transition to another decelerated future era. In our work we explored two different approaches on including the effect of the event horizon in the future evolution of the Universe, within the Buchert framework, and in both cases we got the same qualitative result which showed a future deceleration. We also compared this case with the evolution of the Universe as obtained from the unmodified Buchert framework and here also we found that there is a slowing down of the current acceleration in the future, but the rate of deceleration was faster when the event horizon was considered in our calculations. We also made an extension of our previous study by considering the Universe to be divided into multiple subdomains, and let each subdomain evolve independently of each other, with the aim of recreating the real Universe much better than in our previous model, and then studied the impact of backreaction in the future evolution of the Universe. Here our overall conclusion was that as the

number of subdomains increased the rate of deceleration increased although the magnitude of the maximum value of acceleration also increased correspondingly.

We have worked exclusively with the Buchert framework for studying the effect of backreaction on the evolution of the Universe, but there is some debate on the approach taken in this framework whereby the average of scalar quantities are computed on a space-like hypersurface, as compared to taking the average on the past light cone. The usefulness of the expansion rate averaged on any hypersurface is determined by relating it to observed quantities. It has been observed that the redshift and distance can be expressed in terms of the average geometry alone, provided that the contribution of the null shear is negligible [76]. The task of developing a procedure for light cone averaging is an ambitious programme and till date there is no standard formalism to do so. In a recent paper, three different types of light cone averaging have been proposed [79], though much work remains to be done in order to apply their technique to the problem of cosmic acceleration. In our work with backreaction that dealt with the event horizon we were able to introduce an element of light cone physics from another perspective by considering the effect of inhomogeneities from only those regions present within the event horizon. But much work remains to be done in equating current observed parameters with those obtained from backreaction frameworks no matter which framework is chosen.

BIBLIOGRAPHY

- [1] S. Perlmutter, et. al., *Nature* **391**, 51 (1998); A. G. Riess et. al., *Ap. J.* **116**, 1009 (1998); M. Hicken et al., *ApJ*, **700**, 1097 (2009); M. Seikel, D. J. Schwarz, *JCAP* **02**, 024 (2009).
- [2] E. Komatsu et al., *Astrophys. J. Suppl. Ser.* **180**, 330 (2009).
- [3] S. Weinberg, *Rev. Mod. Phys.* **61**, 1 (1989); S. Weinberg, arXiv:astro-ph/0005265.
- [4] V. Sahni, in Papantonopoulos E., ed., *Lecture Notes in Physics Vol. 653, The Physics of the Early Universe*. Springer, Berlin, p. 141 (2004); E. J. Copeland, M. Sami, and S. Tsujikawa, *Int. J. Mod. Phys. D* **15**, 1753 (2006).
- [5] C. Wetterich, *Nucl. Phys B.* **302**, 668 (1988); B. Ratra, J. Peebles, *Phys. Rev D* **37**, 321 (1988); P. J. E. Peebles and B. Ratra, *Rev. Mod. Phys.* **75**, 559 (2003).
- [6] T. Chiba, T. Okabe, and M. Yamaguchi, *Phys. Rev. D* **62**, 023511 (2000).
- [7] C. Armendariz-Picon, V. F. Mukhanov and P. J. Steinhardt, *Phys. Rev. D* **63**, 103510 (2001) [astro-ph/0006373]; C. Armendariz-Picon, V. F. Mukhanov and P. J. Steinhardt, *Phys. Rev. Lett.* **85**, 4438–4441 (2000) [astro-ph/0004134].
- [8] T. Chiba, *Phys. Rev. D* **66**, 063514 (2002).
- [9] L. P. Chimento and A. Feinstein, *Mod. Phys. Lett. A* **19**, 761 (2004).
- [10] N. Bose, A. S. Majumdar, *Phys. Rev. D* **79**, 103517 (2009).
- [11] N Bose, A. S. Majumdar, *Phys. Rev. D* **80**, 103508 (2009).
- [12] C. Armendariz-Picon, T. Damour, and V. Mukhanov, *Phys. Lett. B* **458**, 209 (1999).

-
- [13] G. R. Dvali, G. Gabadadze and M. Porrati, *Phys. Lett. B* **485**, 208 (2000); S. Capozziello, S. Carloni and A. Troisi, *RecentRes. Dev. Astron. Astrophys.* **1**: 625 (2003) [arXiv:astro-ph/0303041].
- [14] A. Y. Kamenshchik, U. Moschella and V. Pasquier, *Phys. Lett. B* **511**, 265 (2001); N. Bilic, G. B. Tupper and R. D. Viollier, *Phys. Lett. B* **535**, 17 (2002).
- [15] L. Susskind, arXiv:hep-th/0302219.
- [16] T. Padmanabhan, *Phys. Rev. D* **66**, 021301 (2002); A. Sen, *JHEP* **9910**, 008 (1999).
- [17] R. R. Caldwell, *Phys. Lett. B* **545**, 23-29 (2002).
- [18] N. Arkani-Hamed, H. C. Cheng, M. A. Luty and S. Mukohyama, *JHEP* **05**, 074 (2004) [hep-th/0312099].
- [19] A. G. Cohen, D. B. Kaplan and A. E. Nelson, *Phys. Rev. Lett.* **82**, 4971 (1999); S. Thomas, *Phys. Rev. Lett.* **89**, 081301 (2002); S. Hsu, *Phys. Lett. B* **594**, 13 (2004).
- [20] R. D. Sorkin, PRINT-91-0288 (CHICAGO), To appear in Proc. of SILARG VII Conf., Cocoyoc, Mexico, Dec 2-7, 1990; *Int. J. Theor. Phys.* **36**, 2759 (1997) [arXiv:gr-qc/9706002].
- [21] A. Blanchard, M. Douspis, M. Rowan-Robinson and S. Sarkar, *Astron. Astrophys.* **412**, 35 (2005).
- [22] A. Blanchard, M. Douspis, M. Rowan-Robinson and S. Sarkar, *Astron. Astrophys.* **449**, 925 (2006) [arXiv:astro-ph/0512085].
- [23] D. N. Spergel et al. [WMAP Collaboration], *Astrophys. J. Suppl.* **170**, 377 (2007) [arXiv:astro-ph/0603449].
- [24] D. N. Spergel et al. [WMAP Collaboration], *Astrophys. J. Suppl.* **148**, 175 (2003).
- [25] M. Tegmark et al. [SDSS Collaboration], *Phys. Rev. D* **69**, 103501 (2004).
- [26] M. Born and L. Infeld, *Foundations of the new field theory*, *Proc. Roy. Soc. Lond.* **A144** (1934) 425–451.

-
- [27] A. Sen, *Mod. Phys. Lett. A* **17**, 1797 (2002); N.D. Lambert and I. Sachs, *Phys. Rev. D* **67**, 026005 (2003).
- [28] C. Armendariz-Picon and E. A. Lim, *JCAP* **0508**, 007 (2005) [[astro-ph/0505207](#)].
- [29] N. Arkani-Hamed, P. Creminelli, S. Mukohyama and M. Zaldarriaga, *JCAP* **0404**, 001 (2004) [[hep-th/0312100](#)].
- [30] C. Bonvin, C. Caprini, and R. Durrer, *Phys. Rev. Lett.* **97**, 081303 (2006).
- [31] E. Babichev, V. Mukhanov, and A. Vikman, *J. High Energy Phys.* **02**, 101 (2008).
- [32] T. Padmanabhan and T. R. Choudhury, *Phys. Rev. D* **66**, 081301(R) (2002).
- [33] A. Arbey, *Phys. Rev. D* **74**, 043516 (2006).
- [34] R. Scherrer, *Phys. Rev. Lett.* **93**, 011301 (2004).
- [35] P. J. E. Peebles and A. Vilenkin, *Phys. Rev. D* **59**, 063505 (1999); A. S. Majumdar, *Phys. Rev. D* **64**, 083503 (2001); N. J. Nunes and E. J. Copeland, *Phys. Rev. D* **66**, 043524 (2002); K. Dimopoulos, *Phys. Rev. D* **68**, 123506 (2003); M. Sami and V. Sahni, *Phys. Rev. D* **70**, 083513 (2004); A. Gonzales, T. Matos, and I. Quiros, *Phys. Rev. D* **71**, 084029 (2005); I. P. Neupane and C. Scherer, *J. Cosmol. Astropart. Phys.* **05**, 009 (2008).
- [36] J.E. Lidsey, T. Matos, and L.A. Ureña-López, *Phys. Rev. D* **66**, 023514 (2002).
- [37] A. R. Liddle, C. Pahoud, and L. A. Ureña-López, *Phys. Rev. D* **77**, 121301(R) (2008).
- [38] L. P. Chimento, M. Forte, and R. Lazkoz, *Mod. Phys. Lett. A* **20**, 2075 (2005).
- [39] R. Zalaletdinov, *Gen. Rel. Grav.*, **24**, 1015 (1992); *Gen. Rel. Grav.*, **25**, 673 (1993).
- [40] T. Buchert, *Gen. Rel. Grav.*, **32**, 105 (2000); T. Buchert, *Gen. Rel. Grav.* **33**, 1381. (2001).
- [41] T. Buchert, M. Carfora, *Phys. Rev. Lett.* **90**, 031101 (2003).

-
- [42] E. W. Kolb, S. Matarrese, A. Notari and A. Riotto, *Phys. Rev. D* **71**, 023524 (2005).
- [43] S. Räsänen, *J. Cosmol. Astropart. Phys.*, **0402**, 003 (2004); S. Räsänen, *J. Cosmol. Astropart. Phys.*, **0804**, 026 (2008); S. Räsänen, *Phys. Rev. D* **81**, 103512 (2010).
- [44] D.L. Wiltshire, *New J. Phys.* **9**, 377 (2007); *Phys. Rev. Lett.* **99**, 251101 (2007); *Phys. Rev. D* **80**, 123512 (2009).
- [45] M. Gasperini, G. Marozzi, G. Veneziano, *JCAP* **0903**, 011 (2009); *JCAP* **1002**, 009 (2010).
- [46] A. Ishibashi, R. M. Wald, *Classical Quantum Gravity*, **23**, 235 (2006).
- [47] A. Paranjape, T. P. Singh, *Phys. Rev. D* **78**, 063522 (2008); T. P. Singh, arXiv:1105.3450 [astro-ph.CO].
- [48] M. Mattsson, T. Mattsson, *J. Cosmol. Astropart. Phys.* **10**, 021 (2010).
- [49] E. W. Kolb, S. Marra, S. Matarrese, *Phys. Rev. D*, **78**, 103002 (2008).
- [50] A. Wiegand, T. Buchert, *Phys. Rev. D* **82**, 023523 (2010).
- [51] N. Bose, A. S. Majumdar, *MNRAS Letters* **418**, L45 (2011).
- [52] L. P. Chimento, *Phys. Rev. D* **69**, 123517 (2004).
- [53] T. Buchert, M. Carfora, *Class. Quant. Grav.* **25**, 195001 (2008).
- [54] N. Bose, A. S. Majumdar, arXiv:1203.0125 [astro-ph.CO], Accepted for publication in *Gen. Rel. Grav.*
- [55] U. Alam, V. Sahni, T. D. Saini and A. A. Starobinsky, *Mon. Not. Roy. Astron. Soc.* **354**, 275 (2004).
- [56] R. R. Caldwell, M. Kamionkowski and N. N. Weinberg, *Phys. Rev. Lett.* **91**, 071301 (2003); S. Nesseris and L. Perivolaropoulos, *Phys. Rev. D* **70**, 123529 (2004).
- [57] A. R. Liddle and D. H. Lyth, *Cosmological Inflation and Large-Scale Structure*, Cambridge University Press (2000); A. R. Liddle, *An Introduction To Cosmological Inflation*, arXiv:astro-ph/9901124v1.

-
- [58] S. Weinberg, *Cosmology*, Oxford University Press (2008).
- [59] A. H. Guth, *Phys. Rev. D* **23**, 347 (1981).
- [60] A. A. Starobinsky, *Phys. Lett. B* **91**, 99 (1980).
- [61] J. Garriga and V.F. Mukhanov, *Phys. Lett. B* **458**, 219 (1999).
- [62] A. J. Christopherson and K. A. Malik, *Phys. Lett. B* **675**, 159 (2009).
- [63] V. Mukhanov, A. Vikman, *JCAP* **02**, 004 (2006); E. Babichev, *Phys. Rev. D* **74**, 085004 (2006).
- [64] W. Fang, H. Q. Lu, and Z. G. Huang, *Classical Quantum Gravity* **24**, 3799 (2007).
- [65] L. H. Ford, *Phys. Rev. D* **35**, 2955 (1987).
- [66] B. Spokoiny, *Phys. Lett. B* **315**, 40 (1993).
- [67] A. Melchiorri, L. Pagano, and S. Pandolfi, *Phys. Rev. D* **76**, 041301(R) (2007).
- [68] C. Destri, H. J. de Vega, and N. G. Sanchez, *Phys. Rev. D* **77**, 043509 (2008).
- [69] S. Kachru, R. Kallosh, A. Linde, J. Maldacena, L. McAllister, and S. P. Trivedi, *J. Cosmol. Astropart. Phys.* **10**, 013 (2003).
- [70] E. J. Chun, S. Scopel, and I. Zaballa, *J. Cosmol. Astropart. Phys.* **07**, 022 (2008).
- [71] K. Kohri, A. Mazumdar, and N. Sahu, *Phys. Rev. D* **80**, 103504 (2009).
- [72] T. Buchert, *Gen. Rel. Grav.* **40**: 467-527 (2008) [arXiv:0707.2153v3 [gr-qc]].
- [73] T. Buchert, J. Larena, J. M. Alimi, *Class. Quant. Grav.* **23**, 6379 (2006).
- [74] M. Seikel, D. J. Schwarz, *J. Cosmol. Astropart. Phys.*, **02**, 024 (2009)
- [75] K. Bolejko, L. Andersson, *J. Cosmol. Astropart. Phys.* **10**, 003 (2008).
- [76] S. Räsänen, *J. Cosmol. Astropart. Phys.*, **02**, 011 (2009).
- [77] D. Munshi et al., *Phys. Rep.*, **462**, 67 (2008).

-
- [78] E. W. Kolb, C. R. Lamb, arXiv:0911.3852 [astro-ph.CO] (2009).
- [79] M. Gasperini et al., *J. Cosmol. Astropart. Phys.* **07**, 008 (2011).
- [80] N. Bose, A. S. Majumdar, arXiv:xxxxxx [astro-ph.CO].
- [81] Josue De-Santiago and Jorge L. Cervantes-Cota, *Phys. Rev. D* **83**, 063502 (2011); Josue De-Santiago, Jorge L. Cervantes-Cota, David Wands, *Phys. Rev. D* **87**, 023502 (2013); Jorge L. Cervantes-Cota, Alejandro Aviles, Josue De-Santiago, arXiv:1303.2658 [astro-ph.CO].